Reactive Crystallization: A Review

Journal:	*Reaction Chemistry & Engineering*
Manuscript ID	RE-REV-06-2020-000272.R1
Article Type:	Review Article
Date Submitted by the Author:	01-Oct-2020
Complete List of Authors:	McDonald, Matthew; Georgia Institute of Technology, School of Chemical + Biomolecular Engineering Salami, Hossein; Georgia Institute of Technology, School of Chemical + Biomolecular Engineering Harris, Patrick; Georgia Institute of Technology, School of Chemical + Biomolecular Engineering Lagerman, Colton; Georgia Institute of Technology, School of Chemical + Biomolecular Engineering Yang, Ben; US Food and Drug Administration, Center for Drug Evaluation and Research Bommarius, Andreas; Georgia Tech, School of Chemical and Biomolecular Engineering Grover, Martha; Georgia Institute of Technology, School of Chemical & Biomolecular Engineering Rousseau, Ronald; Georgia Institute of Technology, School of Chemical + Biomolecular Engineering

SCHOLARONE™
Manuscripts

Reactive Crystallization: A Review

Matthew A. McDonald,[a] Hossein Salami,[a] Patrick R. Harris,[a] Colton E. Lagerman,[a] Xiaochuan Yang,[b] Andreas S. Bommarius,[a] Martha A. Grover,[a] and Ronald W. Rousseau [a]*

[a] School of Chemical and Biomolecular Engineering, Georgia Institute of Technology, Atlanta, Georgia, 30332

[b] Office of Pharmaceutical Quality, Center for Drug Evaluation and Research, U.S. Food and Drug Administration, Silver Spring, Maryland 20993-0002

Abstract

Reactive crystallization is not new, but there has been recent growth in its use as a means of improving performance and sustainability of industrial processes. This review examines phenomena and processes in which reaction and crystallization are coupled in the production of a desired chemical species. Coverage includes fundamental phenomena, such as solubility, supersaturation, crystal nucleation and growth, and chemical kinetics. Systems examined are divided into two groups, those best described as undergoing ionic reactions (including neutralizations), which have near instantaneous rates and result in the formation of ionic bonds, and those undergoing covalent reactions in which the key step occurs at measurable rates and results in the formation of covalent bonds, Discussion of the latter category also includes the impact of catalysis. Examples of a variety of reactions and applications are enumerated, and special attention is given to the utility of reactive crystallization in chiral resolution. Integration of reactive crystallization into process design, including both batch and continuous operations, and the development and efficacy of modeling, monitoring and control are reviewed. Finally, a perspective addressing needs to advance the usefulness and applications of reactive crystallization is included.

Introduction

Crystallization is used in the production of a wide variety and quantity of products and intermediates, perhaps more than any other separation technique. In different applications,

30   crystallization can separate, concentrate, or purify a specific species or it may be part of

31   diagnostic or analytical procedures. In most applications the most important function of

32   crystallization is to generate a product in a specific solid form. Many medicines, synthetic

33   materials, food ingredients, and specialty and commodity chemicals require crystallization

34   during the transformation from raw materials to product. The process by which chemical species

35   are crystallized often impacts their properties, such as purity, morphology, mean size, and size

36   distribution. Such properties can affect therapeutic capabilities and dissolution profiles of

37   pharmaceuticals, the efficacy of agricultural chemicals, and a variety of material properties.

38   While the use of crystallization is older than the chemical industry, there are aspects of

39   the process that remain poorly understood. Furthermore, the diversity of processes utilizing

40   crystallization and the chemical and physical variations of species crystallized has led to many

41   different methodologies for conducting this operation. The present review focuses on **reactive**

42   **crystallization from solution: that is, those processes in which a chemical reaction produces**

43   **a specific crystallizable species in solution and, thereby, generates a driving force for the**

44   **formation of a crystalline product**. Clearly, the chemical reaction must produce sufficient

45   amounts of the crystallizing species to exceed solubility. While reactive crystallization may

46   fulfill the same functions of crystallization cited earlier, there also are two other important roles

47   that can be played by reactive crystallization: (1) If a reaction is controlled by equilibrium,

48   removal of the reaction product from solution by crystallization pulls the reaction towards the

49   product as dictated by Le Chatelier's principle. (2) Suppose the desired product is an

50   intermediate in a larger reaction network and the yield of that product is reduced by its

51   subsequent reaction. Then the yield can be increased by operating under conditions causing

52   crystallization of the product. As solids, species are stabilized and less likely to undergo

53   subsequent solution-phase reactions.

54   Besides being generated by reaction, the driving force for crystallization can be created or

55   enhanced by solvent removal (for example, by evaporation or transport through a membrane),

56   adjustment of pH, change in temperature, or addition of a nonsolvent. The presence of multiple

57   species in solution complicates the system but is frequently encountered in industrial processes.

58   In a reactive crystallization process, there are necessarily multiple species present—that is, the

59   reactants and products of the reaction—that may impact the solubility of each species, the pH

60   and temperature of the solution, and the kinetics of the reactions and the crystallization.

2

61   As the chemical industry continues to strive towards ambitious goals of process

62   intensification, efficiency enhancements and sustainability, reactive crystallization can be a

63   helpful tool in achieving such goals. Thermal separations dominate the chemical industry and

64   have a huge energy cost; on the other hand, reactive crystallizations can be operated without

65   expenditure of the thermal energy that is required for cooling crystallization, evaporative

66   crystallization, or many other separation processes.[1] The combination of reaction and

67   crystallization can also reduce production time and hold-up of intermediates, thereby reducing

68   the number of operations and eliminating the need to transfer materials between vessels. Use of

69   the same solvent for reaction and crystallization can additionally reduce waste production and

70   the need for wastewater treatment, and it may even eliminate the need to use additional solvents.

71   Reactive crystallization encompasses several fundamental phenomena. Reactant mixing

72   is limited by convection and diffusion, as are the reaction products as they are transported

73   through the bulk liquid to the surface of a growing crystal. New crystals are formed by either

74   primary or secondary nucleation, thereby generating fresh surfaces for growth. The rates at

75   which these kinetic phenomena occur are influenced by mixing, catalyst design, and other

76   engineering decisions, and they determine the size distribution, yield, and other aspects of crystal

77   quality. Moreover, such fundamental considerations work their way into the design,

78   implementation, and control of processes in which reactive crystallization plays the key role.

79   The aims of this review are to (1) describe fundamental thermodynamic and kinetic

80   phenomena important in reactive crystallization, (2) examine reaction types and provide

81   tabulations of references for specific reaction systems, (3) examine the design and control of

82   systems using reactive crystallization, and (4) identify areas for future research. Only

83   crystallization from solution is considered and there is an emphasis on processes involving high-

84   value products such as pharmaceuticals and specialty chemicals. A condensed summary of

85   fundamentals of crystallization and reactive processes is followed by a compilation, with

86   commentary, of recent studies of processes utilizing reactive crystallization. Processes are

87   categorized based on reaction type and relative rates of reaction and crystallization. Finally, the

88   future of reactive crystallization processes is discussed, including what needs to be accomplished

89   for more widespread adoption of this intensified process.

90

91   **Fundamentals**

3

92   ***Solubility.*** Solid-liquid equilibrium thermodynamics determine solute solubility: that is,

93   the maximum mole fraction (or other measure) of the solute in a solution at a specific set of

94   conditions, including temperature, pressure, pH, and solution composition. The governing

95   requirement for solid-liquid equilibrium is that the chemical potential of each component

96   distributed between the two phases is the same in the solid and liquid phases; that is $\mu_i^S = \mu_i^L$.

97   Proceeding from this fundamental expression, a thermodynamic framework for cases involving

98   complex liquid mixtures, multi-component solids, and polymorphs can be developed.[2]

99   Thermodynamics also may determine the state of the solid, which may be anhydrous, a hydrate

100   or solvate, a salt, or one of a family of polymorphs.[*] When the system involves a chemical

101   reaction, the thermodynamics must include interactions of reactants, products, and by-products,

102   all of which greatly complicate the system behavior and make it difficult to formulate working

103   expressions for solute solubility.

104   In reactive crystallization, system conditions usually are selected so that reactants and

105   byproducts[‡] remain in solution, and the driving force for crystallization of the reaction product is

106   created by its synthesis. This was the goal outlined by Encarnacion-Gomez *et al.*[3] and McDonald

107   *et al.*[4] who compared the effect of pH value on solubilities of a product, ampicillin, to those of

108   the reactant, 6-aminopenicillanic acid, and byproduct, phenylglycine, to guide selection of the

109   pH value at which to run the reaction and crystallization. The approach was extended to include

110   systems in which primary products included amoxicillin and cephalexin and corresponding

111   reactants and byproducts.[5]

112   In many instances, empirical relationships, which often are based on simplifying

113   assumptions regarding the fundamental thermodynamics, are used to relate solubility as a

114   function of temperature and composition. Such approaches require experimental measurements

115   of solubilities, and the resulting correlations provide a means of interpreting and interpolating the

---

[*] Hydrates and solvates are sometimes referred to a pseudopolymorphs, but strictly speaking they are distinct chemical entities. Polymorphs, on the other hand, are all the same species, but have different packing structures.
[‡] Reactants are chemical species that are consumed by a reaction; byproducts are produced by a reaction but are not the desired species. Products are generated by a chemical reaction, but the term may also be used to indicate the output from the overall process.

116   data. As an illustration, consider the findings of Hu *et al.*[6] on the solubility of an important

117   intermediate compound, methyl D-(−)-4-hydroxy-phenyl glycinate, $C_9H_{11}NO_3$, in the production

118   of certain β-lactam antibiotics. Over a pH range of 1-13 they showed that the solubility was

119   lowest at the isoelectric point,* which is discussed below. Solubilities increased with solvent

120   polarity, except when water was the solvent, and it was asserted that water was an outlier

121   because of the dominance of the hydrophobic groups in the solute molecule. Temperature had

122   the most significant effect on solubility in both pure and mixed solvents, which was correlated by

123   the Apelblat equation

124
$$\ln x_1 = A + \frac{B}{T} + C \ln T \tag{1}$$

125   where x_1 is the mole fraction of solute 1 and A, B and C are constants fit to data for each solvent

126   or solvent mixture (T in Kelvin).

127   The rationale for the Apelblat equation was developed by Cuevas-Valenzuela *et al.*[7] and

128   it has since been cited in over 400 publications, with each describing its use for a variety of

129   solutes and solvents. In some instances, the third term in the equation can be omitted to obtain

130   the classic van't Hoff relationship

131
$$\ln x_1 = A' + \frac{B'}{T} \tag{2}$$

132   where A' and B' are fitted parameters, and B' is often referred to as the apparent heat of solution

133   (T in Kelvin).

---

* The isoelectric point (pK_I) is the pH at which the species carries no net charge. For a molecule with two proton-labile moieties, like many amino acids, the isoelectric point commonly is taken to be the average of the acid dissociation constant (pK_A) of each moiety.

5

134   Solubilities of amphoteric species,

135 such as amino acids, are lowest at their

136 isoelectric point. At this condition, the solid

137 in equilibrium with the solution is a neutral

138 zwitterion. Addition of acid or base to move

139 the pH value away from the isoelectric point

140 initially causes modest increases in solubility,

141 but then much greater increases occur as pH

142 moves further from the isoelectric point. The

143 distribution of acidic, neutral, and basic forms

Figure 1. Distribution of acidic, neutral, and basic forms of L-serine as a function of pH value.

144 of serine are shown in Figure 1 and illustrate the general behavior of amino acids.[8]

145   The composition of the solid in equilibrium with a coexisting solution of an amphoteric

146 species can vary with pH. Over the pH range that includes the isoelectric point (see Figure 1), the

147 coexisting crystal is the zwitterion (neutral species), but as pH moves towards the lower pK_{A1} the

148 solid species may change from the zwitterion to an acid salt (for example, leucine hydrochloride

149 when HCl is used to reduce pH). Kempkes and van Enckevort[9] presented *in situ* micrographs

150 showing both glutamic acid hydrochloride and glutamic acid crystals coexisting in a 1:1 solution

151 of glutamic acid and HCl in water. Alternatively, addition of a base to a solution near the

152 isoelectric point moves pH towards the higher pK_{A2} and the coexisting solid formed may be a

153 basic salt: for example, sodium leucinate (or leucine sodium) when sodium hydroxide is added to

154 a leucine solution near its upper pK_A. At pH extremes, solubilities of acid or basic salts may be

155 lower than those of the zwitterion and used to enhance recovery of the species of interest. For

156 example, Sano[10] describes the early production of L-glutamic acid hydrochloride by contacting

157 vegetable proteins with HCl, and then processing the recovered acid salt to become monosodium

158 glutamate.

159　　　　Tseng *et al.*[11] measured solubilities of five amino acids over a pH range from 2 to 10 and

160　　used an NRTL model* to describe activity coefficients of the non-ideal solutions. Figueiredo *et*

161　　*al.*[12] developed a methodology for estimating activity coefficients using UNIFAC methods and

162　　the Debye-Hückel equation that they tested successfully against literature data. Additional data

163　　on the effect of pH on the aqueous solubility of a number of amino acids can be found in various

164　　sources.[13-16]

165　　　　The presence of co-solutes and/or impurities can impact the solubility of a species of

166　　interest. McDonald *et al.*[17] showed that during crystallization of cephalexin , the reactants used

167　　to make cephalexin inhibited complete consumption of supersaturation relative to the pure

168　　cephalexin system, by effectively increasing the drug solubility. Hu *et al.*[6] showed that

169　　increasing concentrations of ammonium chloride or D-4-hydroxyphenylglycine methyl ester

170　　hydrochloride increased the solubility of methyl D-(−)-4-hydroxy-phenyl glycinate. This is

171　　particularly important because the ester is a reactant in the synthesis of the glycinate product. Co-

172　　solutes can also decrease solubility; Isakov *et al.*[22] showed that a compound with a valine-to-

173　　isoleucine ratio of 2:1 was formed from solutions containing the two amino acids and the

174　　compound formed a third separate solid phase with lower solubility that contaminated the pure-

175　　component solid phases. The presence of electrolytes in solutions of amphoteric species such as

176　　amino acids also affect the species' solubility. For example, the addition of sodium chloride to

177　　neutral solutions decreased glycine solubility at low sodium chloride concentrations, but then

178　　increased solubility as concentration was increased.[23] The researchers hypothesized that such

179　　behavior is based on ions of the electrolyte shielding the hydrophobic characteristics of the

180　　amino acid. Steendam *et al.*[24] examined how the difference in solubilities of two structurally

181　　similar impurities in solutions of paracetamol (acetaminophen) impacted the properties of

182　　paracetamol crystallized from those solutions. Further work with these species demonstrated that

183　　despite their significant impact on paracetamol crystal properties, the impurities had little

184　　influence on paracetamol solubility at the prescribed impurity concentrations.[25]

---

* The NRTL model (non-random two-liquid model) is an expression used to correlate activity coefficients of species in solution with the composition (expressed as mole fractions) of the solution. Activity coefficients are used to account for solution nonidealities, which usually represent deviations from Raoult's law. UNIQUAC and UNIFAC are group-contribution techniques for predicting activity coefficients.

185   Solubility is a function of solvent composition. For example, Granberg and Rasmuson[26]

186   measured solubilities of paracetamol in 26 solvents and determined ideal solubilities and activity

187   coefficients in the saturated solutions. Also, Jiang and Ni[27] considered how compositions of

188   water-acetic acid mixtures influenced paracetamol solubilities and crystal morphology. Solvent

189   effects on the solubilities of amino acids also have been investigated; the effects of ethanol on

190   aqueous solubilities of twenty amino acids were determined and found to be related to the side

191   chain on the amino acid.[28]

192   The relationship of solubility to the form of a co-existing solid at equilibrium has been

193   observed in the work of Zhang *et al.*[29] who found that hydrogen-bonding ability was a key factor

194   in determining solubility and polymorph formation of clopidogrel hydrogen sulfate (CHS). They

195   used two different experimental procedures to determine solubilities of CHS Forms I and II in

196   five alcohols, two ketones and two acetates. The van't Hoff relationship was used to correlate

197   solubilities in the nine solvents for the two different polymorphic forms. Solubilities in ethyl

198   acetate of Forms I and II, along with that of an amorphous form, were also determined by Lu *et*

199   *al.*[30] Additionally, temperature may determine which of two polymorphs is more soluble in a

200   given solvent, with the one having lower solubility being more stable. In enantiotropic systems

201   the form that has the lowest solubility changes with temperature. While there do not appear to be

202   any studies on reactive crystallization of enantiotropic species, several well-known enantiotropes

203   can be crystallized by reactive crystallization (e.g. *p*-aminobenzoic acid[31, 32]).

204   ***Supersaturation.*** The difference between a system at a given state and at equilibrium

205   represents a driving force for change, which in crystallization is referred to as supersaturation.

206   The formal definition of supersaturation is the difference in chemical potential of a solute at the

207   existing conditions (μ_i) and at equilibrium (μ_i^*): that is, $\mu_i - \mu_i^* = RT \ln\left(a_i / a_i^*\right)$, where a_i and a_i^*

208   are activities of solute *i* in the solution at the existing state and at equilibrium, *T* is absolute

209   temperature and *R* is the gas constant. Activity can be expressed as the product of an activity

210   coefficient (γ_i), mole fraction* and reference-state fugacity; choosing the same reference state for

211   the existing and saturated solutions (for example, pure supercooled liquid at the system

212   conditions) gives

---

* Activities based on other expressions of composition such as concentration (mol/L) can be used.

213
$$\Delta\mu_i = RT \ln \frac{\gamma_i x_i}{\gamma_i^* x_i^*} \tag{3}$$

214   Unless system conditions produce a significant difference between γ_i and γ_i^*, this

215   equation reduces to the simple dimensionless expression

216
$$\frac{\Delta\mu_i}{RT} = \ln \frac{x_i}{x_i^*} \tag{4}$$

217   If the ratio of mole fractions is less than about 1.2, there is less than 10% error in substituting

218    $\left[(x_i/x_i^*)-1\right]$ for $\ln(x_i/x_i^*)$. The dimensionless relative supersaturation σ_i then becomes

219
$$\sigma_i = \frac{x_i - x_i^*}{x_i^*} = S_i - 1 \tag{5}$$

220   where S_i is the ratio of mole fractions and is referred to as the supersaturation ratio. Expressions

221   for systems involving hydrates, partially dissociated electrolytes and mixtures of electrolytes

222   have been developed by Sohnel and Mullin.[33]

223   Mass balances and other operations in crystallization are often more convenient when

224   compositions are expressed in terms of ratios of mass of solute (w_i) per unit mass of solvent (w_s):

225    $X_i = w_i/w_s$. The relative supersaturation and supersaturation ratio can be expressed as

226
$$\sigma_i = \frac{X_i - X_i^*}{X_i^*} = S_i - 1 \tag{6}$$

227   provided $\sum(w_i/M_i) \ll$ where w_i is the mass of solute i in solution and M_i is the

228   molecular weight of i; w_s and M_s are, respectively, the mass of solvent and the solvent molecular

229   weight.

230   Another important way of expressing supersaturation is in terms of concentrations, c_i

231   (mol/L):

232
$$\sigma_i = \frac{c_i - c_i^*}{c_i^*} \tag{7}$$

233   which is valid if the solution molar densities at system conditions and at saturation are

234   approximately the same. Mullin[34] provides an example illustrating a violation of this assumption

235   with mixtures of sucrose, where differences between system conditions and saturation are

236   substantial.

9

237   It may be useful at this point to contrast how supersaturation is generated in reactive

238   crystallization with how it is developed in other settings: here a chemical reaction creates the

239   desired solute. If the system is isothermal and solvent has constant composition and is not being

240   removed, σ can be created only as a species is formed by a chemical reaction. If the system is

241   operating as a batch unit, with reactants added at the start of the process, the concentration of the

242   product, c_i would typically increase from an initial value of zero. Upon exceeding the solubility,

243   c_i^*, the supersaturation ratio, S_i, becomes greater than one, and crystallization can begin to occur

244   and proceed as long as the reaction maintains supersaturation in the system ($S_i > 1$).

245   Reactive crystallization necessarily occurs in the presence of multiple components, in

246   addition to the product. Accordingly, while the product solubility in pure solvent may provide a

247   first approximation to behavior in the reaction solution, such an assumption may be incorrect in

248   describing complicated interactions in the system with multiple species. As described earlier, the

249   effects of other solutes may alter (increase or decrease) product solubility, c_i^*, and therefore

250   supersaturation, and if solubility is increased, there may no longer be a driving force for

251   crystallization. As the objective is to recover pure product, the supersaturation ratio of other

252   species formed in the reaction system must remain below their metastable limits (described in the

253   next section). Otherwise, subsequent separation of species simultaneously crystallized will be

254   required and detract from the efficiency of the process.

255   ***Nucleation and Growth Kinetics.*** The kinetics of crystallization are defined by

256   nucleation and growth phenomena and play a central role in determining the characteristics of a

257   crystalline product, such as crystal size distribution.[*] In this section, nucleation is discussed from

258   the perspective of mechanisms leading to formation of crystals, and growth is recognized as how

259   crystals increase in mass (and size). Kinetics of nucleation and growth are given for several

260   crystallization systems to give context for crystallization kinetics in reactive systems.

261   *Nucleation*, in the context of this manuscript, is formation of a solid crystalline phase

262   from a liquid solution, which often sets the character of the process and is a critical factor in

263   determining product crystal size distributions. Classical nucleation theory (CNT) is based on

---

[*] Agglomeration and breakage, two additional kinetic phenomena that can affect crystal size distribution, are covered by Randolph and Larson,[35] Lewis *et al.*,[36] Ochsenbein *et al.*,[37] and Salvatori and Mazzotti.[38]

264   homogeneous and heterogeneous mechanisms, both of which describe formation of crystals

265   through a process of sequentially combining constituent units to form larger and larger entities

266   until a stable nucleus is produced.[39, 40] Both heterogeneous and homogeneous mechanisms are

267   referred to as primary nucleation because existing crystals play no direct role in the nucleation

268   mechanism. Supersaturation has a highly nonlinear relationship to primary nucleation rate as

269   illustrated by the following equation from classical nucleation theory:[36]

270
$$J = AS\exp\left(-\frac{\phi 16\pi\gamma_{sl}^3 v^2}{3(kT)^3(\ln S)^2}\right) \tag{8}$$

271   where J is the primary nucleation rate, A is a preexponential term, γ_{sl} is interfacial energy

272   between solid and liquid, v is molecular volume, k is the Boltzmann constant, T is absolute

273   temperature, and S is the supersaturation ratio as defined earlier. The term ϕ is an empirical

274   parameter whose value is 1 for homogeneous nucleation (heterogeneous surfaces play no role in

275   the nucleation event) and between 0 and 1 for heterogeneous nucleation (the presence of

276   heterogeneous surfaces lowers the energy barrier to nucleation). Paxton et al.[41] showed the effect

277   of ϕ in distinguishing between homogeneous and heterogeneous nucleation of chicken egg-white

278   lysozyme. Because the effect of supersaturation in the exponential term is much greater than in

279   the preexponential, the equation is often written as:[34]

280
$$J = A'\exp\left(-\frac{\phi 16\pi\gamma_{sl}^3 v^2}{3(kT)^3(\ln S)^2}\right) \tag{9}$$

281   Alternative mechanisms for primary nucleation have been proposed, including a two-step

282   process in which a metastable liquid phase is formed prior to formation of solid. These are

283   reviewed in various sources but are beyond the scope of this review.[36, 42]

284   It is generally recognized that solutions can maintain supersaturation without primary

285   nucleation taking place over modest observation timescales. Classical nucleation theory shows

286   that formation of a stable nucleus at low supersaturations is rare, but then substantial nucleation

287   occurs beyond a threshold referred to as a metastable limit. The region of a phase diagram

288   between solubility and nucleation is referred to as a metastable zone; at a given solute

289   concentration, the difference between the saturation temperature and the temperature at which

290   nucleation occurs is known as the metastable zone width (MSZW). Figure 2 illustrates behavior

11

291   of mixtures of DL-glutamic acid in water by showing solubility and metastable limits obtained

292   when initially undersaturated solutions were cooled at different rates. Clearly, metastable limits

293   are not thermodynamic quantities.

294
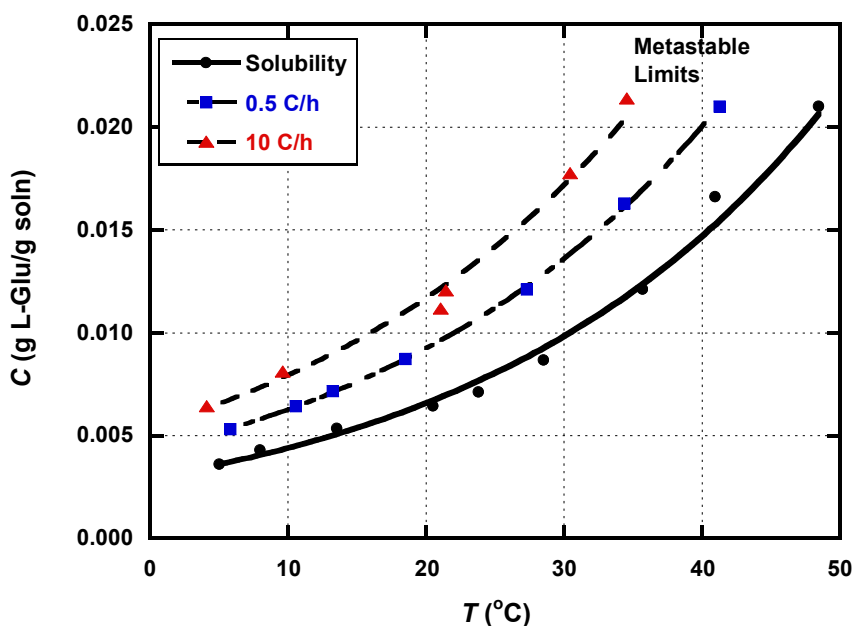
295

296   *Figure 2. Solubility and metastable limits for glutamic acid. Adapted from the work of Svang-Ariyaskul.[43]*

297   Primary nucleation in the metastable zone is unlikely but not impossible. More than 550

298   references emerged from a recent search using key words nucleation and metastable zone,

299   demonstrating the effort that has gone into measuring how the metastable limit varies according

300   to the system in which it is measured. The width of the metastable zone has been measured to be

301   as wide as 55 °C for citric acid ($\sigma \approx 1.4$) with a cooling rate of 0.05 K/min.[44] Kashchiev *et al*.[45]

302   and Kashchiev and van Rosmalen[46] provide a formula for estimating the width of metastable

303   zones. In cooling crystallization, the MSZW increases with increased cooling rate (see Figure 2).

304   Ma *et al*. found the same result for reactant addition rate; they showed that in the reactive

305   crystallization of lithium carbonate, increasing the addition rate led to a larger MSZW.[47]

306   Generally, the MSZW increases as the rate of supersaturation generation increases. Boukerche *et*

307   *al*.[48] found that adding heterogenous solids reduced metastable zone widths and facilitated

308   primary nucleation of different polymorphs. Sparging of inert gases was found to shrink the

309   MSZW for several systems[49] and lessen the induction time.[50]

12

310   Primary nucleation rates are often linked to induction time, which is defined as the

311   elapsed time between a solution becoming supersaturated and observation of nuclei formation.

312   An estimate of this quantity frequently assumes that the time to form a nucleus is much greater

313   than the time required for that nucleus to grow to observable size. The stochastic nature of

314   primary nucleation contributes to variability in induction-time measurements, which have been

315   correlated to probability distribution functions.[51-55] Interestingly, most, if not all, of the studies

316   observing stochastic outcomes are in small volumes (frequently 1 mL). Noting this, other

317   researchers have pointed out that as system volume increases, the observed stochasticity in both

318   induction time and MSZW is diminished.[56, 57] Kadam *et al.*[56] described experiments on

319   paracetamol nucleated from clear 1-mL and 1-L solutions. In the former, MSZWs in many

320   experiments ranged from 7.2 °C to 33.8 °C. Variations in the 1-L experiments were low, having

321   MSZWs between 7.0 °C and 7.5 °C: in other words, near the lower end of the range for 1-mL

322   measurements. Evolving from such observations, Kadam *et al.*[56] proposed what they called the

323   Single Nucleus Mechanism, which postulates that at a given supersaturation a single nucleus

324   forms and ultimately leads to secondary nucleation. Kadam *et al.*[52] extended this analysis by

325   suggesting that MSZW is a volume-dependent stochastic property in which the stochastic nature

326   of primary nucleation is dominant in systems of small volume; however, increasing system

327   volume enhances the probability of primary nucleation, making it deterministic at sufficiently

328   large volumes.

329   Uncertainties associated with primary nucleation lead to the common practice of seeding,

330   which is intentionally adding pre-existing crystals of the desired species into the system expected

331   to produce product crystals. This shift in the controlling phenomenon from primary to secondary

332   nucleation is especially useful in industrial settings where reproducibility of outcomes is a

333   paramount consideration. Moreover, after startup, continuous crystallizers maintain a slurry of

334   crystals which serves to repopulate itself through secondary nucleation. By this mechanism, a

335   metastable polymorph may be produced continuously. Kollges and Vetter predicted by modeling

336   and demonstrated with metastable β-L-glutamic acid that by tuning the residence time of the

337   reactor to the secondary nucleation kinetics (or adjusting the secondary nucleation kinetics by

338   milling) a population of the metastable form could be sustained indefinitely.[58, 59] Similar results

339   were found by Agnew *et al.*[60] for Form II of paracetamol.

13

340   Any mechanism involving existing crystals in the formation of new crystals is referred to

341   as secondary nucleation. In the late 1960s and early 1970s, considerable research identified this

342   form of nucleation as an important aspect of crystal formation, especially in industrial settings.

343   This early work was summarized in a foundational review by Garside and Davey[61] and a later

344   review provided by Agrawal and Paterson.[62] Among several mechanisms of secondary

345   nucleation, contacts or collisions of existing crystals with other crystals, crystallizer internals,

346   circulation pumps and impellers, which is known as contact nucleation or collision breeding, is

347   considered most important. Contact nucleation is characterized by a low-order dependence on

348   supersaturation (compared to primary nucleation) and absence of a metastable region. The latter

349   factor means that substantial secondary nucleation can occur at low supersaturation. Although

350   secondary nucleation is often considered to be a form of attrition,* it need not produce

351   macroscopic damage to parent crystals (those from which secondary nuclei are produced).[63-70]

352   Secondary nucleation kinetics have been examined extensively for stirred-tank

353   crystallizers, with some of the early proposed correlations provided by Grootscholten et al.,[71]

354   Ploss and Mersmann,[72] and others. Lewis et al.[36] summarize such relationships in two related

355   power-law equations that link nucleation rate to variables such as impeller speed, power input,

356   and mass of crystals per unit volume:

357
$$B_{\text{sec}} = k_N G^i N^k M_T^j$$
$$B_{\text{sec}} = k'_N S^a P^b M_T^j$$
(10)

358   where B_{sec} is the secondary nucleation rate [number/volume·time], G is crystal growth rate, N is

359   rotational speed, M_T is a measure of the crystal concentration in the stirred-tank system (usually

360   mass of crystals/volume of either slurry or solvent), S is supersaturation ratio, P is specific power

361   input, and the other quantities are fitted parameters. Such correlations overlook some important

362   process variables, such as type of impeller and existence of baffles or a draft tube and are likely

363   to be most useful in scaling up between similar crystallizer geometries.

364   The roles of primary and secondary nucleation in a batch operation depend on whether

365   seeding is used. Beginning with a clear solution (unseeded) means primary nucleation is an

---

* In this context, attrition is taken to mean removal of small parts of a crystal by abrasion, collision, or friction.

14

366　essential step in crystal formation. Even so, it is likely that crystals resulting from primary

367　nucleation grow and then serve as stimuli for secondary nucleation, analogous to the Single

368　Nucleus Mechanism.[52] Li *et al.*[73] used experiments in which paracetamol was crystallized from

369　clear solutions in ethanol to evaluate models, and then used these models to demonstrate that

370　only a small fraction of the final crystals per batch originated from primary nucleation. The

371　modeling results indicate that the foremost role of primary nucleation is to produce a small

372　number of crystals, which then serve to stimulate secondary nucleation. The overall rate of

373　crystallization in seeded batch and continuous operations is generally dominated by secondary

374　nucleation.

375　　　*Crystal growth* rates depend on how they are measured, and they may be expressed in

376　terms of those measurements. For example, both the linear advance rate of a specific crystal face

377　and the rate of change in a characteristic dimension (which, again, can be determined in a variety

378　of ways) are measures of growth kinetics. The rates of change in the mass of a crystal or a

379　population of crystals also provide growth rates. These seemingly different measures are related

380　through crystal shape and density:

381
$$\frac{dm_{crys}}{dt} = 3\rho\frac{k_v}{k_a}a_{crys}G \tag{11}$$

382　where m_{crys} and a_{crys} are the mass and interfacial area of a crystal, ρ is its density, k_a and k_v are

383　area and volume shape factors (quantities that relate crystal surface area and volume to a selected

384　characteristic dimension), and G is rate of change in the characteristic crystal dimension.

385　　　At least two resistances in series must be overcome for growth to occur: (1) transport (by

386　diffusion or convection) of a solute species though solution to the crystal face and (2)

387　incorporation of solute into a crystal lattice. The rates at which the two processes occur must be

388　equal at steady state, and the growth rate may be expressed in terms of transport coefficients and

389　driving forces associated with each:

390
$$G = k_d\left(c - c_{int}\right) \tag{12}$$

391
$$G = k_r\left(c_{int} - c\right)^r \tag{13}$$

392　where r, k_d, and k_r are fitted parameters, c is solute concentration and c_{int} is solute concentration

393　at the crystal-solution interface. Should the dominant resistance to growth lie in surface

394   incorporation, $c \rightarrow c_{int}$ and $G = k_r \left(c - c* \right)^r$; alternatively, if the dominant resistance is transport

395   to the crystal surface, $c_{int} \rightarrow c*$ and $G = k_d \left(c - c* \right)$.

396   Concepts of how molecules or ions incorporate into a growth face generally are based on

397   either birth-and-spread or screw-dislocation theories. Mechanistic descriptions of these

398   approaches, along with primary sources, are provided in several references.[34, 36] An empirical

399   power-law expression can be used to relate growth kinetics to supersaturation by fitting growth-

400   rate data:

401   $$G = k_G A_G \sigma^g \qquad\qquad (14)$$

402   where k_G is a rate coefficient and A_G is the surface area of the crystals. The exponent g is a fitted

403   parameter with typical values between 1 and 2. This range of values for g encompasses those

404   resulting from the cited theories, but, as demonstrated by Soto and Rasmuson,[74] distinguishing

405   among the birth-and-spread and spiral growth theories is difficult; the empirical power-law is

406   often sufficient.

407   Empirical expressions used to correlate nucleation and growth kinetics should be

408   developed in systems similar to those for which the expressions are to be used. Reactive

409   crystallizations present challenges in that regard because of the inherent presence of species

410   other than a primary crystalline product; in other words, reactants, byproducts, and other species

411   can impact crystallization kinetics of product crystals. The effect can result from changing either

412   the solubility (as discussed previously) or nucleation and/or growth kinetics. Illustrations of the

413   effect on growth kinetics are provided by Capellades et al.[75] who found that impurities from

414   upstream operations impacted the growth rate of the antibiotic ciprofloxacin in a continuous

415   crystallizer, while having little effect on nucleation kinetics. McDonald et al.[17] found that during

416   the reactive crystallization of cephalexin (which is from an antibiotic family that is different from

417   ciprofloxacin) the presence of reactants inhibited crystal growth in a mechanism dependent on

418   both the reactant concentration and cephalexin supersaturation. Neither of these two studies

419   found an effect of co-solutes on nucleation kinetics. Kubota[76] presents a broad review of the

420   impact of co-solute species on crystal growth.

421   ***Chemical Reactions***. Two broad categories of reactions are considered in this review:

422   ionic reactions and covalent reactions. Both will be covered in sections that provide specific

423   examples of such systems.

16

424   Ionic reactions are defined by bonds formed from electrostatic attractions between

425   oppositely charged ions; for example, a positive sodium ion and negative chloride ion in sodium

426   chloride (NaCl). Ionic reactions tend to be very fast; formation of the bond requires only

427   displacement of solvent molecules from the solvation shell and the interaction is governed

428   principally by coulombic forces. Computational work on aqueous NaCl crystallization suggests

429   that the rate limiting step in this reaction between Na^+ and Cl^- is the removal of water from the

430   chloride attachment site on the NaCl crystals.[77] One caveat to these results is the low

431   supersaturations studied. The ability of water to transport protons at a rate faster than expected

432   by diffusion suggests that in neutralizations (see below) the solvent may not pose the same

433   barrier as in inorganic ionic systems like the NaCl system.[78]

434   Neutralizations are a subset of ionic reactions that involve the addition or removal of a

435   proton from a proton-labile functional group such as an acid, amine, or alcohol. Neutralization

436   reaction rates are often considered instantaneous in the reactive crystallization literature.[3, 79-81]

437   The rates are governed by the collision frequency of the reactants; every collision between

438   reactants results in the product being formed, regardless of collision energy or orientation.

439   Therefore, these reactions are often treated as mixing-limited or diffusion-limited. Many studies

440   investigate means of mixing reactants to ensure a uniform reaction,[81-85] with a minireview by

441   Teychene *et al.*[86] The equilibrium composition of these reactions is highly pH-dependent in

442   aqueous systems; in organic solvents equilibrium composition depends on the species as well as

443   the proton capacity of the solvent.

444   Covalent reactions involve forming bonds requiring the sharing of electrons between

445   atoms. These reactions range from very slow to fast and often require a catalyst; both the flow

446   timescale of the reactor and diffusion in and out of the catalyst (if a heterogeneous catalyst is

447   used) may impact the effective reaction rates and overall conversion. While many covalent

448   reactions require a catalyst to proceed at appreciable rates, the presence of the catalyst does not

449   change the reaction equilibrium, which may favor reactants or products, depending on the

450   specific system. Many covalent reactions involve networks or series of reactions, which further

451   complicate reaction equilibria since the products of one reaction are reactants in another.

452   Covalent reactions may also be most amenable to reactive crystallization, as they may benefit

453   from shifts in equilibrium, enhancements in rate and selectivity, isolation of intermediates, and

454   many of the other motivators for implementing a reactive crystallization process.

455   The rate of reaction is described by an equation that expresses the rate of reactant

456   consumption as a function of reactant concentration and reaction conditions (such as

457   temperature, pressure, etc.). The function can be derived empirically, from insight into the

458   reaction mechanism, or through first-principle approaches in computational chemistry. For the

459   simple reaction A → B, the elementary rate equation could be $r = -dc_A/dt = k_1 c_A^n$ where the rate

460   constant k_1 is typically a function of reactor conditions (e.g. temperature), c_A is the concentration

461   of A (mol/L), and the exponent n is the reaction order. If the reverse reaction B → A also occurs

462   then the overall rate equation for A (assuming a first order reaction so that $n = 1$) would be

463   $r = k_1 c_A - k_{-1} c_B$ where the subscript -1 indicates the reverse of the forward reaction.[87]

464   Reaction equilibrium occurs when the rates of the forward and reverse reactions are equal

465   and therefore the overall rate is zero; that is, $dc_A/dt = 0$.* Such conditions are reached when

466   sufficient product has accumulated for the forward (desired) and reverse reactions to have equal

467   rates. The ratio of the forward and reverse rate constants, k_1 and k_{-1}, is the equilibrium constant,

468   $K_{eq} = c_B/c_A$. Equilibrium for a reaction system involving multiple reactions (for example,

469   A $\rightleftharpoons$ B $\rightleftharpoons$ C) means that the concentrations of all species are constant and the reaction

470   equilibrium constant for the overall system is the product of the individual equilibrium constants:

471   $K_{overall} = K_1 K_2$. If the concentration of a compound, such as species B in the above system, is

472   elevated above its solubility, then crystallization removes the species from solution and pulls the

473   reaction further towards its production. Overall equilibrium of the system is reached when there

474   is no driving force for reactions, crystal nucleation, growth, or dissolution (i.e. the chemical

475   potential of each species is the same in all phases, and temperature and pressure are uniform).

476   In reactive crystallization, elementary kinetic expressions may be unknown, in which

477   case empirical relations can be derived. Take for example the reactive crystallization of a crop-

478   protection agent, Z, considered by Bhamidi $et\ al.$[88] The agent is synthesized in the reaction 2A +

479   M → Z with Z crystallizing from the water/methanol reaction solvent. It was empirically

480   determined that consumption of M followed the rate equation $-dc_M/dt = k_1 c_A c_M$ where k_1 is the

481   rate constant, and c_A and c_M are the concentrations of A and M respectively. An Arrhenius

---

* This situation is analogous to solid-liquid equilibrium where the rates of crystallization and dissolution are equal.

18

482   relationship accounted for the dependence of k_1 on temperature, $k_1 = k_0 \exp\left(-E_A/RT\right)$ where k_0

483   is the frequency factor, E_A is the activation energy, R is the universal gas constant, and T is the

484   temperature. They were able to determine the heat of reaction as well as the activation energy

485   and frequency factor using calorimetry. The relatively simple expression used here was sufficient

486   for an economic analysis of the homogeneous uncatalyzed reaction to produce Z.
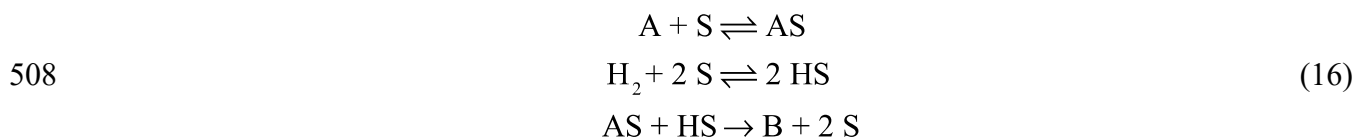
487   Complicated expressions are often required to describe complex reactions, especially

488   those requiring catalysts. Uncatalyzed reactions may only have one or two local energy minima

489   along their reaction pathway; catalyzed reactions, on the other hand, often have a more

490   complicated energy pathway with several transition states and energy minima corresponding to

491   different interactions between the catalyst and reacting species. Each of these steps has the

492   potential to be a rate-limiting transition state, leading to complex rate equations.

493   For example, enzymes, which represent an important class of catalysts, were used in a

494   reactive crystallization leading to deracemization of amino acids.[89] The authors of that study

495   confirmed that in the reactive crystallization the enzyme D-amino acid oxidase followed

496   Michaelis-Menten kinetics:

$$r = c_{enz} \frac{k_{cat}c_A}{K_M + c_A} \tag{15}$$

498   where c_{enz} is the concentration of the enzyme, c_A is the concentration of the reactant, k_{cat} is the

499   catalytic rate constant, and K_M is the Michaelis constant. When the reactant concentration is large

500   ($c_A \gg K_M$), as is often the case, the reaction rate varies only with the enzyme concentration,

501   rendering catalyst concentration an important design variable.[87] When $c_A \ll K_M$ the rate is

502   sensitive only to the reactant concentration.

503   Catalyzed reactions involving two reactants require rate equations of even greater

504   complexity; at different concentration regimes the order of the reaction may appear to change as

505   the rate-limiting step shifts from one state to another. An example is palladium-catalyzed

506   hydrogenolysis, involving hydrogen and a second reactant, which is found in several reactive

507   crystallization systems.[90-93] Yap et $al.$[94] found that these reactions follow the mechanism

$$
\begin{aligned}
A + S &\rightleftharpoons AS \\
H_2 + 2\,S &\rightleftharpoons 2\,HS \\
AS + HS &\rightarrow B + 2\,S
\end{aligned}
\tag{16}
$$

19

509   where A is the species undergoing hydrogenolysis, B is the product, and S denotes a catalytic

510   surface adsorption site; AS and HS indicate adsorbed reactant and hydrogen, respectively. They

511   formulated the rate equation using Langmuir-Hinshelwood kinetics as

$$r = kc_S^2 \frac{K_A c_A \left(K_H c_{H2}\right)^{1/2}}{\left[1 + K_A c_A + \left(K_H c_{H2}\right)^{1/2}\right]^2} \tag{17}$$

512

513   where c_A and c_{H2} represent concentrations of reactants A and H_2, c_S is the surface concentration

514   of active sites S, and K_A, K_H, and k represent the surface adsorption equilibrium constants for the

515   first reaction, the second reaction, and the rate constant of the third reaction, respectively. The

516   number of reactants is not limited to one (as in the above enzyme example) or two (as in the

517   above palladium example) reactants; in general, increasing the number of species increases the

518   complexity of the overall rate equation unless simplifying assumptions can be made.

519   Catalysts may be homogeneous (dissolved in solution) or they may be heterogeneous; in

520   the latter case, the active material often is bound to a porous, inert support. When a catalyst is a

521   solid, for example platinum supported on ceramic or an enzyme immobilized on a polymer, both

522   the rate of reactant consumption at the catalyst surface and the rate of reactant replenishment by

523   diffusion or convection (from the bulk fluid to the surface) may affect the overall reaction

524   kinetics. Solid catalysts are evaluated by their effectiveness factor η, which is defined as the ratio

525   of the observed reaction rate r_{obs} to the reaction rate with rapid mass transfer r.[95] An

526   effectiveness factor close to unity indicates good utilization of the active catalytic material (i.e.

527   the palladium or enzyme on the solid support). An effectiveness factor $\ll 1$ indicates inefficient

528   use of the catalytic material; a re-engineering of the catalyst may increase the effectiveness

529   factor, possibly by changing the size or morphology of the catalyst surface, the catalyst loading,

530   the pore size of the inert support, or other aspects of the catalyst. A similar concept for crystal

531   growth involving resistances in series was described in the previous section, although usefulness

532   of the effectiveness factor for crystal growth is limited.[96]

533   ***Combined Crystallization and Reaction Kinetics***. Taken together, the kinetics of

534   nucleation, growth, and reaction, along with process configuration, determine the quality of the

535   crystal product. For illustrative purposes, four different kinetic scenarios are examined for the

536   first-order reversible reactive crystallization A $\rightleftharpoons$ B $\rightarrow$ B$_{(s)}$ (with $K_{eq} = 1$) taking place in a batch,

537   isothermal, unseeded system: scenario (1) slow reaction and slow crystallization kinetics (1×),

20

538   (2) fast reaction and fast crystallization kinetics (5×), (3) slow reaction and fast crystallization

539   kinetics, and (4) fast reaction and slow crystallization kinetics. For each of the four cases, three

540   different relative rates of nucleation and growth were examined, where the primary and

541   secondary nucleation rates (A' and k_N from Equations 9 and 10, respectively) were increased or

542   decreased by a factor of five. The growth rate was varied to match the concentration profile

543   while compensating for the change in nucleation rate, as is observed experimentally in many

544   well-mixed crystallizers.[97] Details of the simulation are available in the supplementary material.

545   For each case, the concentrations of reactant A and product $B_{(S)}$ over time and endpoint

546   normalized population densities (a representation of the more general crystal size distribution)

547   are shown in Figure 3. Experimental observations of the concentration profile and end-point

548   population density can be used to fit nucleation and growth kinetics.[17] As can be seen, depending

549   on the relative rates of reaction, nucleation, and growth, a batch reactive crystallization can yield

550   a variety of population densities, some of which may not meet product specifications. Bimodal or

551   skewed population densities may be particularly problematic.
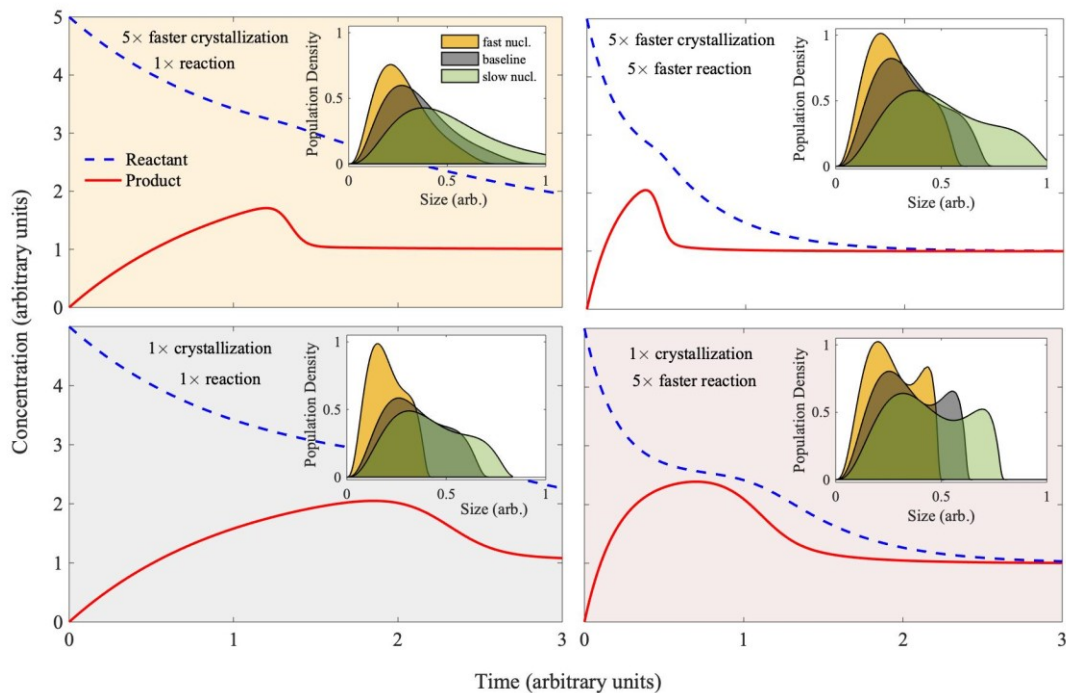
552

553   Figure 3. Quadrant plot showing solution concentrations (normalized by the saturation concentration) of
554   reactants (dashed blue curves) and products (solid red curves) during the first order reaction $A \rightleftharpoons B \rightarrow B_{(s)}$ for
555   baseline reaction and crystallization kinetics (gray, lower left), fast reaction baseline crystallization kinetics (pink,
556   lower right), fast crystallization baseline reaction kinetics (orange, upper left) and fast reaction and crystallization
557   kinetics (white, upper right). The insets depict the population density calculated at baseline nucleation rate (gray),
558   fast nucleation (yellow), and slow nucleation (green); for the different nucleation rates the growth rate was varied

559　*to match the concentration profile. In real systems the growth rate typically varies to match the rate of*
560　*supersaturation generation. The size units and population density have been normalized such that the scale is the*
561　*same in each inset.*

562　　　　The concentrations in Figure 3 have been normalized by the solubility of the product,

563　rendering the solid curve the product supersaturation. As expected, with slower crystallization

564　kinetics a larger supersaturation accumulates before crystal growth can match the rate of the

565　reaction. Crystallization is helping to pull the reaction towards the product, as illustrated by the

566　faster consumption of reactant in cases with faster crystallization kinetics. Sustained higher

567　supersaturations lead to large amounts of primary nucleation and bimodal crystal population

568　densities. If the product B were consumed by a second reaction the sustained higher

569　supersaturation would be expected to further decrease yield and productivity. When the rates of

570　reaction and crystallization are scaled together, comparable population density functions are

571　obtained, as can be seen in the similarity between the bottom left and top right insets in Figure 3.

572　　　　In generalizing Figure 3 one realizes that in reactive crystallization systems the rate of

573　crystallization will always lag the reaction, a consequence of the sequential nature of the process.

574　Enhancing the rate of crystallization (and the benefits of reactive crystallization) can be

575　accomplished by increasing the rate of the reaction, as can be seen comparing the bottom two

576　panes of Figure 3; the faster reacting system spends less time at an elevated supersaturation and

577　reaches a higher peak supersaturation. Alternatively, the kinetics of crystallization can be sped

578　up by techniques such as milling, which is discussed in a later section, to improve overall yield

579　and size distribution. A detailed understanding of the process kinetics is indispensable for

580　producing material with the desired properties in a process with the desired performance.

581　**Types of Reactions**

582　　　　***Crystallization and Ionic Reactions.*** Ionic compounds utilized in applications ranging

583　from pharmaceutical additives[98, 99] to polymer fillers,[100, 101] can be produced via reactive

584　crystallization. Processes involving reactive crystallization can be used for removing

585　contaminants, such as heavy metals, from water,[102-104] or for separating a product, such as

586　lithium carbonate, from solution.[105, 106] Ionic reactions include synthesis of inorganic

587　compounds, formation of salts, and neutralization of organic ions.

588　　　　Reactive crystallization of ionic compounds is based on the reaction between an anion

589　and a cation in solution. The solutions are typically aqueous, but other solvents, such as

590　supercritical CO_2, have been used.[107] The solubility of the target compound is often substantially

591   lower than that of precursors supplying the reacting ions. For sparingly soluble ionic species,

592   solubility is usefully defined in terms of a solubility product. For example, for the species A_aC_c

593   having an anion A with a negative charge $c-$ and a cation C with a positive charge $a+$, the

594   solubility product K_{sp} is given by

595
$$K_{sp} = \left[A^{c-} \right]_{eq}^{a} \left[C^{a+} \right]_{eq}^{c} \tag{18}$$

596   where the bracketed terms represent the concentrations of ions at equilibrium in mol/L. The

597   relative supersaturation σ for the compound A_aC_c may be defined as:

598
$$\sigma = \frac{\left[A^{c-} \right]^{a} \left[C^{a+} \right]^{c} - K_{sp}}{K_{sp}} \tag{19}$$

599    $[A^{c-}]$ and $[C^{a+}]$ are the anion and cation concentrations at system conditions in the same units

600   used for K_{sp}. The time course of ion concentrations during a process can be measured using an

601   ion-selective electrode,[108] a conductivity sensor,[99] or a spectrophotometric probe, such as a UV-

602   vis probe,[109] an IR probe,[110] or a Raman probe.[111] In systems with high ionic strength, Equations

603   18 and 19 should be modified by replacing each concentration with an activity, which is defined

604   as the product of a concentration and an activity coefficient. In systems at low concentration,

605   ions do not interact with each other and the activity coefficient can be assumed to be unity,

606   otherwise, the activity coefficient for each species can be estimated using the Debye-Hückel

607   theory.[112] Note that in some cases (for example, the production of calcium phosphate), the

608   compounds may have several dissociation states, depending on pH value, and the solubility

609   product should be corrected to take that feature into account.[105]

610   A common theme in many ionic reactive crystallization studies is that the reaction between

611   the anion and cation is considered instantaneous. The dynamic behavior of the system is governed

612   by crystal nucleation, growth, and mixing. Fast reaction kinetics contrast with those undergoing

613   covalent reactions such as enzymatic synthesis and crystallization of ampicillin, where the reaction

614   step limits the overall timescale of the process.[113] Rapid reaction kinetics, in addition to the

615   formation of a practically insoluble compound, may lead to very high levels of supersaturation. In

616   such cases, the mixing strategy, especially in fed-batch systems, can have a significant impact on

617   process attributes such as crystal size distribution and shape.[114] Mixing will be discussed further

618   in the process design sections.

23

619   Examples of inorganic compounds produced by reactive crystallization are hydroxides

620   such as nickel[85] and aluminum hydroxide,[115] carbonates such as lithium[98, 106] and calcium

621   carbonate,[116] phosphates such as calcium phosphate,[105] and sulfates such as barium sulfate.[79]

622   Table 1 summarizes some of the representative inorganic ionic reactive crystallization studies

623   and precursor materials used in each. These systems have been examined from different

624   viewpoints, including developing kinetic models for crystal nucleation and growth,[98] prediction

625   and control of particle size distribution,[108] the effect of process parameters such as stirring rate

626   on product size and morphology,[116, 117] and the effect of different additives on polymorph

627   formation.[118]

628   Gas-liquid reactive crystallizations result from contacting liquid and gas phases

629   containing reactants whose combination produces a crystalline product. Many of these systems

630   involve synthesis of carbonates through direct injection of CO_2 gas into the crystallizer.[117, 119, 120]

631   The gaseous CO_2 gets absorbed by the liquid phase to form the carbonate ion:[120]

$$CO_{2(g)} + H_2O \rightarrow CO_3^{2-} + 2H^+ \tag{20}$$

633   The carbonate ions then react with cations to produce solid species. Several groups have studied

634   the effect of different gas-injection variables such as bubble size and CO_2 mole fraction on the

635   structural and chemical properties of the crystal product. For instance, Matsumoto et al.[117]

636   controlled the polymorphic form of calcium carbonate crystals by manipulating the CO_2-to-N_2

637   ratio of the inlet gas. Varma et al.[120] used the same method with different dispersion agents,

638   including citrate ions and polyacrylic acid, for producing calcium carbonate nanocrystals. These

639   systems can be used both for the recovery of metals from solutions and potential removal of CO_2

640   from industrial gas streams.[120, 121]

641   A similar approach was proposed and illustrated for production of hydroxides by

642   injecting ammonia gas into the crystallization solution to produce hydroxide ions:[101]

$$NH_{3(g)} + H_2O \rightarrow NH_4^+ + OH^- \tag{21}$$

644   In these gas-liquid-solid cases, the absorption of gaseous reactant into the liquid phase can affect

645   the supersaturation and kinetics of the process. Attempts have been made to model this transport

646   limitation, such as proposing a double-film theory-based mass-transfer model.[122-124]

647   Table 1 highlights some of the studies of reactive crystallization in the types of inorganic

648   systems discussed above. The studies include continuous and batch processes with various

24

649   reactor configurations. In inorganic systems the focus tends to be crystallization-centric, as seen

650   from the last column in the table. The listed works either give insight into a specific

651   crystallization phenomenon, such as growth mechanism, size control, or polymorph control, or

652   are case studies on process designs for recovery of a certain species, such as nickel from

653   wastewater or CO_2 from flue gas. In the coming sections it will be shown that many desirable

654   features of reactive crystallization, such as equilibrium modification and intermediate isolation,

655   are more common in organic systems.

656   *Table 1. A list of representative studies on the reactive crystallization of ionic compounds with the*
657   *precursors used and the focus of the work. $MgDS_2$ stands for dodecyl sulfate, FB for fluidized bed, and CSD for*
658   *crystal size distribution.*

Product	Reference No.	Reactant 1	Reactant 2	Focus
Carbonate				
Li_2CO_3	[106]	LiOH	CO_2	Li and CO_2 recovery
Li_2CO_3	[98]	Li_2SO_4	Na_2CO_3	Crystallization kinetics
Li_2CO_3	[125]	LiCl	Na_2CO_3	Growth morphology
Li_2CO_3	[121]	LiCl	CO_2	Growth mech./product characterization
Li_2CO_3	[126]	LiCl	Na_2CO_3	Effect of additives on shape/size
$CaCO_3$	[116]	$Ca(OH)_2$	Na_2CO_3	Crystal polymorph control
$CaCO_3$	[117]	$CaNO_3$	CO_2	Crystal polymorph control
$CaCO_3$	[120]	$Ca(OH)_2$	CO_2	Nanocrystal formation
$CaCO_3$	[127]	$CaCl_2$	Na_2CO_3	Crystal polymorph control
$CaCO_3$	[128]	$CaCl_2$	Na_2CO_3	Crystal polymorph control
$CaCO_3$	[118]	$CaCl_2$	$NaHCO_3$	Effect of additives on size/morphology
$CaCO_3$	[129]	$Ca(OH)_2$	CO_2	Effect of additives on size/morphology
$CaCO_3$	[119]	$Ca(OH)_2$	CO_2	Crystallization kinetics
$MgCO_3$	[130]	$Mg(OH)_2$	CO_2	Effect of gas flow/stirring on process
$NiCO_3$	[102]	$NiSO_4$	Na_2CO_3	Fluidized bed reactor design
$NiCO_3$	[131]	$NiSO_4$	Na_2CO_3	Metal recovery and effect of seeding
$BaCO_3$	[108]	BaS	Na_2CO_3	Crystallization kinetics and CSD
$BaCO_3$	[132]	$BaCl_2$	Na_2CO_3	Crystallization kinetics
$BaCO_3$	[133]	$BaCl_2$	$(NH_4)_2CO_3$	Crystallization kinetics and morphology
Hydroxide				
$Ni(OH)_2$	[85]	$NiSO_4$	NaOH	Study of airlift-loop reactor
$Ni(OH)_2$	[134]	$NiSO_4$	NaOH	Ni recovery from wastewater
$Al(OH)_3$	[115]	$NaAl(OH)_4$	$NaHCO_3$	Crystallization kinetics and morphology
$Mg(OH)_2$	[99]	$Mg(NO_3)_2$	NaOH	Crystallization kinetics
$Mg(OH)_2$	[101]	$MgCl/DS_2$	NH_3	Impact of metal source on shape
$Ca(OH)_2$	[135, 136]	$CaCl_2$	NaOH	Crystallization kinetics
Phosphate				
$CaClH_2PO_4$	[105]	$CaCl_2$	H_3PO_4	Process design for PO_4 recovery
$CaHPO_4$	[137]	$Ca(NO_3)_2$	K_3PO_4	Effect of additives on size/shape
$MgHPO_4$	[138, 139]	$MgCl_2$	NaH_2PO_4	FB reactor for phosphate removal
$MgHPO_4$	[140]	$MgSO_4$	$NH_4H_2PO_4$	Effect of pH on product solid phase
Sulfate				
$BaSO_4$	[79]	$BaCl_2$	Na_2SO_4	Process optimization
$BaSO_4$	[114]	$BaCl_2$	Na_2SO_4	Effect of mixing on CSD
$BaSO_4$	[83]	$BaCl_2$	Na_2SO_4	Effect of ultrasound on nucleation

659

660   Examples of organic ionic products from reactive crystallizations include calcium[141] and

661   magnesium[142] carboxylates, amines with carboxylic acid anions,[80] and amphoteric molecules

25

662   such as amino acids.[143] Together these reactions are termed neutralizations because they remove

663   acids or bases from solution. They are highly pH-dependent as many species only possess the

664   required charge in a specific pH range. Some neutralizations are fermentation-based where the

665   primary reactant is glucose, although many other nutrients are needed by the fermenting

666   microbes. The motivation for each of the cited works on organic ionic reactions is different, and

667   ranges from demonstration of continuous reactive crystallization in a chemical plant[144] to yield

668   enhancement by product sequestration[145] to crystal size optimization.[146] Applications of organic

669   ionic reactive crystallizations include pharmaceutical development, carbon capture, and

670   production of chemicals from renewable platforms.

671   Specially tailored amines are used to remove carboxylates or other anions selectively

672   from solution. Custelcean et al.[147] engineered a m-benzene-(bis-iminoguanidine) (m-BBIG)

673   anion for crystallization of an amino-carbonate salt for direct air capture and sequestration of

674   carbon dioxide. A much different application was described by Sturm et al.[148] who used

675   diphenylamine to crystallize the pharmaceutical compound cefdinir from a solution of impurities.

676   In addition to carboxylates, specialty amines can be used in reactively crystallizing other highly

677   soluble anions. Custelcean et al.[149] synthesized urea functionalized amines to remove sulfate

678   from a nuclear-waste simulant and examined the competition between accelerated reaction

679   kinetics and increased solubility as the system temperature is increased. In these cases,

680   engineered amines were used to remove specific anions by reactive crystallization,

681   Amines can also be removed from solution through reactive crystallization. However,

682   unlike the cases for carboxylic acids, simple ammonium salts tend to have high solubility,[150]

683   which means complex anions are needed to form salts with low solubility. Aakeroy et al.[151]

684   screened 105 potential reactive crystallizations of amines with carboxylates and found 30

685   combinations in which crystal products resulted, although the kinetics of these reactions and the

686   possible role of solvent evaporation are unclear. Quon et al.[80] developed a continuous approach

687   to crystallize the amine drug aliskiren as the hemifumarate salt. Cole et al.[152] produced the amine

688   drug prexasertib as the lactate salt. While many amines are crystallizable as carboxylate salts, the

689   applications are mostly limited to specialty and pharmaceutical chemicals produced in low

690   volumes. General guidance for producing solid amines takes advantage of the reduced solubility

691   of the free amine compared to their salts,[150] reacting the amine salt with a hydroxide to

692   crystallize the free amine.

26

693   Reactive crystallization may be used to control the pH in a fermenter, as in the synthesis

694   of carboxylic acids such as citric, lactic, gluconic, and itaconic acids. Synthesis of the acids

695   decreases the pH in the fermenter, and at high concentration can halt the fermentation. Addition

696   of a neutralizing base such as one of the calcium compounds $Ca(OH)_2$, CaO, or $CaCO_3$ stabilizes

697   pH and causes many carboxylic acids to crystallize as calcium salts,[153] which may further benefit

698   the fermentation by sequestering inhibitory products.[154] Magnesium compounds are also used,

699   but to a lesser extent.[155] Reactive crystallization with a calcium neutralizing agent is not always

700   the most economical approach to separating carboxylic acids[153, 156].

701   Figure 4 illustrates several alternative operating procedures for reactive crystallization in

702   the production of carboxylic acids. Line AB′ represents neutralization with a calcium compound

703   that produces a saturated solution at B′ while Line AB represents neutralization with a soluble

704   base such as sodium hydroxide. The need for neutralization can be avoided by engineering acid-

705   tolerant strains of the fermenting microorganism, in which case the operating line of the

706   fermentations may be represented by Line AC.[157]
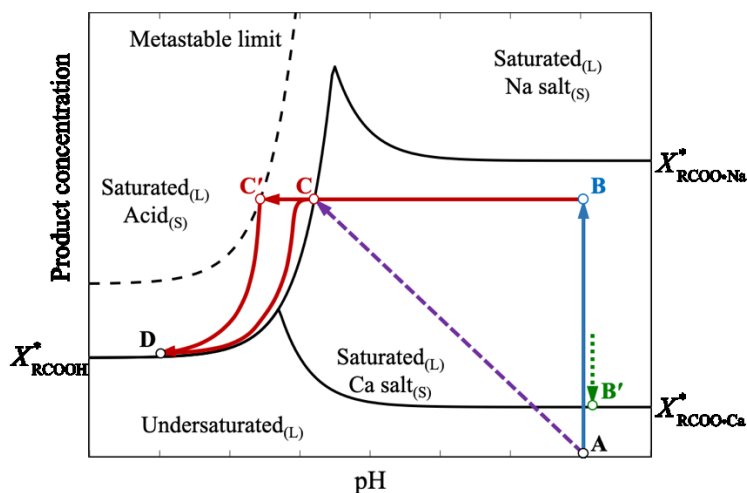
707

708   *Figure 4. Concentration of product species in the fermentation broth as a function of broth pH for*
709   *metastability, saturation, and process operating lines for the reactive crystallization of an organic acid produced by*
710   *fermentation. Black solid curves are solubilities; the black dashed curve is a metastable limit. Line AB represents*
711   *fermentation at constant pH with neutralization by NaOH. Line AB' represents fermentation with neutralization by*
712   *Ca(OH)₂. Line BC represents acidification of solution with mineral acid. Curve CD follows the product solubility as*
713   *it is crystallized. Line AC follows fermentation using an acid-tolerant microorganism. Point C' represents conditions*
714   *at which unseeded crystallization is initiated.*

715   Changes in solubility with pH often are exploited to isolate carboxylic acids. For

716   example, after microbial production by fermentation, cinnamic acid,[158] furan dicarboxylic

717   acid,[159] and fumaric acid[160] is recovered by lowering the pH of the fermentation broth. Paths of

27

718 acidification are illustrated in Figure 4, which represent a case in which either seed crystals are

719 added to initiate nucleation (curve BCD) or primary nucleation at the metastable limit is

720 followed (curve BC′D). Acidification after fermentation and continuous neutralization with Ca^{2+}

721 are two competing methods to isolate the product acid from a fermentation broth. The same

722 process is used to isolate amino acids, although amino acids with multiple acid and base moieties

723 have more complex solubility curves than shown for the monoprotic acid in Figure 4.[161]

724   The inverse of acidification, deprotonation of an amine by a strong base, is also feasible.

725 However, there are fewer studies of these systems as solid amines are typically limited to

726 specialty chemicals and pharmaceuticals. For example, Diab et al.[162] optimized the continuous

727 production of nevirapine with a final reactive crystallization step between sodium hydroxide and

728 nevirapine hydrochloride.

729   Acidification of an organic acid by a strong mineral acid is at the boundary between ionic

730 and covalent reactions; the product itself is covalent (e.g. RCOOH), but the reactants are ionic

731 (e.g. $RCOO^- + H^+$), and the reaction kinetics are fast ($\sim 10^{10}$ mol/sec), which is why acidification

732 is discussed in this section. The organic acid, after receiving a proton from the dissociated strong

733 acid, crystallizes from solution, as exemplified by the chemical equation

734       $$6\text{-APA}^- + \text{HCl} \rightarrow 6\text{-APAH}_{(s)} + \text{Cl}^- \tag{22}$$

735   Typically, though not always, the neutral form of organic acids (or bases) tends to be less

736 soluble than the negatively (or positively) charged deprotonated (or protonated) form in aqueous

737 solution. Ferreira et al.[163] exploit this feature to produce the beta-lactam antibiotic precursor 6-

738 aminopenicillanic acid (6-APA). 6-APA is produced enzymatically from penicillin G at neutral

739 pH where it exists primarily in a soluble, dissociated state. After complete conversion of

740 penicillin G to 6-APA the solution is acidified to the isoelectric point, pH 3, and the zwitterionic

741 6-APA crystallizes.

742   McDonald et al.[17] used the extremely fast kinetics of acid/base reactions to study

743 crystallization kinetics in the reactive crystallization of cephalexin. Cephalexin, which can be

744 produced by a slow enzymatic reactive crystallization,[164] was instead crystallized by reacting

745 HCl with a solution of cephalexin sodium. The reaction is mass-transfer controlled and, with

746 sufficient agitation, can be considered instantaneous. By adding the reactants of the enzymatic

747 system to the cephalexin sodium solution, cephalexin nucleation and growth could be studied in

28

748   a manner representative of the enzymatic process without needing to deconvolute the enzyme

749   reaction kinetics and crystallization kinetics.

750   Table 2 lists reactive crystallizations involving organic acids and bases and their salts.

751   The diversity of listed compounds is much greater than was the case for inorganic reactive

752   crystallizations. The cited studies are also more wide ranging as these species tend not to be the

753   model compounds used to study phenomena but are industrial products or intermediates with

754   economic motivators for an intensified process.

755   *Table 2. A list of representative studies on the reactive crystallization of acids and bases in which a species*
756   *is crystallized as a salt or is crystallized as an acid (or base) by acidification with a stronger acid (or base).*

Product	Reference No.	Reactant 1	Reactant 2	Focus
Organic Salts				
Aliskiren hemifumarate	80	Aliskiren free base	Fumaric acid	Optimization of purity and yield
Aliskiren hemifumarate	144	Aliskiren free base	Fumaric acid	Control of crystallization in an integrated continuous plant
Amino acid bicarbonates	143	K and Na salts of amino acids	CO_2	Found enhanced carbon capture using precipitating CO2 absorbing solvents
m-BBIG carbonate	147	*m*-BBIG (see text for abbr.)	CO_2	Improved ligand for reversible crystallization for CO2 direct air capture
Sodium cefuroxime	146, 165	Cefuroxime	Sodium acetate	Control of mixing and particle size distribution, stability of product
Ca citrate	166	Citric acid	CaO	Large amount of gypsum byproduct, from *A. niger* fermentation
Ca gluconate	167	Glucose	$Ca(OH)_2$, $CaCO_3$	Crystallization during fermentation in *A. niger* inhibits oxygen transfer
Mg 6-hydroxynicotinate	168	Nicotinic acid	MgO	Hydroxylated by *A. xylosoxidans*. Improved yield
Ca lactate	145	Glucose	$Ca(OH)_2$	*B. coagulans* fermentation. 75% yield increase, 1.7x productivity increase
Mg lactate	142	Glucose	MgO	Reduction in water use by 40% and nutrient use by 43%
Ca malate	169	Ca fumarate		Used overexpressed fumarase, better kinetics with solubilized Ca fumarate
Ca malonate	141	Glucose	$Ca(OH)_2$	Fermentation with *P. kudriavzevii*
1-PEA DPPA salt	170	*i*PA-DPPA	Acetophenone	Conversion increase from 19% to 91% by shifting equilibrium (see text for abbreviations)
Pyridinium salts	151	2-aminopyridine derivative	Carboxylic acids	Screening for new salts and cocrystals. 105 pyridine/carboxylate pairs tested
Ca succinate	171	Glucose	$Ca(OH)_2$	Review of several fermentation technologies
NH4 succinate	155	Glucose	Ammonia	Future directions discussed, enhanced regeneration (succinate back to succinic acid) with ammonium salt.
TREN-tris-urea sulfate	149	1,1′,1″-(nitrilotris(ethane-2,1-diyl))tris(3-(pyridin-3-yl)urea	Na_2SO_4	Sulfate recovery from nuclear waste by crystallization with engineered ligands, kinetic and equilibrium study
Acids/Bases				
6-amino-penicillanic acid	163	6-APA NH4 salt	HCl	Growth and solubility in presence of precursor and byproduct

Amoxicillin trihydrate	172	Amoxicillin hydrochloride	NaOH	Nucleation and growth in the presence of impurities
Ampicillin trihydrate	173	Ampicillin sodium	HCl	Monitoring with online PAT
BACE inhibitor	92	BACE inhibitor hydrochloride	NaOH	Purification, control of particle size, control of fouling
Cefixime trihydrate	174	Cefixime disodium	HCl	Control of crystal morphology in a mixing limited reaction
Cephalexin monohydrate	17	Cephalexin sodium	HCl	Nucleation and growth in the presence of precursor molecules
Cinnamic acid	175	Sodium cinnamate	HCl	Templating agents reduce induction time
Ciprofloxacin	176	Ciprofloxacin sodium	HCl	Continuous process in flow
Fumaric acid	160	Glucose	Na_2CO_3, H_2SO_4	Optimize of fermenter neutralization to compete with benzene route
Fumaric acid	157	Glucose Starch	KOH	Review with optimization of feedstocks and organism engineering
Furan dicarboxylic acid	159	Hydroxymethyl furancarboxylate	O_2, H_2SO_4	Recovery of terephthalic acid alternative from *P. putida* fermenter
Glutamic acid	79	Monosodium glutamate	HCl	Continuous manufacturing, control of size and productivity
Glutamic acid	177, 178	Monosodium glutamate	H_2SO_4	Modeling, control, and parameter estimation
Glutamic acid	179, 180	Monosodium glutamate	H_2SO_4	Control of reactive crystallization
p-Hydroxybenzoic acid	158	*p*-Hydroxy-benzoate	HCl	Electrochemically induced crystallization by manipulation of local pH
Itaconic acid	181	Glucose	NaOH, HCl	Fermentation by *A. terreus*. Inhibition overcome by product removal
Malic acid	182	Fumaric acid	H_2SO_4	Fumarase in *S. cerevisiae* as catalyst. Continuous process with electro-dialysis. Yield up from 78% to 91%
Nevirapine	162	Nevirapine hydrochloride	NaOH	Continuous manufacturing, including reactive crystallization, of API
Riboflavin	183	Glucose	NaOH	Review of riboflavin fermentation processes

757

758   ***Crystallization and Covalent Reactions.*** Covalent reactions are inherently more complex

759   than ionic reactions; the bonding moieties tend to be bulky with a variety of characteristics

760   (polarity, hydrophobicity, size, etc.) playing a role in the nature and strength of bonds formed.

761   This section addresses that complexity by dividing covalent systems into three broad categories:

762   non-catalytic, catalytic, and biocatalytic reactions. Lastly, reactive crystallization for chiral

763   resolution, an application with enormous industrial importance and unique operating

764   considerations, is discussed.

765   Dividing covalent reactive crystallization according to the use and nature of catalysts

766   assists in comparing the different process conditions each reaction type requires. Uncatalyzed

767   reactive crystallization is accomplished by controlling only the reactant concentrations and

768   crystallizer conditions (e.g. solvent composition, temperature, etc.). However, catalyzed

769　processes can be adjusted with variation of catalyst properties and loading. Reactive

770　crystallization utilizing traditional metal catalysts may have wider operating ranges than

771　uncatalyzed processes as the catalyst helps decouple reaction rates from important crystallization

772　conditions, such as temperature and solvent composition. Biocatalytic processes are constrained

773　by limited biocatalyst stability, but reactive crystallization is often applied to biocatalytic

774　processes as a means of overcoming other catalyst deficiencies, for example poor selectivity.[184]

775　Chiral resolution by reactive crystallization may be accomplished with any of the listed catalytic

776　strategies provided the reaction, which racemizes the enantiomers, is much faster than the

777　crystallization and prevents nucleation of the undesired form. Chiral resolution is given its own

778　section because of this unusual (in the context of the other examples) operating requirement and

779　industrial importance. Reactive crystallization enables chiral resolution by diastereomeric

780　resolution,[185] preferential crystallization,[186] enantiomeric enrichment,[89] and attrition enhanced

781　deracemization.[187]

782　　　　*Uncatalyzed covalent reactive crystallization.* The literature has relatively few examples

783　of covalent reactive crystallizations that do not use a catalyst. However, one prominent class

784　involves synthesis of amides by coupling amines with acid chlorides.[84, 122, 188] The amines and

785　acid chlorides often have higher solubility than the resulting amides, making these products good

786　candidates for reactive crystallization. Liu *et al.*[122] used a fed-batch system as the rate of reactant

787　addition provided adequate control over the rate of reaction and rate of generation of

788　supersaturation. As is typical of most crystallization processes, decreased supersaturation

789　suppressed nucleation and increased mean crystal size. Covalent reactions typically cannot be

790　considered instantaneous, and their rate is a strong function of temperature. In the system studied

791　by Liu *et al.*,[122] raising the temperature was shown to have a stronger effect on increasing

792　product solubility compared to the impact on reaction rate; the outcome was an overall lower

793　supersaturation at higher process temperatures and, concomitantly, larger mean crystal size.

794　While this result is important to note, the competition between increasing reaction rate and

795　solubility with temperature is system-specific and results from a single system cannot be used to

796　predict the outcome for other chemistries.

797　　　　As another example of uncatalyzed covalent reactive crystallization, Jiang and Ni[189]

798　studied the synthesis of paracetamol from 4-aminophenol and acetic anhydride. The same

799　authors investigated several different types of reactors, including batch and continuous

800   oscillating-baffle reactors and concluded that combining reaction and crystallization improved

801   yield by limiting the extent of further paracetamol reactions.[190] It was also found that the growth

802   mechanism for paracetamol was different in an aqueous solvent from that in a predominately

803   acetic acid solvent. Crystal shape also depended on the solvent composition, in qualitative

804   agreement with the observed change in growth kinetics.

805   Reactive crystallization can provide a framework to understand biological assembly,

806   supporting a means for chemical selection and evolution. For example, the assembly of peptide-

807   like polymers into paracrystalline assemblies is driven by uncatalyzed polycondensation

808   reactions. Thioesters of racemic amino acids undergo polymerization and then beta-sheet

809   assembly, providing a selection for isotactic peptides.[191] In a more recent study, peptide aldehyde

810   monomers first polymerize, driving a liquid-liquid phase separation from which beta-sheet

811   crystals nucleate and grow. The resulting peptides are highly monodisperse, supporting a

812   secondary nucleation mechanism for templated polymerization.[192]

813   It is difficult to adjust the rate of reaction independent of the rate of crystal growth in

814   uncatalyzed reactive crystallizations; both are sensitive to temperature, composition, and

815   concentration. While the lack of a catalyst makes the process simpler, it may complicate

816   production of a specified size, shape, and form of crystal if the reaction rate cannot be adequately

817   controlled.

818   *Inorganic catalyzed covalent reactive crystallization.* Combining catalysis with reactive

819   crystallization results in complex but useful processes. For example, hydrogenolysis is a

820   commonly encountered reaction that takes place on metal catalysts. Hansen *et al.*[92] published a

821   workup of a BACE (beta-site amyloid precursor protein cleaving enzyme) inhibitor, with

822   potential as an anti-Alzheimer's drug, involving hydrogenolysis of a precursor by hydrogen gas

823   in an aqueous environment with a palladium-on-carbon catalyst. The API (active pharmaceutical

824   ingredient) crystallized in the reaction environment, which made reclaiming the solid catalyst

825   difficult. Rather than pursue a solid-solid separation, acid was added to the reaction solvent to

826   increase the API solubility and allow the catalyst to be filtered off. After catalyst recovery the

827   API was deprotonated by reaction with sodium hydroxide and crystallized based on the

828   acidification mechanism described in the ionic reaction section.

829   Reactive crystallization to produce terephthalic acid (TPA), a precursor to the ubiquitous

830   polymer polyethylene terephthalate, by oxidizing *p*-xylene can improve the impurity profile of

32

831   the resulting product.[193] Species formed during the oxidation, which is catalyzed by soluble

832   cobalt/manganese catalysts with bromine promoter, are shown in Figure 5. Incomplete oxidation

833   leads to the formation of 4-carboxybenzaldehyde (4-CBA), which can incorporate into the

834   terephthalic acid crystals. Rejection of 4-CBA during crystallization of terephthalic acid is

835   paramount as 4-CBA terminates polymerization. Wang et al.[193] found that 4-CBA was

836   incorporated to a greater extent when the TPA growth rate was faster and seed crystals were not

837   used. They developed a process with slow feed rate and higher temperature to minimize impurity

838   incorporation, while maintaining the same mean crystal size.
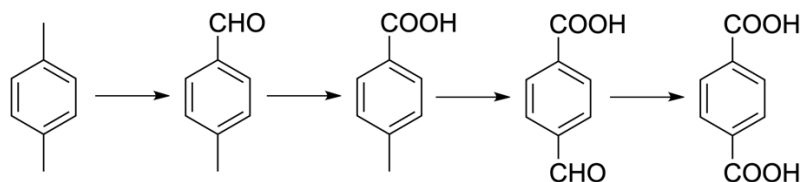
839

840   *Figure 5. Successive oxidation in the conversion of p-xylene (left) to TPA (right). CBA (second from right)*
841   *can incorporate into TPA crystals at high concentration, requiring tuning reaction conditions to prevent buildup of*
842   *CBA while maintaining slow formation of TPA for crystal size control.*

843   *Biocatalytic covalent reactive crystallization.* In this section, biocatalytic reactions are

844   described that crystallize products formed from specific reactants. There has already been some

845   discussion on reactive crystallization as it pertains to fermentation, which can be considered a

846   highly non-selective form of biocatalysis (glucose is converted into a myriad of products). In the

847   biocatalysis community reactive crystallization is sometimes referred to as *in situ* product

848   crystallization, ISPC (a subset of *in situ* product removal, ISPR). Hulsewede et al.[194] provide a

849   minireview on ISPC; here ISPC is discussed in the general framework of reactive crystallization.

850   Biocatalytic processes are well-positioned to benefit from reactive crystallization. Many

851   biocatalysts, such as whole live cells, are poisoned by high concentrations of products, which can

852   be reduced by reactive crystallization.[195] Other biocatalysts, such as resting or whole dead cells,

853   may catalyze undesired reactions with the desired product as reactant, but utilization of reactive

854   crystallization can insulate that product from further reaction.[196] Purified enzymes, while highly

855   specific and more resistant to poisoning, often catalyze reactions with equilibrium coefficients on

856   the order of unity leading to low yields; reactive crystallization can shift equilibrium towards

857   products.[197]

858   Synthesis of beta-lactam antibiotics is a well-studied example of a biocatalytic reactive

859   crystallization. Ferreira et al.[198] have demonstrated good recyclability of an immobilized

860   penicillin G acylase (PGA) for production of ampicillin in saturating conditions. The three main

861   reactions catalyzed by PGA are shown in Figure 6 for ampicillin; they are synthesis (desired,

862   top), reactant hydrolysis (undesired, left), and product hydrolysis (undesired, right). Using PGA

863   entrapped in agarose gel particles afforded only slight mass transfer resistance in the catalyst

864   particle.[198] After some time, the solution saturated and ampicillin crystallized because the

865   reactants, phenylglycine methyl ester (PGME) and 6-APA, are both more soluble than ampicillin

866   on a molar basis. Once again, the crystallization made reclaiming the catalyst difficult and so the

867   product was dissolved after filtration, leaving behind the immobilized enzyme for recycling.

868   Another study used a soluble version of the same enzyme to increase the selectivity towards

869   ampicillin by >50% by sequestering the product from enzymatic hydrolysis by crystallization.[4]
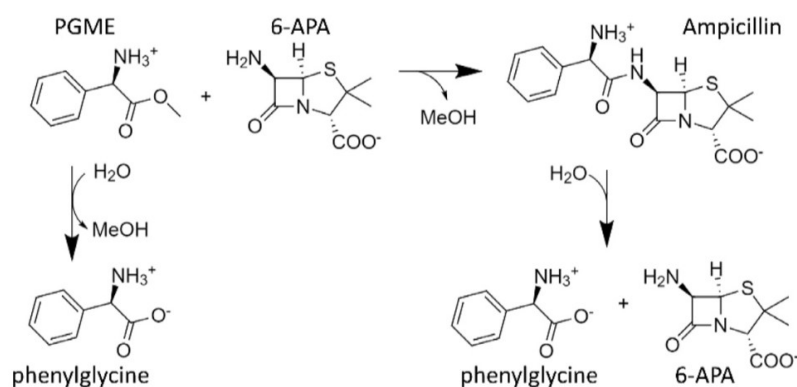
870

871 *Figure 6. PGA-catalyzed synthesis of ampicillin (desired, top), hydrolysis of phenylglycine methyl ester,*
872 *PGME (undesired, left), and hydrolysis of ampicillin (undesired, right).*

873   The value of the biocatalyst (relative to the value of the product) often dictates whether

874   the catalyst is immobilized on a solid, which enables catalyst recovery and reuse, or is soluble,

875   enabling product recovery by filtration. In the case of ampicillin, the product is less valuable than

876   the enzyme, which must be recycled repeatedly for economic sustainability; since solid-solid

877   separations are difficult, the product crystals may be re-dissolved to enable recovery of the

878   enzyme in solid form.[198] With the simplified recovery of a solid biocatalyst comes the challenge

879   of catalyst engineering: choosing a particle size and material to avoid mass-transfer limitations

880   and efficiently utilize the active material, for example PGA in Figure 6.[184] When catalyst

881   recovery is a nonissue, and trace catalyst does not impact downstream quality, e.g. heavy metal

882   toxicity, a reactive crystallization with a dissolved catalyst may be preferable.

883   Recently, a biocatalytic process with reactive crystallization to produce the HIV drug

884   islatravir has been described.[199] The reactive crystallization involves four dissolved enzymes.

885   The three final reactions to islatravir are reversible, so crystallization helps shift the equilibrium

886   towards the product, and the fourth enzyme catalyzes a reaction to consume a byproduct and

887   further improve the yield of islatravir (see Figure 7). The high value of the product favors its

888   recovery by filtration and use of fresh enzyme for each batch. Upstream of the reactions shown

889   in Figure 7 product recovery by filtration is not favorable, and five immobilized enzymes are

890   used. The starting solution for the reactive crystallization is the filtrate from the reactions

891   catalyzed with immobilized enzyme. The relative harmlessness of enzymes (compared to heavy

892   metals) and the value of the reaction products favor reactive crystallization processes.

893   Furthermore, the strong specificity of enzymes enables coupling many reactions to transform

894   soluble reactants to the desired insoluble product. A more recent study of the same system used

895   crystallization of the byproduct (previously consumed by the fourth enzyme) as a calcium salt to

896   drive the reaction further; the improvement in reaction yield (82% versus 76%) outweighed the

897   difficulty of recrystallization.[200]
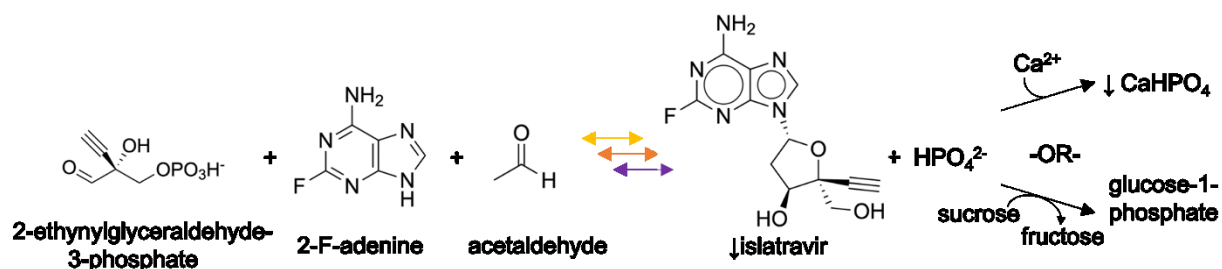
898

899   *Figure 7. Enzymatic synthesis of islatravir by three enzymes in a single vessel from an alkyne precursor*
900   *(also produced enzymatically). Islatravir crystallization helps drive the reaction to the right; consumption of the*
901   *phosphate byproduct by (top) reaction with calcium and crystallization of calcium phosphate or (bottom) enzymatic*
902   *reaction with sucrose pulls the reaction further towards the product. Adapted from Huffman et al.[199]*

903   Many chemistries that do not seem plausible with biocatalytic processes could be

904   implemented with biocatalytic reactive crystallization. For example, equilibrium favors removal

905   of CO_2 from carboxylic acids, not carboxylation by addition of CO_2. However, Ren *et al.*[201]

906   overcame the unfavorable reaction equilibrium when they carboxylated phenols with a

907   decarboxylase enzyme (which, as the name suggests, typically catalyzes removal of CO_2) by

908   crystallizing the products as quaternary ammonium salts, improving the yield from 40% to 97%.

909   Table 3 lists several examples of the three types of covalent reactive crystallizations

910   discussed, non-catalytic, catalytic, and biocatalytic. The product, reactants, and focus of the

911   study are listed for each entry in Table 3. The focuses are varied, reflecting the wide-ranging

912   applications of covalent reactive crystallization.

913   *Table 3. A list of representative studies on covalent reactive crystallization processes, divided based on*
914   *catalyst usage and type.*

Product	Reference No.	Reactant 1	Reactant 2	Focus
Uncatalyzed				
Paracetamol	[189]	4-aminophenol	Acetic anhydride	Impurity content, crystal shape, growth and nucleation kinetics
Paracetamol	[190]	4-aminophenol	Acetic anhydride	Continuous oscillating baffled reactor
2,4,6-triamino-1,3,5-trinitro-benzene	[122]	2,4,6-trichloro-1,3,5-trinitro-benzene	Ammonia	Gas, liquid, solid phase. Effect of feed rate and temperature on particle size in bubble column reactor
Dithiocarbamate (DTC)	[88]	DTC-precursor	Formaldehyde	Narrow CSD, avoid oiling out and spherulites, optimize productivity
Amides	[84]	Acid chlorides	Amines	Plug flow reactor crystallizer, examined fouling
Inorganic catalyst				
Terephthalic acid (TPA)	[193]	*p*-xylene	Oxygen	Intermediate impurity incorporation, Co/Mn catalyst, Br promoter
TPA	[202]	*p*-xylene	Oxygen	Evaporative cooling of exothermic reaction to avoid fouling
TPA	[203]	*p*-xylene	Oxygen	Two reactive crystallizers in series to eliminate intermediate impurity
BACE inhibitor	[92]	Isoxazidoline derivative	Hydrogen	Difficulty separating Pd/C catalyst from solid product, redissolved
Relebactam	[204]	Carboxybenzyl relebactam	Hydrogen, silylating agent	Pd/C, DABCO then HOAc. *In situ* protect/deprotect with crystallization
Akt kinase inhibitor	[91]	Amine precursor	Methyl phenylacetate	Cs_2CO_3 catalyst, impurity rejection
		Boronate precursor	Chloropyridine derivative	Pd catalyzed Suzuki coupling, enhance yield and selectivity
Hedgehog pathway inhibitor	[93]	Carboxybenzyl protected API	Hydrogen	Solids formed on Pd/C catalyst, form HCl salt instead
Biocatalytic				
Ampicillin	4	6-amino penicillanic acid (6-APA)	Phenylglycine methyl ester (PGME)	Improved enzymatic yield with crystallization
Ampicillin	[173]	6-APA	PGME	Reactive crystallization of product and byproduct, phenylglycine
Ampicillin	[198]	6-APA	PGME	Taylor-Couette flow reactor to suspend slurry with low shear
Ampicillin, Amoxicillin, Cephalexin	[205]	6-APA, 7-amino-desacetoxy-cephalosporanic acid (7-ADCA)	Phenylglycine amide, 4-hydroxy-phenylglycine amide	Used supersaturated reactants for three different pen G acylase catalyzed reactions
Ampicillin	[206]	6-APA	Phenylglycine amide	Fed batch, solid reactants dissolving, solids purity versus conversion
Amoxicillin, Cephalexin	5, 113	6-APA, 7-ADCA	PGME	Continuous reactive crystallization modeling, size, purity, yield
Cephalexin	[207]	6-APA	Phenylglycine nitrile	Complex product with 1,5-dihydroxynaphthalene (reduced sol.)
Islatravir	[199]	2-Ethynyl-glyceraldehyde-3-phosphate	2-F-adenine	Three reactions in series, crystallization pulls equilibrium right
Methyl trans-3-(4-methoxy-phenyl) glycidate	[208]	Racemate		Lipase immobilized on membrane to facilitate enzyme recovery from crystals. Deracemization
Levodione	154, 195	4-oxoisophorone		Reduction by live *S. cerevisiae*, crystallization reduce over-reduction

Nicotinamide	[209]	3-cyano pyridine	water	Avoid overhydration to nicotinic acid by crystallization
Methionine, phenylalanine	[210]	Racemate	Ammonia borane, oxygen	Deracemization
Alanine	[196]	Aspartic acid		Deracemization, whole cell (dead) *Pseudomonas dacunhae* catalyst
2,3- and 2,6-dihydroxybenzoate	[201]	Resorcinol Catechol	$KHCO_3$	Use of quaternary ammonium salts to increase yield from 40% to 97%
Allo-threonine	[211]	threonine		Isomerase reaction, solid reactant and product, constant liquid composition
Z-aspartame	[212]	Carboxybenzyl aspartate	Phenylalanine methyl ester	Two enzymes tested, reaction kinetics
L-Homo-phenylalanine	[213]	2-oxo-4-phenyl-butryic acid	L-aspartate	Fed batch to overcome substrate inhibition
L-phenylglycine	[214]	Phenyl-glyoxylate	L-glutamate	Thermophilic enzyme, crystallization shifted equilibrium to products
Peptides	[215-219]	Amino acid with protected amine	Unprotected amino acid	Improving yield, conversion

915

916   In the carboxylation example by Ren *et al.*[201] the product formed is an organic salt, but it

917   is discussed in the covalent section of this review because the rate-limiting step is the formation

918   of covalent bonds (carboxylation). The kinetics of this process are more representative of those

919   found for other covalent and biocatalytic reactive crystallizations. The same behavior is observed

920   in fermentation with continuous neutralization by calcium hydroxide; the rate-limiting step is not

921   the reaction between carboxylate and neutralizing base, but rather production of the acid by the

922   microorganism. The product, a dissociated acid, is ionic, but the rate-limiting reaction that

923   produced the acid forms covalent bonds. Neutralization in batch at the end of the fermentation

924   may also be practiced, in which case the ionic reaction between Ca^{2+} and the carboxylate is rate-

925   limiting. The use of a second species, such as Ca^{2+} for carboxylates, to form a less-soluble

926   complex with the product is a common application of reactive crystallization.

927   Enzymatic peptide synthesis is thermodynamically unfavorable in aqueous solutions, but

928   reactive crystallization enables even thermodynamically-controlled reactions to achieve high

929   yields, especially when using a second species to promote crystallization. For example, the

930   thermolysin-catalyzed synthesis of the artificial sweetener aspartame (L-asp-L-phe-OMe) is used

931   in a 10,000 ton/year-scale process with 96% yield in the enzymatic step.[220, 221] Carboxybenzyl L-

932   aspartate (Z-asp) is coupled with equimolar L-phenylalanine methyl ester (L-phe-OMe) at

933   neutral pH in purely aqueous solution. The anion generated at neutral pH values, Z-aspartame

934   (Z-asp-L-phe-OMe), forms an insoluble salt with cationic D-phe-OMe, Z-asp-L-phe-OMe·D-

935   phe-OMe. Racemic DL-phe-OMe is employed in 2:1 molar ratio with Z-aspartate such that the

936   L-enantiomer is consumed in the reaction and the D-enantiomer promotes crystallization.

37

937   Eichhorn *et al.*[217] demonstrated that reactive crystallization of thermolysin-catalyzed dipeptide

938   couplings leads to high yields with a wide range of amino acids and their derivatives. In a high-

939   solids medium (only about 10% aqueous solution), at the kilogram scale, mixing limits the

940   reaction rate. In theoretical work on peptide synthesis, Erbeldinger *et al.*[216] and Ulijn *et al.*[215]

941   showed that high yield is the consequence of reactive crystallization and that above a threshold

942   of product solubility, yield switches from low values to values of almost 100%.

943   The work of Hulsewede *et al.*[170] described a nearly 5-fold increase in the yield of 1-

944   phenylethylamine (1-PEA), synthesized by a transaminase enzyme, by reactively crystallizing

945   the 1-PEA. Starting with acetophenone and isopropylammonium-3,3-diphenylpropionate (*i*PA-

946   DPPA), the enzyme transfers the amine group from *i*PA to acetophenone and the resulting 1-

947   PEA crystallized as a salt with DPPA. The crystal product was a salt, but the rate-limiting step is

948   the enzyme-catalyzed covalent reaction. The DPPA was present in stoichiometric quantity

949   throughout the reaction since the *i*PA was fed as the DPPA salt. It was found that low reaction

950   equilibrium (19%) could be overcome by coupling to the favorable crystallization of 1-PEA-

951   DPPA and 92% conversion could be reached. The general process, illustrated in Figure 8, is also

952   applicable to similar chemistries.[222]
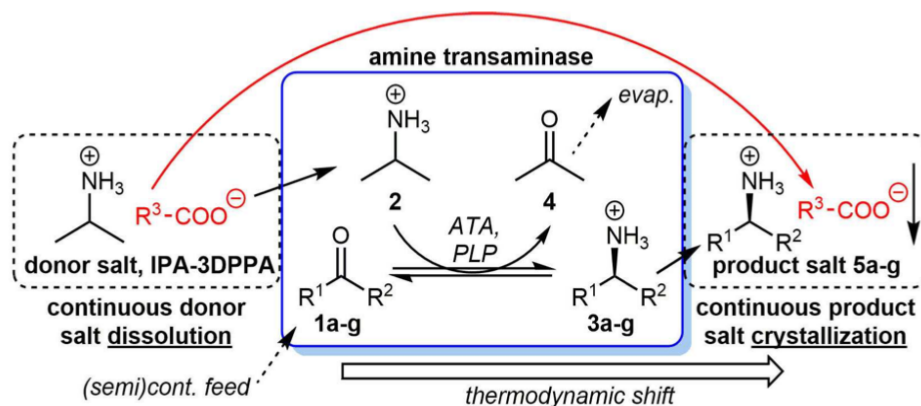
953

954   *Figure 8. Reaction scheme of the amine transaminase (ATA, cofactor pyridoxal phosphate, PLP) catalyzed*
955   *stereoselective amination of a ketone with iPA donor amine. The amine product forms a salt with the anion from the*
956   *amine donor. In the main text, $R_1 = C_6H_5$, $R_2 = CH_3$, and $R_3 = DPPA$. Reprinted with permission from Hulsewede et*
957   *al.[170] copyright 2019, John Wiley and Sons.*

958   Depending on the nature of the interactions between the product and the second species,

959   the resulting crystals may be called salts (coulombic interactions) or cocrystals.[223-225] In the

960   previous example, 1-PEA is crystallized as a salt of DPPA, but numerous examples can be found

961   where the final solid is a cocrystal. As an illustration, the yield of cephalosporin antibiotics can

962   be increased by reactive crystallization with an aromatic species to isolate the antibiotic product,

963   which is an intermediate in an enzymatic cascade. The process has been demonstrated for

964   cefaclor (yield increased from 57% to 80%),[226] cephalexin (42% to 67%),[227] and cephradine

965   (yield not evaluated).[228] Recent published work on cocrystallization has focused on discovery

966   and/or prediction of cocrystal-forming systems,[229, 230] which could make reactive crystallization

967   practical for a wider range of products if co-formers[*] promoting crystallization can be identified

968   for more products. Other applications of cocrystallization include: improved solids handling,[231]

969   solubility,[232] stability,[233] and pharmaceutical activity,[234] Karimi-Jafari et al. reviewed the entire

970   topic.[235]

971   Carbamazepine has been a favorite model compound for cocrystal research and is the

972   only compound for which cocrystallization kinetics have been published. Gagniere et al.[236]

973   qualitatively examined the rates of cocrystallization in the carbamazepine-nicotinamide system

974   while Rodriguez-Hornedo et al.[237] used Raman spectroscopy to monitor the nucleation and

975   growth of carbamazepine-nicotinamide from a slurry of the individual solids. Kudo and

976   Takiyama[238] have worked out much of the thermodynamics of reactive cocrystallization in the

977   carbamazepine-saccharin system. Each of these studies highlights the difficulties designing

978   reactive crystallizations with multiple small molecules, namely complex phase diagrams with at

979   least three solids (more with chiral compounds and if cocrystals with several stoichiometries

980   exist) and uncertain driving forces for complexation.

981   *Chiral Resolution.* Enantiomers are prevalent in pharmaceutically active compounds,

982   with one enantiomer typically being responsible for clinical activity and, in some cases, the

983   mirror compound having deleterious effects. Both left and right enantiomers have the same

984   solubility, vapor pressure, partition coefficients, etc. (in achiral solvents), making their separation

985   by traditional methods very difficult. Many non-biological reactions are agnostic of chirality, the

986   products are racemic mixtures that, by definition, contain equal amounts of the two enantiomers.

987   Producing a compound with a single chirality often involves a deracemization step. Provided a

988   racemizing reaction (a reversible reaction interconverting the two enantiomers) occurs with

---

[*] The FDA defines a co-former (or coformer) as one of the two different molecules in the same crystal lattice, forming a co-crystal. More information can be found at https://www.fda.gov/media/81824/download

39

989   appreciable speed, the left- and right-hand enantiomers (S and R) will exist in a 1:1 ratio in

990   solution, irrespective of removal of one of the enantiomers from solution by crystallization.

991   Conglomerate-forming systems are ones in which each of the two enantiomers form

992   enantiomerically pure crystals that may be produced as a physical mixture if crystallized

993   together. Racemate-forming systems produce crystals in a single lattice structure with a 1:1 ratio

994   of the two enantiomers. Conglomerate-forming systems are more amenable to resolution by

995   reactive crystallization, and are estimated to comprise 5-20% of all enantiomeric systems with

996   racemates making up the remainder.[239, 240] Reviews of several techniques for enhancing

997   enantiomeric purity, some involving reactive crystallization, are provided by Lorenz and Seidel-

998   Morgenstern,[241] Palmans,[242] and Brands and Davies.[185] In the following discussion, special

999   emphasis is given to a class of covalent reactive crystallizations used to recover enantiomerically

1000   pure products.

1001   Crystallization can result in deracemization in four ways: (1) by formation of a

1002   diastereomeric salt with a chiral resolving agent, (2) by preferential crystallization, (3) by

1003   selectively subjecting the undesired enantiomer to racemization with an asymmetric reaction,

1004   thereby enriching the solution in the preferred enantiomer and facilitating its crystallization, and

1005   (4) by attrition-enhanced deracemization of conglomerate-forming enantiomers.

1006   Diastereomeric resolution, or crystallization with a resolving agent, sometimes referred to

1007   as "classical resolution," takes advantage of differences in interactions between two chiral

1008   molecules. In this process, two enantiomers of a single species are reacted with a single

1009   enantiomer of another compound (resolving agent) to form two diastereomers that have different

1010   properties, including solubilities. The two diastereomers may then be separated by crystallizing

1011   the less soluble of the two. The desired free enantiomer is then recovered by reversing the

1012   reaction that formed the diastereomer.

1013   An illustration of diastereomeric resolution is the production of the unnatural amino acid

1014 R-(−)-2-phenylglycine, R-PG, mentioned previously in reference to certain beta-lactam

1015   antibiotics. In the commercial process, a racemic mixture of phenylglycine (RS-PG) is reacted

1016   with (1S)-(+)-camphor-10-sulfonic acid, S-CS, to produce two diastereomeric salts, RS-PG-CS

1017   and SS-PG-CS. The former has a lower aqueous solubility (5.75 g/100 g at 25 °C) than the latter

1018   (>150 g/100g, 25 °C), which facilitates separation.[243] Racemization of RS-PG in the presence of

40

1019　　one equivalent of *S*-CS and half an equivalent of hydrochloric acid (to keep zwitterionic PG from

1020　　crystallizing) leads to greater than 90% yield of *R*-PG from *RS*-PG.

1021　　　　The simultaneous use of multiple resolving agents has been shown to enhance resolution,

1022　　likely by inhibiting nucleation of the undesired diastereomeric salt.[244] Brands and Davies[185] list

1023　　many systems for which diastereomeric salt resolution has proven successful. The utility of this

1024　　method is demonstrated by its use in the production of large quantities of (*S*)-naproxen, (*R*)-

1025　　phenylglycine, and (*R*)-4-hydroxyphenylglycine.[241] Diastereomeric resolution can be used to

1026　　resolve individual enantiomers of conglomerate-forming and racemate-forming compounds.

1027　　Figure 9 represents the resolution of the *S* enantiomer of a conglomerate forming compound by

1028　　addition of resolving agent *S*[†]. The apex represents pure solvent, while the lower left vertex is

1029　　pure *S* or *SS*[†] and the lower right vertex represents pure *R*. Using process analytical technology

1030　　(PAT, discussed further in the process design section) one would observe the solution

1031　　composition following the solid black curve from Point A to Point B, with movement up and to

1032　　the right due to crystallization and movement left due to racemization.
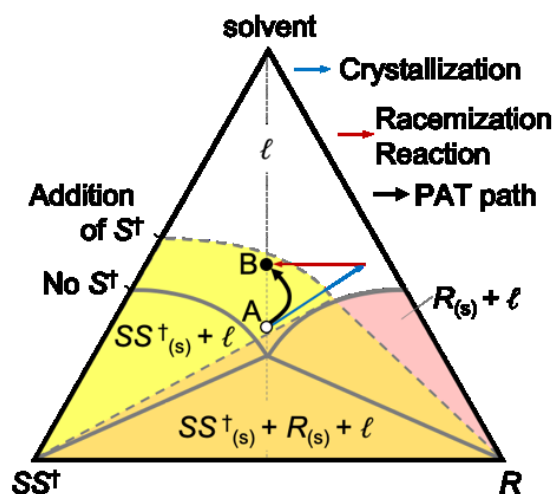
1033

1034　　　　*Figure 9. Isothermal ternary phase diagram for diastereomeric resolution. The phase equilibrium before*
1035　　*addition of the resolving agent is symmetrical, shown by bold gray curves, while after addition the resulting*
1036　　*diastereomer SS[†] phase equilibrium is asymmetric, shown by dashed gray curves, enabling crystallization of only*
1037　　*the desired enantiomer. During the process, the solution moves from Point A (undersaturated) to B upon addition of*
1038　　*S[†] with concurrent racemization in solution.*

1039　　　　Preferential crystallization utilizes the addition of seed crystals to solutions of

1040　　enantiomers in the metastable zone to initiate nucleation and subsequent growth of a single

1041　　enantiomer from a racemic solution. The methodology is useful for conglomerate-forming

1042　　systems. Seed crystals of the desired enantiomer are added, and the supersaturation is held within

1043   the metastable zone. The seed crystals grow and breed new crystals of the desired chirality while

1044   the undesired enantiomer remains in solution; primary nucleation must not occur as it would

1045   initiate crystallization of the undesired enantiomer. Simultaneously subjecting the solution to a

1046   racemization reaction enhances the yield of the seeded species. Yoshioka[245] summarized several

1047   examples of preferential crystallization of amino acids, both proteogenic and unnatural, with

1048   racemization by catalytic salicylaldehyde. Petrusevska-Seeback *et al.* give an example of

1049   combining preferential crystallization with enzymatic racemization .[246] Supersaturation may be

1050   generated by cooling, pH adjustment or other means. Figure 10 shows the preferential

1051   crystallization of *S* by acidification reactive crystallization, where $pH_1 > pH_2 > pH_3$ and the

1052   solubility decreases with decreasing pH value.
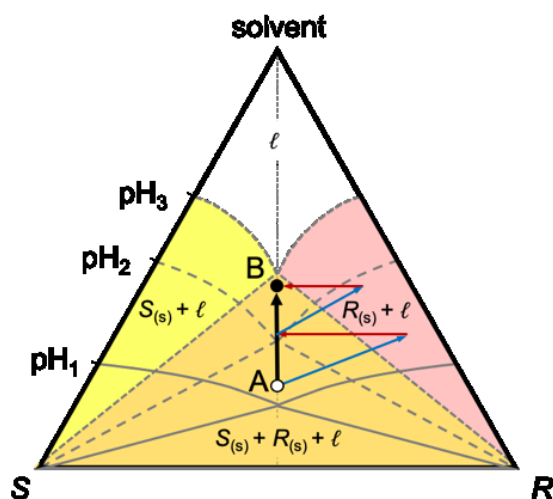
1053

1054   *Figure 10. Ternary phase diagram for preferential crystallization of S by addition of S seed crystals.*
1055   *Supersaturation is generated by decreasing the pH from pH₁ to pH₃ while a racemization reaction converts excess R*
1056   *in solution to restore a 1:1 ratio of R:S in solution. Again, the bold black curve from Point A to Point B represents*
1057   *the solution composition observed by PAT, while the blue arrows represent movement due to crystallization and the*
1058   *red arrows movement due to racemization.*

1059   <u>Enantiomeric enrichment</u> followed by crystallization is especially valuable if an

1060   enantiomerically pure product is to be recovered from a racemate-forming system. Enrichment in

1061   the present context means that the relative proportion of the desired enantiomer in solution is

1062   increased to an extent that crystallization of enriched pure enantiomer is feasible. Enrichment of

1063   a specific enantiomer can be accomplished in several ways. For example, Johnson *et al.*[247] used

1064   an asymmetric palladium catalyst in route to an API, producing the desired enantiomer at a

1065   solution enantiomeric excess of 95%; crystallization was used to upgrade the enantiomeric

1066   excess of the solid to >99%. Encarnacion-Gomez *et al.*[210] used a chemo-enzymatic

1067   stereoinversion reaction system to enrich the concentration of a desired enantiomer to

1068   appropriate concentrations for crystallization of the pure enantiomer. They demonstrated the

1069   process using racemic mixtures of phenylalanine and of methionine and recovered crystals of the

1070   desired pure enantiomer from each system. Harriehausen et al.[248] suggested several process

1071   configurations that combined enantioselective chromatography with enzymatic racemization to

1072   recover pure enantiomer with nearly complete extinction of the undesired enantiomer. Figure 11

1073   shows enantiomeric enrichment in a racemate forming system by reacting R to S followed by

1074   crystallization in a racemate-forming system. The middle cone-shaped region identifies

1075   conditions corresponding to equilibrium between crystals of the racemate and the solution. The

1076   objective of enantiomeric enrichment is to move from the central region to the yellow region,

1077   thereby facilitating crystallization of the desired enantiomer.
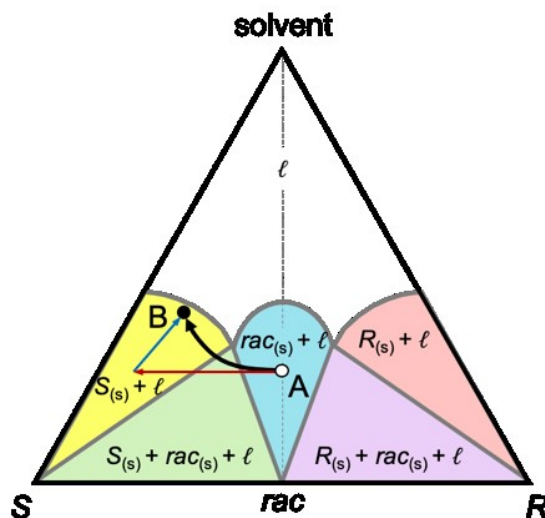
1078

1079   *Figure 11. The ternary phase diagram for enantiomeric enrichment in a racemate-forming system. The*
1080 *enantiomeric enriching reaction occurs under supersaturated conditions, but high conversion ensures only the*
1081 *desired enantiomer is crystallized. Again, the bold black curve from Point A to Point B represents the solution*
1082 *composition observed by PAT, while the blue arrow represents movement due to crystallization and the red arrow*
1083 *movement due to an enantioselective isomerization reaction.*

1084   <u>Attrition-enhanced deracemization</u>, sometimes referred to as "Viedma ripening," was

1085   observed originally by Viedma[249] and explored further by Viedma[250] and Blackmond.[251, 252] The

1086   original observations were on aqueous solutions of sodium chlorate, a species that is achiral in

1087   solution but which, on crystallization, produces chiral crystals. Experiments included seeding

1088   with mixtures of R and S chiral crystals that had been subjected to attrition before being added to

1089   the system and which were subject to continuous attrition by the presence of glass beads that

1090   were added to the stirred system. After stirring for a sufficiently long period, the resulting

43

1091   crystals were found to be enantiomerically pure *R* or *S*. Later work found similar behavior for

1092   conglomerate-forming enantiomers that underwent rapid racemization reactions and, therefore,

1093   maintained the ratio of enantiomers in solution near 1:1. Examples of such systems include: an

1094   amino acid derivative N-(2-methylbenzylidene)-phenylglycine amide;[253] aspartic acid, one of

1095   two conglomerate forming proteogenic amino acids;[250] and an imine that is the key component in

1096   clopidogrel.[254] Spix *et al.*[255] converted the racemate-forming amino acids alanine and

1097   phenylalanine to conglomerate-forming salts alanine 4-chlorobenzene sulfonic acid and

1098   phenylalanine 2,5-xylenesulfonic acid. After deracemization of the salts, the free amino acids

1099   were recovered by neutralizing the salts with alkali.

Reactive Crystallization Process Design

1101   Development of reactive crystallization processes for use at the industrial scale is a

1102   challenging multi-objective problem. The generation of a given product by reactive

1103   crystallization involves simultaneous fundamental thermodynamic and kinetic phenomena,

1104   including reaction, mass transfer, and crystal nucleation and growth, all coupled with the

1105   engineering aspects of reactor design, configuration, control, and product recovery. While each

1106   of these has been well-studied in the literature, decisions for process design, optimization, and

1107   control are often unique to the system of interest.

1108   Reactive crystallization processes generate supersaturation by synthesizing a product

1109   through a reaction, concomitantly increasing the concentration of the product and leading to

1110   crystallization. The rates of the reaction and crystallization steps guide strategies for reactor

1111   design and control. In cases where fixed operating conditions favor both reaction and

1112   crystallization, reactive crystallization can be performed in a single vessel. For example, many of

1113   the ionic reactions mentioned earlier produce a sparingly soluble compound in an instantaneous

1114   reaction and fall into this category. Other cases may require the steps to be temporally or

1115   spatially separated, several configurations of which are illustrated in Figure 12. Temporally

1116   separated processes include well-mixed batch or semi-batch designs in which synthesis reactions

1117   occur, followed by a shift in temperature or pH to promote subsequent crystallization of the

1118   product. Processes that are spatially separated utilize multiple vessels or different segments of a

1119   vessel—first performing the reaction to generate supersaturation and then feeding the mixture

1120   into a second vessel for crystallization. Process intensification in the form of combining both

1121   reaction and crystallization steps into a single vessel is likely to lead to savings in capital and

1122   operating costs as the technology matures,[256, 257] but like many aspects of design problems, the

1123   potential benefit is system-dependent.
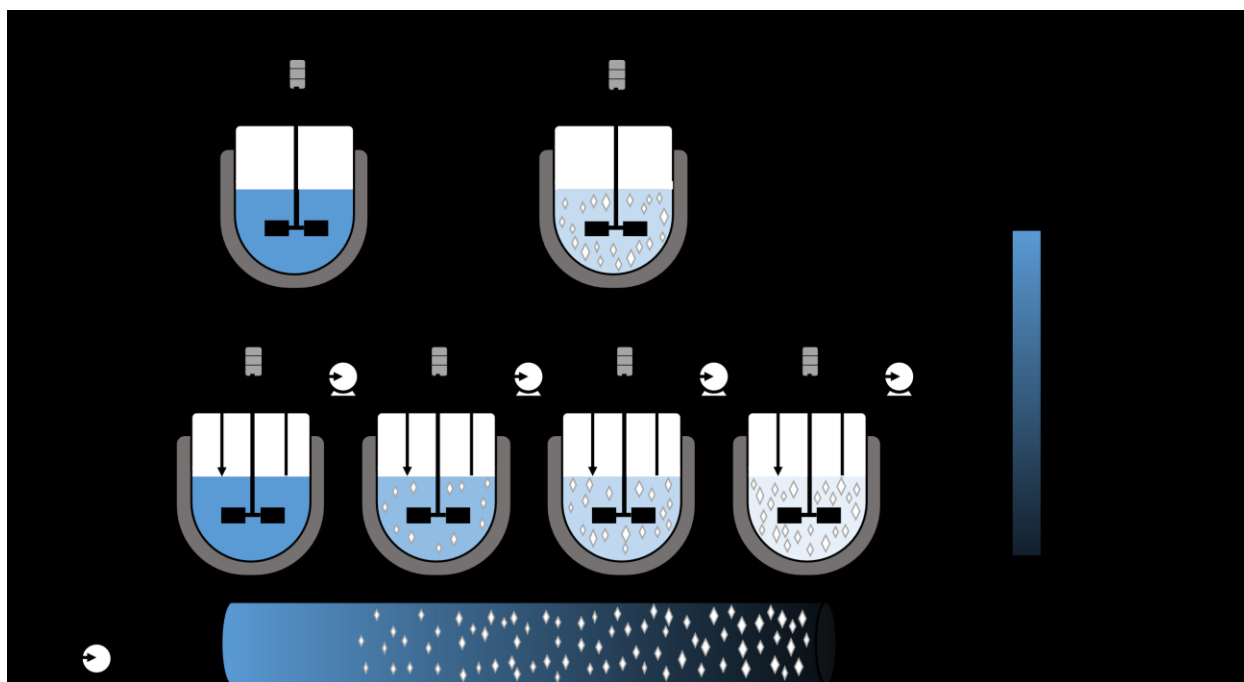
1124

1125   *Figure 12. (a) Temporal separation of reaction and crystallization favoring conditions in a well-mixed*
1126   *batch reactor; (b) Spatial separation of reaction and crystallization favoring conditions in continuous well-mixed*
1127   *reactors (above) and tubular reactors (below).*

1128   Key factors in process design for reactive crystallization include the presence of multiple

1129   components (sometimes with more than one crystallizing), effects of mixing on crystallization

1130   kinetics, the necessity of maintaining mutually beneficial operating conditions for reaction and

1131   crystallization, and the need for producing crystals that can be readily separated from a reaction

1132   slurry. In instances where a heterogeneous catalyst is used to facilitate a desired reaction,

1133   separating the catalyst from product crystals represents an additional challenge. As crystal shape

1134   and size distributions are strongly influenced by supersaturation, process control is also a unique

1135   challenge due to the generation of supersaturation from a reaction rather than by temperature

1136   manipulations, evaporation, or anti-solvent addition. In the following discussion, challenges

1137   unique to reactive crystallization process design and control that focus on the aforementioned

1138   issues are discussed in more detail.

1139   ***Reactor Design.*** Design and implementation of reactive crystallization systems rely

1140   heavily on reaction and crystallization kinetics. A strong distinction between the operation of a

1141   reactive crystallizer and a traditional crystallizer is that reactive crystallization conditions must

45

1142   satisfy *both* the reaction *and* the crystallization. For example, an enzymatic reaction usually

1143   requires benign temperatures (20 to 37 °C), aqueous conditions, and near-neutral pH values. If

1144   these conditions promote crystallization of the desired product, then reaction and crystallization

1145   may be conducted in the same vessel. If the conditions for reaction do not permit crystallization

1146   of the product, then using multiple vessels may need to be investigated. Alternatively, the

1147   conditions within the vessel may be varied over the time course of the reactive crystallization or

1148   across the volume of the reactor (specifically for tubular reactors). For example, Jiang *et al*.[190]

1149   varied the temperature across a tubular reactor to allow for enhanced reaction kinetics in the

1150   upstream section and improved crystallization kinetics in the downstream section.

1151   Configurations of vessels in which reactive crystallizations are conducted usually are

1152   similar to those of non-reactive crystallizers. The perfectly mixed continuous crystallizer, which

1153   is often referred to as a mixed-suspension mixed-product removal (MSMPR) crystallizer,* is an

1154   idealized version of a continuous stirred-tank crystallizer. A similar vessel may serve as a batch

1155   crystallizer with feed added at time zero and product removed at a designated endpoint. In a

1156   semi-batch (or fed-batch) unit, one or more feed streams is added during the course of a run and

1157   product removed at the designated endpoint. More details on these generic configurations, which

1158   often have to do with mixing, are available in general references on industrial crystallization.[36,

1159   258]

1160   Most applications of reactive crystallization described in the literature focus on batch or

1161   semi-batch systems. While these are often relatively simple to design and operate, continuous

1162   reactive crystallization processes offer several benefits. Advantages of continuous systems have

1163   been outlined specifically for pharmaceuticals manufacturing by Lee *et al*.[259] and Acevedo *et*

1164   *al*.[260] Some of these benefits include higher process capacity and productivity, more efficient use

1165   of raw materials and energy, production of fewer intermediate compounds, and more robust

1166   control. The design and use of various arrangements of reactive crystallization equipment for

1167   batch, semi-batch and continuous operation are covered in the following discussion.

---

* The MSMPR crystallizer is a useful model for continuous stirred-tank crystallizers. The assumptions of perfect mixing and uniformity of residence time distributions of solvent and crystals of all sizes are approximations often approached in actual systems.

1168　　　　*Batch and semi-batch systems.* The use of a batch reactor allows for adjustment of

1169　　process parameters during the time course of the reactive crystallization, such as decreasing the

1170　　temperature or adjusting the pH value towards the end of a batch so as to crystallize more

1171　　product and increase the overall process yield. For example, in the enzymatic synthesis of beta-

1172　　lactam antibiotics shown in Figure 6, the solution pH value typically decreases as the reaction

1173　　progresses due to the formation of acidic products. The lower pH value further decreases the

1174　　solubility of the product, improving product crystallization and yield.[4, 261]

1175　　　　Batch and semi-batch reactive crystallization processes are operated in well-mixed

1176　　reactors that allow for implementation of on-line PATs, are robust, and are more resistant to

1177　　clogging and encrustation issues than tubular reactors. Also, these well-mixed reactors are often

1178　　highly modular, allowing for the inclusion of baffles, a draft tube,[262] or different impeller types

1179　　to enhance mixing.[263] Cao *et al.*[85] used an airloop-lift reactor (ALR) to improve mixing for the

1180　　batch reactive crystallization of $Ni(OH)_2$ over traditional impeller stirring. Another alternative to

1181　　traditional impeller-stirred reactors is the Taylor-Couette reactor used by Ferreira *et al.*,[198] which

1182　　uses a combination of inner rotating and outer stationary cylinders to gently mix the slurry of

1183　　crystals and catalyst particles in the region between the cylinders (Figure 13). The design is used

1184　　to protect the catalyst particles, which are susceptible to the shear stress induced by an impeller

1185　　in a conventionally mixed reactor. Often, traditional impeller stirring may be adequate for a

1186　　system, but for very fast reactions, the various parameters involving mixing and reactant addition

1187　　rate or novel techniques of mixing may need to be investigated to achieve a desirable crystal size

1188　　distribution.

1189　　　　In the case of fast reactions in semi-batch systems, mixing and the method and rate of

1190　　reactant addition significantly impacts the product size distribution. Åslund and Rasmuson[264]

1191　　studied the effect of stirring rate, impeller type, reactant concentration, reactant feed rate, and

1192　　feed position (e.g. surface level, bulk liquid, next to impeller feeds) on the size distribution of

1193　　benzoic acid crystals formed via reactive crystallization. The rate of addition of the reactant

1194　　hydrochloric acid, reactant concentration, and stirring rate significantly influenced the product

1195　　size distribution. As the stirring rate was increased, the size of resulting crystals increased up to a

1196　　maximum where crystal size began to decrease; the type of impeller and feed position had a

1197　　lesser effect on the product size distribution, especially at higher stirring rates. Chen *et al.*[114]

1198　　investigated mixing during reactive crystallization of barium sulfate. Three separate scales of

1199   mixing, Kolmogorov, turbulent, and convective, were proposed in a new mixing model

1200   composed of viscous deformation and molecular diffusion in a slab element. The model was

1201   used to give accurate predictions of the effect of stirring speed, feed location, and viscosity on

1202   particle sizes. Zauner and Jones[265, 266] investigated the effect of feed rate, feed concentration,

1203   feed tube diameter, impeller type and stirring rate on particle size for the reactive crystallization

1204   of calcium oxalate and calcium carbonate. Overall, the results of the aforementioned mixing

1205   studies suggest that poor mixing conditions promote a higher rate of primary nucleation, leading

1206   to a larger number of nuclei and a size distribution of smaller final crystals.

1207   *Continuous systems.* As in batch systems, the stirred tank is the most commonly-used

1208   vessel in continuous systems, but alternative geometries have also been proposed and

1209   implemented. Several examples of alternatives to the stirred-tank crystallizer are shown in

1210   Figure 13. These include Taylor-Couette, impinging jet, airlift loop, continuous flow inversion,

1211   and oscillatory baffled crystallizers. Examples (a), (b), and (c) in Figure 13 approximate

1212   MSMPRs, while (d) and (e) are used to provide near plug-flow behavior.
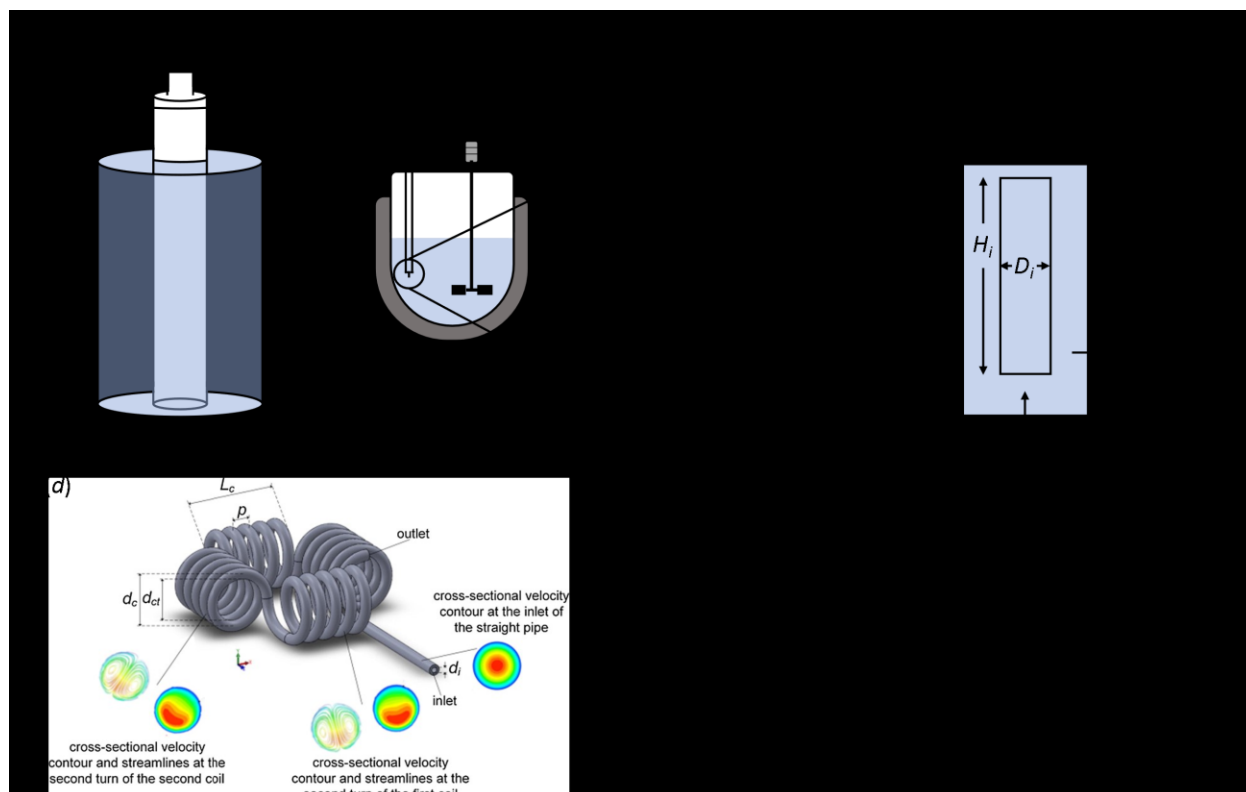
1213

1214   *Figure 13. Summary of novel reactive crystallizers; (a) Taylor-Couette,[198, 267] (b) Impinging jet mixer,[165] (c)*
1215   *airlift loop,[85] (d) continuous flow inverter – Reprinted with permission from Kurt et al.[268] copyright 2017, Elsevier,*
1216   *(e) continuous oscillatory baffled.[190]*

48

1217   For reactions of short timescales, often a reactor that is nearly perfectly mixed is used due

1218   to its robust operation and the ease of implementing process analytical technologies (which are

1219   discussed later and may include *in situ* microscopy, Raman and IR spectroscopy, and particle

1220   size analysis). Well-mixed reactors such as an MSMPR are also used when high supersaturation

1221   is not desired, such as when high supersaturation promotes the formation of an undesired

1222   polymorph or a finer crystal size distribution. For reactions in which high reactant concentrations

1223   are preferred, a single well-mixed reactor may not be the best design because it operates at outlet

1224   conditions; that is, conditions throughout the vessel correspond to those at the outlet. However,

1225   the use of a plug-flow reactor may introduce clogging concerns.[269] To address this issue, Hu *et*

1226   *al.*[270] utilized multiple MSMPR reactors in series to approach plug-flow behavior for a second-

1227   order reaction in which high reactant concentration was needed to achieve high conversions.

1228   When the reaction proceeds much faster than crystallization (both nucleation and

1229   growth), techniques such as wet-milling or sonocrystallization can promote nucleation and more

1230   rapid consumption of supersaturation. Yang *et al.*[271] and Acevedo *et al.*[272] showed that wet

1231   milling in a continuous crystallizer increased the yield, operating as a promoter of both primary

1232   and secondary nucleation for paracetamol in two different solvents. Use of wet-milling has also

1233   been shown to enable deracemization of conglomerates by combining the principles of

1234   preferential crystallization and Viedma ripening.[273] Sonocrystallization, or the application of

1235   ultrasound to a crystallizer, has been shown to hasten crystallization in batch.[274] Hatakka *et al.*[180]

1236   used sonocrystallization to selectively produce a single polymorph during the batch reactive

1237   crystallization of L-glutamic acid while experiments without sonication resulted in a mixture of

1238   polymorphs. The authors concluded that the polymorphic purity results from reduced

1239   supersaturation due to enhanced nucleation by sonication. Wet-milling and sonocrystallization

1240   can both lead to narrower, finer size distributions as a result of increased nucleation.[275, 276]

1241   Slower reactions may require the use of multiple vessels in series to achieve higher

1242   conversions. Mo and Jensen[277] demonstrated the use of a micro-CSTR cascade for two separate

1243   solid-forming reactions: (1) the reaction of glyoxal and cyclohexylamine to form the practically

1244   insoluble N,N'-dicyclohexylethylenediimine and (2) the sulfonylation of 2-octanol which

1245   produced the sparingly soluble side product triethylamine hydrochloride. For the first reaction, a

1246   six-unit CSTR cascade (15-minute total residence time) was needed to reach nearly 100%

1247   conversion while the second reaction only required three CSTRs to achieve 100% conversion.

49

1248   Effective control of process parameters such as temperature and pH, often important variables in

1249   determining the reaction and crystallization rates, is typically achieved in well-mixed reactors

1250   with the inclusion of probes, a thermal jacket, and addition of acid or base. Process control will

1251   be discussed in more detail below.

1252   Mixing intensity may be an issue in continuous reactive crystallization. Like batch

1253   crystallizers, if the reaction utilizes a catalyst that is susceptible to high shear, a Taylor-Couette

1254   style reactor may be operated with a feed and continuous product removal. Aggregation of

1255   mixing-induced nuclei may also be a concern, leading to a wide crystal size distribution (CSD).

1256   Liu *et al.*[165] found that incorporation of an impinging jet mixer in the continuous reactive

1257   crystallization of the antibiotic sodium cefuroxime resulted in a narrower CSD and improved

1258   product stability compared to a traditional impeller-stirred reactor. Jung *et al.* found a similar

1259   decrease in the size distribution using a Taylor-Couette reactor for calcium hydroxide production

1260   because the more gentle mixing discouraged agglomeration.[278]

1261   Continuous tubular reactors such as plug flow reactors (PFRs) are frequently used in the

1262   chemical industry. Higher overall concentrations of reactants across the length of the reactor lead

1263   to higher conversions for positive-order reactions. For reactive crystallization, unlike in a well-

1264   mixed tank, temperature or pH value may be varied along the length of the reactor, allowing for

1265   the enhancement of reaction or crystallization kinetics in different sections. Jiang and Ni[190]

1266   varied the temperature across a continuous oscillatory baffled crystallizer (COBC), a type of

1267   continuous tubular reactor designed to achieve plug flow at low fluid velocities, such that higher

1268   temperatures in the initial segments favored the reaction and lower temperatures towards the

1269   outlet improved the rate of crystallization. Kurt *et al.*[268] achieved near plug-flow behavior of

1270   slurry by designing and operating a coiled flow inverter (CFI) crystallizer for the reactive

1271   crystallization of calcium carbonate. The inverting flow and helically coiled tubing enhanced

1272   mixing via formation of Dean and Taylor vortices, which increased secondary flow

1273   perpendicular to the primary flow direction. Others have physically segmented plugs of slurry by

1274   injecting inert gas spacers.[279] All of these crystallizers enhance mixing and slurry suspension by

1275   achieving a more plug-flow-like flow profile than conventional PFRs. Increased turbulence using

1276   these novel designs permits the use of reactors with larger diameters and shorter lengths to

1277   achieve the same residence times. In general, using small-diameter tubing to achieve adequate

1278   turbulence and slurry suspension is a concern in PFRs because of clogging. Polster *et al.*[84]

50

1279   attempted to design a continuous reactive crystallization process for a BACE inhibitor using a

1280   PFR, but eventually settled on an MSMPR due to clogging inside the reactor tubing. Oroskar and

1281   Turian[280] developed the following correlation to estimate the critical slurry velocity, which is

1282   defined as the velocity required to suspend particles and prevent their deposition in a tube or

1283   pipe:

1284
$$\frac{v_c}{\sqrt{gd(s-1)}} = 1.85C^{0.15}(1-C)^{0.36}\left(\frac{d}{D}\right)^{-0.38}\left(\frac{D\rho_l\sqrt{gd(s-1)}}{\mu}\right)^{0.090} x^{0.30} \qquad (23)$$

1285   All dimensional variables are in SI units and v_c represents the critical velocity, d the equivalent

1286   spherical particle size, C the fractional slurry density, D the pipe diameter, ρ_l the liquid density,

1287 μ the liquid viscosity, and s the ratio of the liquid-to-solid density. Here, x is a correlation factor

1288   estimated using the fraction of particles above the critical velocity generally approximated to be

1289   unity. This correlation may be used to estimate the minimum diameter of a PFR to avoid

1290   clogging keeping in mind that the minimum diameter, while providing the most turbulence, must

1291   be large enough to accommodate the largest crystals.

1292   Another downside of using continuous tubular reactors is that the composition of the

1293   suspension cannot be easily manipulated after the inlet. Thus, controlling the pH can be difficult

1294   (especially for reactions involving acids and bases), which may lead to unintended changes in

1295   reaction or crystallization kinetics across the reactor. Controlling pH is a special challenge in

1296   working with enzymes as biocatalysts typically work in very narrow, well-regulated pH

1297   environments. As a solution, Jiang and Ni[190] used multiple sampling ports across the length of a

1298   tubular reactor to learn more about the slurry by off-line analysis. Another issue arises when a

1299   continuous tubular reactor requires seed crystals to initiate crystallization; either the reactor must

1300   be fed seed crystals or a recycle stream must be incorporated to introduce crystals at the inlet,

1301   complicating the design and operation of the reactor. In contrast, a well-mixed reactor (for

1302   example, an MSMPR unit) does not face this issue as it operates with a suspension of crystals

1303   that participate in secondary nucleation and foster crystal breeding during continuous operation.

1304   ***Modelling, Monitoring, and Process Control.*** A control scheme for reactive

1305   crystallization processes depends on the nature of the species being produced and its desired

1306   characteristics. Various factors such as temperature,[193] pH,[127] and the presence of additives[281]

1307   can dictate the final crystal properties in specific processes. More generally, control of

1308   supersaturation and seeding have the greatest effect on crystal size distribution, crystal shape,

1309   and polymorphic form. Compared to crystallization alone, supersaturation may be more difficult

1310   to control in a reactive crystallization process because it can only be manipulated indirectly via

1311   adjusting the reaction rate. Extreme examples are near-instantaneous reaction rates, typical of

1312   ionic systems, where the only manipulation of the reaction rate is through the supply of reactants.

1313   Slow-reacting systems are also difficult to control as the solution stays near saturation ($S \approx 1.0$).

1314   Reactive crystallization models that couple the kinetics of the three governing phenomena of

1315   chemical reaction, nucleation, and crystal growth are constructed to narrow an operating window

1316   that will provide a desired CSD, crystal shape, and polymorph.[5, 113] From models, the

1317   development of process control algorithms for reactant flow rate or seed-crystal addition can be

1318   tuned to optimize robust production of the desired crystal properties.

1319   One of the earliest and most general models for semi-batch reactive crystallization

1320   processes focused on developing reactive phase equilibrium equations and diagrams based on

1321   reaction equilibria where the products are non-soluble and instantly form a solid.[282] While useful

1322   for identifying reaction conditions and simulating reactor performances that generate only solid

1323   products, this model focused on hypothetical examples and did not include the kinetics of

1324   nucleation and growth that determine CSD and crystal shape. Kelkar and Ng[283] expanded this

1325   model to include nucleation and growth kinetics for MSMPR crystallizers. Their model included

1326   the steps for reactions in solution generating supersaturation, nucleation, and linear growth rate

1327   of crystals from supersaturated product in solution. Applying their model for process design,

1328   they studied the reaction rate under different reactor throughput conditions, dissolution rates, and

1329   mass transfer rates. The effect of different reaction rates, nucleation rates, and growth rates on

1330   the product weight fraction distribution was also predicted.

1331   The previously discussed models primarily focus on using hypothetical kinetic

1332   parameters to simulate reactor performance, while only a few studies have been directed towards

1333   process optimization. Choong and Smith[284] further expanded semi-batch reactive crystallization

1334   models by including a population balance to allow for the optimization of CSD. Assuming

1335   perfect mixing, the initial amount of reactants, feed addition time, and number of feeds were

1336   considered to be design variables for two optimization problems: (1) maximizing crystal size

1337   with a constraint of maximum coefficient of variation of the size distribution and (2) minimizing

1338   the coefficient of variation subject to a constraint of minimum average crystal size. A stochastic

1339   optimization framework was then used to circumvent traditional pitfalls such as nonconvergence

1340   or suboptimal solutions in highly nonlinear systems.[284] The model neglected secondary

1341   nucleation with the rate of nuclei generation being defined by Equation (9). Within that

1342   limitation, their model allowed for devising nonlinear control policies that could be implemented

1343   in a semi-batch reactive crystallization process.

1344   While the studies discussed above are not exhaustive, they have developed models that

1345   present the primary features of reactive crystallization processes and strategies for their

1346   optimization. Other reactive crystallization models include more specific studies on modelling

1347   and control of enantiomer and polymorph crystallization,[285] multi-objective optimization and

1348   generation of Pareto-optimal solutions for desired crystal properties,[286] incorporation of seeding

1349   strategies,[287] resistances in double-film mass transfer models for gas-liquid systems,[121] and

1350   effects of macro- and micromixing regimes on crystal size distributions.[114] System-specific

1351   models to predict control profiles for optimal mean crystal size and narrow CSD have also been

1352   developed for ampicillin,[288] barium carbonate,[108] aluminum hydroxide,[115] and 2,4,6 -triamino-

1353   1,3,5-trinitrobenzene.[122] Similar models for continuous reactive crystallization have also been

1354   developed but focus primarily on instantaneous reaction kinetics[287] or are specific to a given

1355   system[5, 113] and examples in the literature are still quite limited in the literature.

1356   Reactive crystallization process modeling and process evaluation would not be robust

1357   without in-line monitoring using PAT and sensors to obtain qualitative and quantitative data on

1358   the evolution of the solution and crystal phases.[289] The use of PAT is important for process

1359   monitoring, which in turn allows for analyses of reaction and crystallization mechanisms and

1360   process control. A summary of PATs common to reactive crystallization processes is shown in

1361   Figure 14. Attenuated total reflectance-Fourier transform infrared (ATR-FTIR) coupled with

1362   multivariate models is often used to analyze the liquid-phase composition during the process, as

1363   it has low solid-phase sensitivity.[29, 290, 291] Raman spectroscopy can be used to quantify solution

1364   or crystal composition for molecules that can undergo large polarization changes and thus exhibit

1365   strong Raman scattering. Raman measurements are especially useful in systems with co-

1366   crystallization or multiple polymorphs to distinguish different solids.[180, 237, 290, 291] Focused beam

1367   reflectance measurement (FBRM) estimates the evolution of chord-length distributions of

1368   crystals (a proxy for, but fundamentally different from, the crystal size distribution) in real

1369   time.[84, 98, 146, 173, 270, 292] Coupled with system-dependent algorithms, chord-length distributions

1370   can be directly related to crystal size distributions; however, substantial work is required to

1371   transform chord-length distributions for comparison with size distributions obtained by laser

1372   diffraction or optical imaging.[293, 294] Particle vision and measurement (PVM) can provide *in situ*

1373   estimates of crystal size and shape by observing crystals in a crystallizer or a reactor as

1374   transformations take place. PVM has been shown to be especially useful in observing polymorph

1375   shifts,[295] agglomeration,[88, 296] and crystal growth under different process conditions.[292] Other

1376   monitoring techniques include HPLC for offline solution composition measurements and laser

1377   diffraction particle size analyzers coupled with image analysis to collect information about

1378   particle size and shape. Crystal structure can be further characterized offline with x-ray

1379   diffraction (XRD) and x-ray powder diffraction (PXRD). For products that undergo color

1380   changes upon degradation, a stability chamber and transmittance measurements using UV to

1381   obtain color-grade data can be used to evaluate purity of the final product. These methods are

1382   performed offline after crystal isolation but they do provide metrics for confirmation and

1383   calibration of online measurements or process stability.[297] PATs are often combined to give a

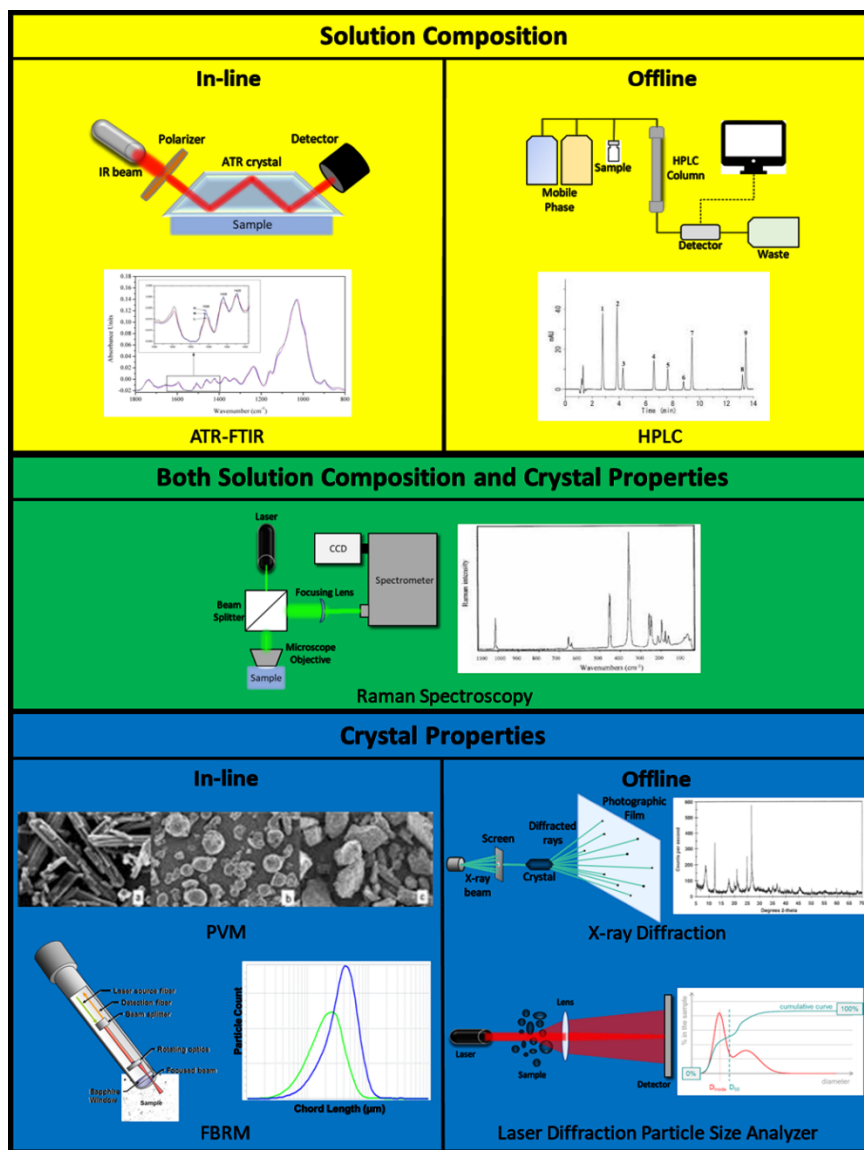1384   more complete view of the reaction and crystallization phenomena.

Figure 14. Common PAT used for characterizing composition and concentration of species in solution as well as crystal properties. Representative data outputs from each PAT are shown.

1385   Control of final product properties can be achieved without modelling the system of

1386   interest but requires a detailed understanding of how different process parameters affect qualities

1387   of the solution and crystal phases. Polster *et al.*[84] developed a continuous reactive crystallization

1388   process for production of an API for clinical trials and studied experimentally how crystallizer

1389   residence time, temperature, solvent composition, and recycle configuration impacted size

1390   distribution, final blend flow function coefficients, yield, and tapped density. The control

1391   strategy then focused on feedback control of reactant flow rates and pH adjustments.

1392   In any control application, model-free control is simpler and easier to implement

1393   compared to model-based optimal control, but the latter can provide superior performance if an

1394   accurate model is available. A representative example for how PAT can assist in modelling,

1395   monitoring, and optimal control during the development of a large-scale process is the reactive

1396   crystallization of glutamic acid from monosodium glutamate and sulfuric acid.[298] A common

1397   control strategy in batch antisolvent or cooling crystallizations is to determine the optimal

1398   supersaturation trajectory for the process as a function of some manipulated variable such as

1399   temperature or anti-solvent flow rate and to design a feedback control system to maintain the

1400   optimal state using ATR-FTIR for direct measurement of solution concentrations.[299, 300] Direct

1401   concentration control commonly used in antisolvent or cooling crystallizations is often difficult

1402   to employ in reactive crystallizations due to strong process nonlinearities that can arise from

1403   coupled reaction, dilution, and crystallization dynamics. For instance, the desired supersaturation

1404   trajectory in the reactive crystallization of glutamic acid is dome-shaped, and conventional

1405   concentration control cannot be used at many operating points because it would require a

1406   reduction in volume to hit the desired trajectory. However, volume is constantly increasing from

1407   the startup of the system due to the addition of reactants. A variation of direct concentration

1408   control known as Just-in-Time-Learning, JITL, can be employed to build a nonlinear model-

1409   predictive control strategy based on extended predictive self-adaptive control that accounts for

1410   nonlinearities.[301] This method is used to identify a set of empirical state-space models along the

1411   desired process trajectory.[177] JITL has also been coupled with system models to include batch-to-

1412   batch model predictive control strategies.[302]

1413   Glutamic acid crystallization is further complicated by the existence of two polymorphs;

1414   the desired α form is thermodynamically metastable and eventually transforms into the undesired

1415   but stable β form. Obtaining the metastable α form requires a detailed monitoring and control

1416   process. Alatalo et al.[290] showed that ATR-FTIR measurements coupled with thermodynamic

1417   modeling in a multivariate partial least squares model were effective in accurately measuring

1418   glutamic acid concentrations in solution over the course of the reaction. By using coupled ATR-

1419   FTIR and Raman spectroscopy measurements, Qu et al.[291] determined that formation of the

1420   stable β polymorph was favored at high supersaturation. They speculated that this was due to the

1421   β form having a higher barrier to nucleation than the α form. The in-line monitoring techniques

1422   allowed discovery of the formation of the β polymorph at conditions of high global

56

1423   supersaturation and in regions of poor mixing, especially those where feed was introduced above

1424   the liquid surface in the crystallizer. Alatalo *et al.*[298, 303] further extended this work to the design

1425   of a closed-loop feedback control algorithm based on the ATR-FTIR measured concentration of

1426   glutamic acid in solution and adjustment of the sulfuric acid feed rate with a PID controller. Such

1427   an arrangement allowed control of supersaturation and the formation of the α polymorph in a 50-

1428   L reactor.

Perspectives and Future Directions for Reactive Crystallization

1430   Reactive crystallization provides opportunities for process intensification and product

1431   improvements, which could be favorable to product economics. In this section the necessary

1432   developments needed for reactive crystallization to advance to new applications are outlined,

1433   with emphasis on the need for more data, improved PAT, advanced crystallizer design, and

1434   better understanding of reaction and crystallization mechanisms. Brief guidance for adaptation of

1435   existing processes or creation of new processes for reactive crystallization is given. Finally,

1436   possible future enhancements centered on reactive crystallization, primarily continuous

1437   manufacturing and hybrid systems, are outlined.

1438   ***Kinetics: distinguishing reactive crystallization from other separation techniques.***

1439   Utilizing crystallization, and therefore reactive crystallization, in industrial processes presents

1440   unique challenges with respect to product quality: namely those associated with meeting criteria

1441   on crystal size, size distribution, purity and form. Such challenges must be met while also

1442   satisfying the usual process requirements of yield and economics. Advancing reactive

1443   crystallization to where it can increase the yield of a product, while at the same time meeting

1444   quality criteria, is a great challenge. Environmental and economic sustainability add urgency that

1445   new manufacturing processes are implemented and matured.

1446   Some specific studies of how reactive crystallization can fit into a useful process have

1447   already been published.[84, 113] However, relating reactive crystallization to meet final product

1448   specifications including purity, size distribution, morphology (including polymorphic form and

1449   crystal shape), and more, remains a difficult task. For example, a few authors have undertaken

1450   the task of optimizing simulated reactive crystallization processes,[79, 282, 284] but bypassed the

1451   significant effort required to characterize the reaction kinetics and crystallization kinetics in the

1452   combined reactive crystallization environment.

57

1453   Several authors have shown that the kinetics of crystal growth and nucleation, which

1454   together with system configuration determine product crystal size distribution, can vary in the

1455   presence of other species such as reactants and byproducts.[17, 75, 76] Elucidating reaction and

1456   crystallization kinetics in complex environments requires large volumes of data, which can come

1457   from either high-throughput or data-rich experiments. High-throughput experimentation involves

1458   measuring reaction and crystallization (that is, nucleation and growth) rates across a large

1459   sampling of process conditions and compositions to predict complex process features such as

1460   crystal size distribution. Data-rich experimentation, on the other hand, uses a smaller number of

1461   experiments, but with collection of high-dimensional data, such as crystal size distribution,

1462   which can be used to work backwards and determine reaction and crystallization kinetics. Both

1463   approaches enable the required level of description for designing new reactive crystallization

1464   processes, and substantial progress has been made towards both ends; however, each approach

1465   also comes with its own hurdles and challenges.[304-306]

1466   Reactive crystallizations typically take place in more complex solutions than cooling,

1467   antisolvent, or evaporative crystallization; PAT tools that are effective in such complex solutions

1468   would enable more accurate modeling and precise control of reactive crystallization processes.

1469   Taking ATR-FTIR as an example, each dissolved species contributes to the overall IR spectrum,

1470   and through careful construction of calibration models the concentration of each species can be

1471   extracted from the overall spectrum.[110, 307, 308] However, the presence of uncharacterized species

1472   such as impurities, intermediates, byproducts, or catalysts, can break calibration models, and the

1473   work required to characterize all species and their combination may be too laborious or even

1474   impossible (e.g. non-isolatable intermediates). Improved baselining algorithms and regression

1475   techniques may make calibration model construction more manageable, such as recent work by

1476   Maggioni et al.[111] based on blind source separation and independent component analysis

1477   requiring only single point calibration with robustness against unknown species. The

1478   methodology was demonstrated on mixtures of simple oxyanions and did not perform as well

1479   when the anions' spectra overlapped. For many reactive crystallizations the reactants,

1480   intermediates, and products have similar functional groups and IR spectra; continued

1481   chemometric development is required for general solution phase monitoring by spectroscopic

1482   methods. Additionally, many species may only be present at low concentration compared to the

1483   reactants and products. In the production of terephthalic acid the intermediate 4-CBA has a

1484   maximum concentration of <10% of the total concentration of aromatics, leading to 1% 4-CBA

1485   in the final product. Using control to minimize the 4-CBA concentration is difficult as improved

1486   spectroscopic analysis would be needed to quantify the small amount of 4-CBA in such a

1487   complex solution (see Figure 5).[193, 309]Likewise, in the enzymatic production of beta-lactam

1488   antibiotics the undesired byproduct phenylglycine (see Figure 6) may crystallize and contaminate

1489   the antibiotic slurry. Detecting the nucleation of phenylglycine amounts to detecting a change in

1490   phenylglycine concentration of <10 mmol/L in a solution with >100 mmol/L 6-APA and PGME,

1491   both of which have IR spectra with significant overlap with phenylglycine, and has proven to be

1492   very challenging with ATR-FTIR.[310]

1493   Improvement in the characterization of solids will also benefit reactive crystallization

1494   process design and process control. In the case of beta-lactams the ability to distinguish between

1495   antibiotic crystals and byproduct crystals *in situ* could circumvent the challenges associated with

1496   solution-phase monitoring. FBRM has been used to indicate polymorph transformation in

1497   paracetamol[311] and in-situ microscopy with machine learning has been demonstrated for

1498   classifying individual crystals versus agglomerates.[37] Both FBRM and *in situ* microscopy are

1499   restricted to use in slurries of low solids concentration.[312, 313] Reactive crystallization would

1500   benefit considerably from the development of techniques that can identify new particle types

1501   with minimal training data and calibration effort, especially since many systems involve solid

1502   reactants dissolving, reacting, and crystallizing.[196, 206, 314, 315] A promising development for these

1503   systems, where solution concentration cannot quantify reaction conversion, are composite PAT

1504   arrays and crystallization informatics.[289] An array of complimentary sensors combined with

1505   process expertise has been shown to enable quantification of different solids concentrations in

1506   other solution-mediated solids transformations, such as polymorph transformations[316] and

1507   hydrate-to-anhydrate transformations;[317] application to a reactant-to-product transformation

1508   follows naturally.

1509   ***Determining the applicability and utility of reactive crystallization.*** Heuristics to

1510   identify when a reactive crystallization could enhance a process do not exist and should be

1511   created. It is often assumed that the product must be less soluble than the reactants, however fed-

1512   batch and continuous stirred-tank reactors (with independent solution and solids residence times)

1513   can enable reactive crystallization even when the product is more soluble. Use of co-formers can

1514   decrease the solubility of the product below that of the reactants, also enabling productive

1515   reactive crystallization. A brief guide to how reactive crystallization can improve a process is

1516   presented in Table 4, below.

1517   *Table 4. A list of useful heuristics for recognizing when reactive crystallization is advantageous and/or*
1518   *feasible.*

Product Type	
Inorganic	Reactive crystallization almost always possible, preferable with sparingly soluble compounds, mixing control key to supersaturation control and size control
Organic Ionizable	Usually possible with appropriate counter-ion. Preferable for temperature-sensitive compounds and hydrates. Ideal for isolating intermediates, overcoming reaction equilibrium. Requires modest aqueous solubility in charged state
Organic Nonionic	Should be evaluated on a case by case basis. Examples of successful processes include covalent reactions eliminating charged groups in aqueous solution (e.g. amide bond formation) or creating charged groups in nonpolar solvents (e.g. hydrogenolysis)
Critical Quality and Process Attributes	
Yield, Productivity, Selectivity, Sustainability	Reactive crystallization ideal for improving yields and selectivity by shifting equilibrium, isolating inhibitory products, protecting reactive intermediates
Purity, Form, Solvate	Complex composition in reaction mixture can increase number of possible impurities, may change form preference from pure solution, reaction solvents may limit solvate options
Crystal Size Distribution	Fast reactions, i.e. neutralizations and acidifications, will create a fines-dominated CSD. Slow reactions and seeding typically give large crystals. Reaction rate modification by catalyst engineering can enable fine-tuning of CSD
Methods of Reactive Crystallization	
Neutralization	Reactive crystallization by neutralization ideal for intermediate process steps, e.g. isolating an intermediate as a calcium salt before dissolving salt for further processing. Limited by neutralizing agents, usually calcium, magnesium, and ammonium
Acidification	Ionizable compounds typically least soluble in protonated (neutrally charged) form, ideal for removing acids/bases from complex mixtures of nonionic species
Covalent reaction	System specific, often catalyst dependent. Least generalizable but most opportunity for process improvement. Requires that the catalyst be in a form that can easily be separated from the crystal product

1519

1520   ***Continuous manufacturing.*** The end-to-end integrated continuous manufacturing

1521   paradigm is becoming increasingly important in the pharmaceutical industry, due in large part to

1522   the potential benefits of lower costs, shorter supply chains, smaller footprints, and better quality

1523   monitoring and controls with PAT.[259, 318, 319] In this relatively new paradigm in pharmaceutical

1524   manufacturing, reactive crystallization processes should be designed to be adapted to the whole

1525   process, rather than considered as an independent unit operation. For example, traditional batch

1526   operations may allow operational flexibility over a range of conditions, such that the reaction

1527   time can be shortened or extended based on the extent of reaction; such alterations are not easily

1528   made in continuous reactors.

1529   Control of raw materials to an integrated reactive crystallization is important, as: (1) raw

1530   materials often include insoluble particles requiring a clarification bypass system beforehand;[320]

1531   (2) variability in raw materials (like differences in purity or water content) could result in lower

1532   yield or higher impurity profile. Batch processes have more flexibility to handle raw material

1533   variability; different control strategies for continuous reactive crystallization may be more or less

1534   amenable to mitigating the risks of variability in raw material composition, based on the

1535   frequency and extent of the irregularity.

1536   ***Novel reactive crystallization process designs.*** Process intensification has been cited as

1537   one of the primary reasons for implementing a reactive crystallization process. Further

1538   intensification can be found with examples of evaporative reactive crystallization,[202] cooling

1539   reactive crystallization,[321] membrane-assisted reactive crystallization,[322, 323] liquid-liquid

1540   extraction reactive crystallization,[181] and chromatography-assisted reactive crystallization.[241, 324]

1541   In each case multiple techniques may be applied simultaneously: for example, a reaction

1542   occurring in one liquid phase, crystallization occurring in a second liquid phase, and rapid mass

1543   transfer between phases;[322] or sequentially: for example, a reactive crystallization occurring at

1544   high temperature with fast reaction kinetics followed by cooling to reduce solubility and generate

1545   supersaturation while sacrificing reaction speed.[89]

1546   Most complex chemical processes require catalysts to control reactions and produce

1547   desired products. Using stoichiometric amounts of catalysts is often undesirable from the

1548   standpoints of process economics as well as purification. Catalysts must be recovered for

1549   sustainability and product purity. Separating solid catalysts from a crystal slurry can be

1550   prohibitively difficult; several examples of reactive crystallization followed by dissolution for

1551   the purpose of catalyst recovery have already been discussed.[92, 198] Alternatively a soluble

1552   catalyst can be used and retained/recovered via ultrafiltration, which may work well for

1553   dissolved biocatalysts as bio-macromolecules can be separated from small molecules with

1554   ease.[182, 325] Nanofiltration, which has proven useful for removing impurities during

1555   crystallization,[326] may be useful for recovery of non-biologic soluble catalysts. However,

1556   membranes are subject to fouling and are not compatible with all solvents, substrates, and

1557   catalysts, in which case the pursuit of solid-solid separations based on size, density, or other

1558   properties may be preferable. Examples of such solid-solid crystal-catalyst separators include

1559   hydrocyclones,[141] elutriation,[327] and sieves.[198]

1560   Further research into the fundamentals of crystallization in complex environments, i.e.

1561   with multiple solutes, solvents, and surfaces, will enable future synthesis and separation

1562   processes with improved yield and sustainability.

1563   **Concluding remarks**

1564   As process designers continue to experiment with novel methods of increasing economic

1565   and environmental sustainability, reactive crystallization has become increasingly attractive as a

1566   means to those ends. Reactive crystallization is not particularly new, as ionic compounds have

1567   been synthesized by reactive crystallization since the beginning of the chemical industry.

1568   However, new applications of reactive crystallization promise to make possible new processes

1569   and improve existing ones. New applications of ionic reactive crystallization include capturing

1570   greenhouse gases as carbonates, recovering minerals from wastewater, and enabling fermentation

1571   routes to platform chemicals. Covalent reactive crystallization, while less developed, has more

1572   promise as a tool to enhance existing reactions or overcome the kinetic and equilibrium

1573   limitations of formerly untenable reactions. Biocatalytic processes could benefit the most, as

1574   those systems are most sensitive to accumulations of products and intermediates. Additionally,

1575   crystallization plays a dominant role in processes to separate enantiomers, where the

1576   combination of a racemization reaction and crystallization can lead to enantiomeric excess

1577   greater than 99%. The design of reactive crystallization systems follows closely the design of

1578   crystallizers in general. Crystallization is a highly nonlinear process; controlling crystallization

1579   coupled with a reaction is difficult but many control strategies and reactor designs have proven

1580   effective for specific cases. The future of reactive crystallization rests on collection of more data

1581   and generalization of findings from disparate case studies, which is the primary aim of this

1582   review. While this review may not be exhaustive, it should serve as a starting point for the design

1583   of reactive crystallization processes for any type of compound across many scales of industry.

62

Conflicts of Interest

Acknowledgements

References

1. D. S. Sholl and R. P. Lively, *Nature*, 2016, **532**, 435-437.
2. A. S. Teja and R. W. Rousseau, *Chemical Thermodynamics for Industry*, 2004, 230-242.
3. L. G. Encarnación-Gómez, A. S. Bommarius and R. W. Rousseau, *Industrial & Engineering Chemistry Research*, 2016, **55**, 2153-2162.
4. M. A. McDonald, A. S. Bommarius and R. W. Rousseau, *Chemical Engineering Science*, 2017, **165**, 81-88.
5. M. A. McDonald, A. S. Bommarius, R. W. Rousseau and M. A. Grover, *Computers & Chemical Engineering*, 2019, **123**, 331-343.
6. W. Hu, S. Wang, A. Liang and J. Wang, *Journal of Chemical & Engineering Data*, 2017, **62**, 69-79.
7. J. Cuevas-Valenzuela, Á. González-Rojas, J. Wisniak, A. Apelblat and J. R. Pérez-Correa, *Fluid Phase Equilibria*, 2014, **382**, 279-285.
8. H. Charmolue and R. W. Rousseau, *AIChE Journal*, 1991, **37**, 1121-1128.
9. L. J. M. Kempkes and W. J. P. van Enckevort, *CrystEngComm*, 2015, **17**, 1483-1490.
10. C. Sano, *The American Journal of Clinical Nutrition*, 2009, **90**, 728S-732S.
11. H.-C. Tseng, C.-Y. Lee, W.-L. Weng and I. M. Shiah, *Fluid Phase Equilibria*, 2009, **285**, 90-95.
12. B. R. Figueiredo, F. A. Da Silva and C. M. Silva, *Industrial & Engineering Chemistry Research*, 2013, **52**, 16044-16056.
13. C.-Y. Lee, J.-T. Chen, W.-T. Chang and I. M. Shiah, *Fluid Phase Equilibria*, 2013, **343**, 30-35.
14. A. A. Pradhan and J. H. Vera, *Fluid Phase Equilibria*, 1998, **152**, 121-132.
15. R. Carta and G. Tola, *Journal of Chemical & Engineering Data*, 1996, **41**, 414-417.
16. M. G. Brown and R. W. Rousseau, *Biotechnology Progress*, 1994, **10**, 253-257.
17. M. A. McDonald, G. D. Marshall, A. S. Bommarius, M. A. Grover and R. W. Rousseau, *Crystal Growth & Design*, 2019, **19**, 5065-5074.
18. J. C. Givand, A. S. Teja and R. W. Rousseau, *AIChE Journal*, 2001, **47**, 2705-2712.
19. J. Givand, B.-K. Chang, A. S. Teja and R. W. Rousseau, *Industrial & Engineering Chemistry Research*, 2002, **41**, 1873-1876.

20. I. Kurosawa, A. S. Teja and R. W. Rousseau, *Fluid Phase Equilibria*, 2004, **224**, 245-249.

21. I. Kurosawa, A. S. Teja and R. W. Rousseau, *Industrial & Engineering Chemistry Research*, 2005, **44**, 3284-3288.

22. A. I. Isakov, E. N. Kotelnikova, S. Muenzberg, S. N. Bocharov and H. Lorenz, *Crystal Growth & Design*, 2016, **16**, 2653-2661.

23. J. Lu, X.-J. Wang, X. Yang and C.-B. Ching, *Journal of Chemical & Engineering Data*, 2006, **51**, 1593-1596.

24. R. R. E. Steendam, L. Keshavarz, B. de Souza and P. J. Frawley, *The Journal of Chemical Thermodynamics*, 2019, **133**, 85-92.

25. L. Keshavarz, R. R. E. Steendam, M. A. R. Blijlevens, M. Pishnamazi and P. J. Frawley, *Crystal Growth & Design*, 2019, **19**, 4193-4201.

26. R. A. Granberg and Å. C. Rasmuson, *Journal of Chemical & Engineering Data*, 1999, **44**, 1391-1395.

27. M. Jiang and X.-W. Ni, *Chemical Engineering and Processing-Process Intensification*, 2018, **131**, 20-26.

28. N. A. Bowden, J. P. M. Sanders and M. E. Bruins, *Journal of Chemical & Engineering Data*, 2018, **63**, 488-497.

29. T. Zhang, Y. Liu, S. Du, S. Wu, D. Han, S. Liu and J. Gong, *Crystal Growth & Design*, 2017, **17**, 6123-6131.

30. J. Lu, J. Wang and S. Rohani, *Cryst. Res. Technol.*, 2012, **47**, 505-510.

31. J. F. Black, R. J. Davey, R. J. Gowers and A. Yeoh, *CrystEngComm*, 2015, **17**, 5139-5142.

32. M. Svärd, F. L. Nordström, E.-M. Hoffmann, B. Aziz and Å. C. Rasmuson, *CrystEngComm*, 2013, **15**, 5020-5031.

33. O. Söhnel and J. W. Mullin, *Chemical Engineering Science*, 1978, **33**, 1535-1538.

34. J. W. Mullin, *Crystallization*, Butterworth-Heinemann, Fourth edition edn., 2001.

35. A. D. Randolph and M. A. Larson, *Theory of Particulate Processes*, Academic Press, San Diego, 2 edn., 1988.

36. A. Lewis, M. Seckler, H. Kramer and G. Van Rosmalen, *Industrial Crystallization: Fundamentals and Applications*, Cambridge University Press, 2015.

37. D. R. Ochsenbein, T. Vetter, S. Schorsch, M. Morari and M. Mazzotti, *Crystal Growth & Design*, 2015, **15**, 1923-1933.

38. F. Salvatori and M. Mazzotti, *Crystal Growth & Design*, 2018, **18**, 5957-5972.

39. S. Ghader, M. Manteghian, M. Kokabi and R. S. Mamoory, *Chem. Eng. Technol.*, 2007, **30**, 1129-1133.

40. V. I. Kalikmanov, in *Nucleation Theory*, Springer Netherlands, Dordrecht, 2013, DOI: 10.1007/978-90-481-3643-8_3, pp. 17-41.

41. T. E. Paxton, A. Sambanis and R. W. Rousseau, *Langmuir*, 2001, **17**, 3076-3079.

42. P. G. Vekilov, *Crystal Growth & Design*, 2010, **10**, 5007-5019.

43. A. Svang-Ariyaskul, Georgia Institute of Technology, 2010.

44. H. Groen and K. J. Roberts, *Journal of Physical Chemistry B*, 2001, **105**, 10723-10730.

45. D. Kashchiev, D. Verdoes and G. M. Vanrosmalen, *Journal of Crystal Growth*, 1991, **110**, 373-380.

46. D. Kashchiev and G. M. van Rosmalen, *Cryst. Res. Technol.*, 2003, **38**, 555-574.

64

1668 47. S. Ma, C. Li, J. Gao, H. Yang, W. Tang, J. Gong, F. Zhou and Z. Gao, *Industrial &*
1669 *Engineering Chemistry Research*, 2020, **59**, 7765-7776.
1670 48. M. Boukerche, D. Mangin, J. P. Klein, O. Monnier and C. Hoff, *Chemical Engineering*
1671 *Research and Design*, 2010, **88**, 1474-1478.
1672 49. K. Wohlgemuth, A. Kordylla, F. Ruether and G. Schembecker, *Chemical Engineering*
1673 *Science*, 2009, **64**, 4155-4163.
1674 50. T. Kleetz, F. Funke, A. Sunderhaus, G. Schembecker and K. Wohlgemuth, *Crystal*
1675 *Growth & Design*, 2016, **16**, 6797-6803.
1676 51. S. Jiang and J. H. ter Horst, *Crystal Growth & Design*, 2011, **11**, 256-261.
1677 52. S. S. Kadam, S. A. Kulkarni, R. C. Ribera, A. I. Stankiewicz, J. H. ter Horst and H. J. M.
1678 Kramer, *Chemical Engineering Science*, 2012, **72**, 10-19.
1679 53. G. M. Maggioni and M. Mazzotti, *Faraday Discussions*, 2015, **179**, 359-382.
1680 54. G. M. Maggioni and M. Mazzotti, *Crystal Growth & Design*, 2017, **17**, 3625-3635.
1681 55. G. M. Maggioni, L. Bosetti, E. dos Santos and M. Mazzotti, *Crystal Growth & Design*,
1682 2017, **17**, 5488-5498.
1683 56. S. S. Kadam, H. J. M. Kramer and J. H. ter Horst, *Crystal Growth & Design*, 2011, **11**,
1684 1271-1277.
1685 57. N. Kubota, *Journal of Crystal Growth*, 2012, **345**, 27-33.
1686 58. T. Köllges and T. Vetter, 2017.
1687 59. T. Köllges and T. Vetter, *Organic Process Research & Development*, 2019, **23**, 361-374.
1688 60. L. R. Agnew, T. McGlone, H. P. Wheatcroft, A. Robertson, A. R. Parsons and C. C.
1689 Wilson, *Crystal Growth & Design*, 2017, **17**, 2418-2427.
1690 61. J. Garside and R. J. Davey, *Chemical Engineering Communications*, 1980, **4**, 393-424.
1691 62. S. G. Agrawal and A. H. J. Paterson, *Chemical Engineering Communications*, 2015, **202**,
1692 698-706.
1693 63. L. Bosetti and M. Mazzotti, *Crystal Growth & Design*, 2020, **20**, 307-319.
1694 64. R. Tyrrell, B. De Souza and P. J. Frawley, *Crystal Growth & Design*, 2018, **18**, 617-622.
1695 65. T. Mueansichai, A. E. Flood, T. Stelzer and J. Ulrich, *Cryst. Res. Technol.*, 2013, **48**, 38-
1696 50.
1697 66. H. Briesen, *Chemical Engineering Science*, 2009, **64**, 661-672.
1698 67. B. Biscans, *Powder Technology*, 2004, **143-144**, 264-272.
1699 68. C. Gahn and A. Mersmann, *Chemical Engineering Science*, 1999, **54**, 1273-1282.
1700 69. C. Gahn and A. Mersmann, *Chemical Engineering Science*, 1999, **54**, 1283-1292.
1701 70. S. Wang, A. Mersmann and M. Kind, *Journal of Crystal Growth*, 1990, **99**, 1104-1107.
1702 71. P. A. M. Grootscholten, L. D. M. V. D. Brekel and E. J. De Jong, *Chemical Engineering*
1703 *Research and Design*, 1984, **62**, 179-189.
1704 72. R. Ploß and A. Mersmann, *Chem. Eng. Technol.*, 1989, **12**, 137-146.
1705 73. H. Li, Y. Kawajiri, M. A. Grover and R. W. Rousseau, *Industrial & Engineering*
1706 *Chemistry Research*, 2017, **56**, 4060-4073.
1707 74. R. Soto and Å. C. Rasmuson, *Crystal Growth & Design*, 2019, **19**, 4273-4286.
1708 75. G. Capellades, H. Wiemeyer and A. S. Myerson, *Crystal Growth & Design*, 2019, **19**,
1709 4008-4018.
1710 76. N. Kubota, *Cryst. Res. Technol.*, 2001, **36**, 749-769.
1711 77. M. N. Joswiak, B. Peters and M. F. Doherty, *Crystal Growth & Design*, 2018, **18**, 6302-
1712 6306.
1713 78. S. A. Fischer, B. I. Dunlap and D. Gunlycke, *Chemical Science*, 2018, **9**, 7126-7132.

65

1714 79. H.-Y. Wang and J. D. Ward, *Journal of the Taiwan Institute of Chemical Engineers*,
1715 2016, **65**, 28-42.
1716 80. J. L. Quon, H. Zhang, A. Alvarez, J. Evans, A. S. Myerson and B. L. Trout, *Crystal*
1717 *Growth & Design*, 2012, **12**, 3036-3044.
1718 81. S. Yu, Y. Zhang and X. Z. Wang, *Organic Process Research & Development*, 2019, **23**,
1719 177-188.
1720 82. P. N. Mandare and V. G. Pangarkar, *Chemical Engineering Science*, 2003, **58**, 1125-
1721 1133.
1722 83. Z. Guo, A. Jones and N. Li, *Chemical Engineering Science*, 2006, **61**, 1617-1626.
1723 84. C. S. Polster, K. P. Cole, C. L. Burcham, B. M. Campbell, A. L. Frederick, M. M.
1724 Hansen, M. Harding, M. R. Heller, M. T. Miller, J. L. Phillips, P. M. Pollock and N.
1725 Zaborenko, *Organic Process Research & Development*, 2014, **18**, 1295-1309.
1726 85. T. Cao, Z. Weipeng, C. Jingcai and Y. Chao, *Chinese Journal of Chemical Engineering*,
1727 2018, **26**, 196-206.
1728 86. S. Teychené, I. Rodríguez-Ruiz and R. K. Ramamoorthy, *Current Opinion in Colloid &*
1729 *Interface Science*, 2020, **46**, 1-19.
1730 87. H. S. Fogler, *Essentials of Chemical Reaction Engineering*, Pearson Education, 4th edn.,
1731 2010.
1732 88. V. Bhamidi, K. Dumoleijn, D. Guha, S. K. Kirk, A. De Bruyn and A. K. Pymer, *Organic*
1733 *Process Research & Development*, 2019, **23**, 342-354.
1734 89. L. G. Encarnación-Gómez, A. S. Bommarius and R. W. Rousseau, *Chemical Engineering*
1735 *Science*, 2015, **122**, 416-425.
1736 90. R. L. Hartman, *Organic Process Research & Development*, 2012, **16**, 870-887.
1737 91. P. Grongsaard, P. G. Bulger, D. J. Wallace, L. Tan, Q. Chen, S. J. Dolman, J. Nyrop, R.
1738 S. Hoerrner, M. Weisel, J. Arredondo, T. Itoh, C. Xie, X. Wen, D. Zhao, D. J. Muzzio, E.
1739 M. Bassan and C. S. Shultz, *Organic Process Research & Development*, 2012, **16**, 1069-
1740 1081.
1741 92. M. M. Hansen, D. J. Jarmer, E. Arslantas, A. C. DeBaillie, A. L. Frederick, M. Harding,
1742 D. W. Hoard, A. Hollister, D. Huber and S. P. Kolis, *Organic Process Research &*
1743 *Development*, 2015, **19**, 1214-1230.
1744 93. T. A. Martinot, B. C. Austad, A. Côté, K. M. Depew, D. Genov, L. Grenier, J. Helble, A.
1745 Lescarbeau, S. Nair and M. Trudeau, *Organic Process Research & Development*, 2015,
1746 **19**, 1693-1702.
1747 94. A. J. Yap, A. F. Masters and T. Maschmeyer, *ChemCatChem*, 2012, **4**, 1179-1184.
1748 95. J. B. Rawlings and J. G. Ekerdt, *Chemical Reactor Analysis and Design Fundamentals*,
1749 Nob Hill Pub, Llc, 2002.
1750 96. J. Garside, *Chemical Engineering Science*, 1971, **26**, 1425-1431.
1751 97. G. R. Youngquist and A. D. Randolph, *AIChE Journal*, 1972, **18**, 421-429.
1752 98. S. Zhao, J. Gao, S. Ma, C. Li, Y. Ma, Y. He, J. Gong, F. Zhou, B. Zhang and W. Tang,
1753 *Processes*, 2019, **7**, 248.
1754 99. L. Lu, Q. Hua, J. Tang, Y. Liu, L. Liu and B. Wang, *Cryst. Res. Technol.*, 2018, **53**,
1755 1700130.
1756 100. W. Zuiderduin, C. Westzaan, J. Huetink and R. Gaymans, *Polymer*, 2003, **44**, 261-275.
1757 101. Y. Gao, H. Wang, Y. Su, Q. Shen and D. Wang, *Journal of Crystal Growth*, 2008, **310**,
1758 3771-3778.
1759 102. V. T. Costodes and A. E. Lewis, *Chemical Engineering Science*, 2006, **61**, 1377-1385.

1760 103. A. Rajbanshi, B. A. Moyer and R. Custelcean, *Crystal Growth & Design*, 2011, **11**, 2702-
1761   2706.
1762 104. L. Peng, H. Dai, Y. Wu, Y. Peng and X. Lu, *Chemosphere*, 2018, **197**, 768-781.
1763 105. Y. Liu and H. Qu, *Journal of Environmental Chemical Engineering*, 2016, **4**, 2155-2162.
1764 106. Y. Jiang, C. Liu, X. Zhou, P. Li, X. Song and J. Yu, *Energy Sources, Part A: Recovery,*
1765   *Utilization, and Environmental Effects*, 2019, 1-13.
1766 107. A. M. López-Periago, N. Portoles-Gil, P. Lopez-Dominguez, J. Fraile, J. Saurina, N. A
1767   liaga-Alcalde, G. T obias, J. A. Ayllón and C. Domingo, *Crystal Growth & Design ,*,
1768   2017, **17**, 2684- 2872.
1769 108. W. Zhang, F. Zhang, L. Ma, Y. Jie, Y. Jing and X. Huaping, *Crystal Growth and Design*,
1770   2019, **19**, 3616-3626.
1771 109. A. N. Saleemi, C. D. Rielly and Z. K. Nagy, *Crystal Growth & Design*, 2012, **12**, 1792-
1772   1807.
1773 110. D. J. Griffin, M. A. Grover, Y. Kawajiri and R. W. Rousseau, *Chemical Engineering*
1774   *Science*, 2014, **116**, 77-90.
1775 111. G. M. Maggioni, S. Kocevska, M. A. Grover and R. W. Rousseau, *Industrial &*
1776   *Engineering Chemistry Research*, 2019, **58**, 22640-22651.
1777 112. J. Prausnitz, R. Lichtenthaler and E. de Azevedo, *Englewood Cliffs, New Jersey*, 1986.
1778 113. M. A. McDonald, A. S. Bommarius, M. A. Grover and R. W. Rousseau, *Computers &*
1779   *Chemical Engineering*, 2019, **126**, 332-341.
1780 114. J. Chen, C. Zheng and G. A. Chen, *Chemical Engineering Science*, 1996, **51**, 1957-1966.
1781 115. Y. Li, Y. Zhang, C. Yang, L. Chen and Y. Zhang, *Chemical Engineering Science*, 2010,
1782   **65**, 4906-4912.
1783 116. M. Kitamura, H. Konno, A. Yasui and H. Masuoka, *Journal of Crystal Growth*, 2002,
1784   **236**, 323-332.
1785 117. M. Matsumoto, T. Fukunaga and K. Onoe, *Chemical Engineering Research and Design*,
1786   2010, **88**, 1624-1630.
1787 118. K.-J. Westin and Å. C. Rasmuson, *Desalination*, 2003, **159**, 107-118.
1788 119. H. Yagi, A. Iwazawa, R. Sonobe, T. Matsubara and H. Hikita, *Industrial & Engineering*
1789   *Chemistry Fundamentals*, 1984, **23**, 153-158.
1790 120. S. Varma, P. C. Chen and G. Unnikrishnan, *Materials Chemistry and Physics*, 2011, **126**,
1791   232-236.
1792 121. Y.-Z. Sun, X.-F. Song, M.-M. Jin, W. Jin and J.-G. Yu, *Industrial & Engineering*
1793   *Chemistry Research*, 2013, **52**, 17598-17606.
1794 122. R. Liu, M. Huang, X. Yao, S. Chen, S. Wang and Z. Suo, *Journal of Crystal Growth*,
1795   2018, **491**, 6-15.
1796 123. S. Wachi and A. G. Jones, *Chemical Engineering Science*, 1991, **46**, 1027-1033.
1797 124. S. Wachi and A. G. Jones, *Chemical Engineering Science*, 1991, **46**, 3289-3293.
1798 125. L. Pastero, F. R. Massaro and D. Aquilano, *Crystal Growth and Design*, 2007, **7**, 2749-
1799   2755.
1800 126. P. Taborga, I. Brito and T. A. Graber, *Journal of Crystal Growth*, 2017, **460**, 5-12.
1801 127. M. Kitamura, *Journal of Colloid and Interface Science*, 2001, **236**, 318-327.
1802 128. W.-S. Kim, I. Hirasawa and W.-S. Kim, *Industrial & Engineering Chemistry Research*,
1803   2004, **43**, 2650-2657.
1804 129. L. Xiang, Y. Wen, Q. Wang and Y. Jin, *Materials Chemistry and Physics*, 2006, **98**, 236-
1805   240.

1806	130.	B. Han, H. Qu, H. Niemi, Z. Sha and M. Louhi-Kultanen, *Chem. Eng. Technol.*, 2014, **37**,
1807		1363-1368.
1808	131.	Y. Shimizu and I. Hirasawa, *Chem. Eng. Technol.*, 2012, **35**, 1588-1592.
1809	132.	P. Nore and A. Mersmann, *Chemical Engineering Science*, 1993, **48**, 3083-3088.
1810	133.	P.-C. Chen, G. Y. Cheng, M. H. Kou, P. Y. Shia and P. O. Chung, *Journal of Crystal*
1811		*Growth*, 2001, **226**, 458-472.
1812	134.	C.-H. Lee and C.-H. Lee, *Korean Journal of Chemical Engineering*, 2005, **22**, 712-716.
1813	135.	B. Tomazic, R. Mohanty, M. Tadros and J. Estrin, *Journal of Crystal Growth*, 1986, **75**,
1814		339-347.
1815	136.	B. Tomazic, R. Mohanty, M. Tadros and J. Estrin, *Journal of Crystal Growth*, 1986, **75**,
1816		329-338.
1817	137.	H. Tsuge, Y. Tanaka, S. Yoshizawa and T. Kuraishi, *Chemical Engineering Research*
1818		*and Design*, 2002, **80**, 105-110.
1819	138.	C.-C. Su, R. R. M. Abarca, M. D. G. de Luna and M.-C. Lu, *Journal of the Taiwan*
1820		*Institute of Chemical Engineers*, 2014, **45**, 2395-2402.
1821	139.	C.-C. Su, L. D. Dulfo, M. L. P. Dalida and M.-C. Lu, *Separation and Purification*
1822		*Technology*, 2014, **125**, 90-96.
1823	140.	F. Abbona, H. L. Madsen and R. Boistelle, *Journal of Crystal Growth*, 1982, **57**, 6-14.
1824	141.	*United States Pat.,* 2019.
1825	142.	Y. Wang, D. Cai, C. Chen, Z. Wang, P. Qin and T. Tan, *Bioresource Technology*, 2015,
1826		**198**, 658-663.
1827	143.	L. V. van der Ham, E. L. V. Goetheer, E. S. Fernandez, M. R. M. Abu-Zahra and T. J. H.
1828		Vlugt, in *Absorption-Based Post-combustion Capture of Carbon Dioxide*, ed. P. H. M.
1829		Feron, Woodhead Publishing, 2016, pp. 103-119.
1830	144.	H. Zhang, R. Lakerveld, P. L. Heider, M. Tao, M. Su, C. J. Testa, A. N. D'Antonio, P. I.
1831		Barton, R. D. Braatz, B. L. Trout, A. S. Myerson, K. F. Jensen and J. M. B. Evans,
1832		*Crystal Growth & Design*, 2014, **14**, 2148-2157.
1833	145.	K. Xu and P. Xu, *Bioresource Technology*, 2014, **163**, 33-39.
1834	146.	W. J. Liu, C. Y. Ma, J. J. Liu, Y. Zhang and X. Z. Wang, *AIChE Journal*, 2017, **63**, 967-
1835		974.
1836	147.	R. Custelcean, N. J. Williams, K. A. Garrabrant, P. Agullo, F. M. Brethomé, H. J. Martin
1837		and M. K. Kidder, *Industrial & Engineering Chemistry Research*, 2019, **58**, 23338-
1838		23346.
1839	148.	2002.
1840	149.	R. Custelcean, N. J. Williams and C. A. Seipp, *Angewandte Chemie International*
1841		*Edition*, 2015, **54**, 10525-10529.
1842	150.	R. J. Ouellette and J. D. Rawn, in *Organic Chemistry*, eds. R. J. Ouellette and J. D.
1843		Rawn, Elsevier, Boston, 2014, pp. 803-842.
1844	151.	C. B. Aakeröy, A. Rajbanshi, Z. J. Li and J. Desper, *CrystEngComm*, 2010, **12**, 4231-
1845		4239.
1846	152.	K. P. Cole, J. M. Groh, M. D. Johnson, C. L. Burcham, B. M. Campbell, W. D. Diseroad,
1847		M. R. Heller, J. R. Howell, N. J. Kallman, T. M. Koenig, S. A. May, R. D. Miller, D.
1848		Mitchell, D. P. Myers, S. S. Myers, J. L. Phillips, C. S. Polster, T. D. White, J. Cashman,
1849		D. Hurley, R. Moylan, P. Sheehan, R. D. Spencer, K. Desmond, P. Desmond and O.
1850		Gowran, *Science*, 2017, **356**, 1144.

1851   153.   Q. Li and J. Xing, in *Production of Platform Chemicals from Sustainable Resources*, eds.
1852   Z. Fang, J. R. L. Smith and X. Qi, Springer Singapore, Singapore, 2017, DOI:
1853   10.1007/978-981-10-4172-3_8, pp. 231-262.
1854   154.   E. M. Buque-Taboada, A. J. Straathof, J. J. Heijnen and L. A. Van der Wielen,
1855   *Biotechnology and Bioengineering*, 2004, **86**, 795-800.
1856   155.   M. L. A. Jansen and W. M. van Gulik, *Current Opinion in Biotechnology*, 2014, **30**, 190-
1857   197.
1858   156.   C. S. López-Garzón and A. J. J. Straathof, *Biotechnology Advances*, 2014, **32**, 873-904.
1859   157.   C. A. Roa Engel, A. J. J. Straathof, T. W. Zijlmans, W. M. van Gulik and L. A. M. van
1860   der Wielen, *Applied Microbiology and Biotechnology*, 2008, **78**, 379-389.
1861   158.   J. Urbanus, R. Bisselink, K. Nijkamp, J. Ter Horst, D. Verdoes and C. Roelands, *Journal
1862   of Membrane Science*, 2010, **363**, 36-47.
1863   159.   F. Koopman, N. Wierckx, J. H. de Winde and H. J. Ruijssenaars, *Bioresource
1864   Technology*, 2010, **101**, 6291-6296.
1865   160.   I. C. Gangl, W. A. Weigand and F. A. Keller, *Applied Biochemistry and Biotechnology*,
1866   1990, **24**, 663-677.
1867   161.   Y. Usuda, Y. Hara and H. Kojima, in *Amino Acid Fermentation*, eds. A. Yokota and M.
1868   Ikeda, Springer Japan, Tokyo, 2017, DOI: 10.1007/10_2016_36, pp. 289-304.
1869   162.   S. Diab, D. T. McQuade, B. F. Gupton and D. I. Gerogiorgis, *Organic Process Research
1870   & Development*, 2019, **23**, 320-333.
1871   163.   J. S. Ferreira, A. J. Straathof, X. Li, M. Ottens, T. T. Franco and L. A. van der Wielen,
1872   *Industrial & Engineering Chemistry Research*, 2006, **45**, 6740-6744.
1873   164.   R. P. Elander, *Applied Microbiology and Biotechnology*, 2003, **61**, 385-392.
1874   165.   W. J. Liu, C. Y. Ma and X. Z. Wang, *Procedia Engineering*, 2015, **102**, 499-507.
1875   166.   M. Berovic and M. Legisa, in *Biotechnology Annual Review*, ed. M. R. El-Gewely,
1876   Elsevier, 2007, vol. 13, pp. 303-343.
1877   167.   S. Ramachandran, P. Fontanille, A. Pandey and C. Larroche, *Food Technology &
1878   Biotechnology*, 2006, **44**.
1879   168.   H. G. Kulla, *CHIMIA International Journal for Chemistry*, 1991, **45**, 81-85.
1880   169.   M. Furui, N. Sakata, O. Otsuki and T. Tosa, *Biocatalysis*, 1988, **2**, 69-77.
1881   170.   D. Hülsewede, J. N. Dohm and J. von Langermann, *Advanced Synthesis & Catalysis*,
1882   2019, **361**, 2727-2733.
1883   171.   K.-K. Cheng, X.-B. Zhao, J. Zeng, R.-C. Wu, Y.-Z. Xu, D.-H. Liu and J.-A. Zhang,
1884   *Applied Microbiology and Biotechnology*, 2012, **95**, 841-850.
1885   172.   S. Feng, N. Shan and K. J. Carpenter, *Organic process research & development*, 2006,
1886   **10**, 1212-1218.
1887   173.   L. G. Encarnación-Gómez, A. S. Bommarius and R. W. Rousseau, *Reaction Chemistry &
1888   Engineering*, 2016, **1**, 321-329.
1889   174.   S. Yu, Y. Zhang and X. Z. Wang, *Organic Process Research & Development*, 2019,
1890   DOI: 10.1021/acs.oprd.8b00190.
1891   175.   J. Urbanus, C. P. M. Roelands, J. H. ter Horst, D. Verdoes and P. J. Jansens, *Food and
1892   Bioproducts Processing*, 2008, **86**, 116-121.
1893   176.   H. Lin, C. Dai, T. F. Jamison and K. F. Jensen, *Angewandte Chemie International
1894   Edition*, 2017, **56**, 8870-8873.
1895   177.   Q.-L. Su, R. D. Braatz and M.-S. Chiu, *Journal of Process Control*, 2014, **24**, 415-421.
1896   178.   Q. L. Su, M. S. Chiu and R. D. Braatz, *AIChE Journal*, 2014, **60**, 2828-2838.

1897 179. H. M. Alatalo, H. Hatakka, M. Louhi-Kultanen, J. Kohonen and S. P. Reinikainen,
1898   *Chemical Engineering & Technology: Industrial Chemistry-Plant Equipment-Process*
1899   *Engineering-Biotechnology*, 2010, **33**, 743-750.
1900 180. H. Hatakka, H. Alatalo, M. Louhi-Kultanen, I. Lassila and E. Hæggström, *Chem. Eng.*
1901   *Technol.*, 2010, **33**, 751-756.
1902 181. A. Eggert, T. Maßmann, D. Kreyenschulte, M. Becker, B. Heyman, J. Büchs and A.
1903   Jupke, *Separation and Purification Technology*, 2019, **215**, 463-472.
1904 182. N. Pandurić, A. Šalić and B. Zelić, *Biochemical Engineering Journal*, 2017, **125**, 221-
1905   229.
1906 183. S. K. Schwechheimer, E. Y. Park, J. L. Revuelta, J. Becker and C. Wittmann, *Applied*
1907   *Microbiology and Biotechnology*, 2016, **100**, 2107-2119.
1908 184. H. Salami, C. E. Lagerman, P. R. Harris, M. A. McDonald, A. S. Bommarius, R. W.
1909   Rousseau and M. A. Grover, *Reaction Chemistry & Engineering*, 2020, DOI:
1910   10.1039/D0RE00276C.
1911 185. K. M. J. Brands and A. J. Davies, *Chemical Reviews*, 2006, **106**, 2711-2733.
1912 186. K. Würges, K. Petruševska-Seebach, M. P. Elsner and S. Lütz, *Biotechnology and*
1913   *Bioengineering*, 2009, **104**, 1235-1239.
1914 187. L.-C. Sögütoglu, R. R. Steendam, H. Meekes, E. Vlieg and F. P. Rutjes, *Chemical Society*
1915   *Reviews*, 2015, **44**, 6723-6732.
1916 188. J. R. Dunetz, J. Magano and G. A. Weisenburger, *Organic Process Research &*
1917   *Development*, 2016, **20**, 140-177.
1918 189. M. Jiang and X.-W. Ni, *Journal of Crystal Growth*, 2019, **523**, 125150.
1919 190. M. Jiang and N. Xiong-Wei, 2019, **23**, 882-890.
1920 191. R. A. Illos, G. Clodic, G. Bolbach, I. Weissbuch and M. Lahav, *Origins of Life and*
1921   *Evolution of Biospheres*, 2009, **40**, 51.
1922 192. C. Chen, J. Tan, M.-C. Hsieh, T. Pan, J. T. Goodwin, A. K. Mehta, M. A. Grover and D.
1923   G. Lynn, *Nature Chemistry*, 2017, **9**, 799.
1924 193. Q. Wang, Y. Cheng, L. Wang, H. Xu and X. Li, *Industrial & Engineering Chemistry*
1925   *Research*, 2008, **47**, 5861-5870.
1926 194. D. Hülsewede, L. E. Meyer and J. von Langermann, *Chemistry–A European Journal*,
1927   2019, **25**, 4871-4884.
1928 195. E. M. Buque-Taboada, A. J. Straathof, J. J. Heijnen and L. A. Van Der Wielen, *Applied*
1929   *Microbiology and Biotechnology*, 2006, **71**, 1-12.
1930 196. S. Takamatsu and D. D. Ryu, *Biotechnology and bioengineering*, 1987, **32**, 184-191.
1931 197. J. M. Woodley, *Computers & Chemical Engineering*, 2017, **105**, 297-307.
1932 198. A. L. Ferreira, R. L. Giordano and R. C. Giordano, *Industrial & Engineering Chemistry*
1933   *Research*, 2007, **46**, 7695-7702.
1934 199. M. A. Huffman, A. Fryszkowska, O. Alvizo, M. Borra-Garske, K. R. Campos, K. A.
1935   Canada, P. N. Devine, D. Duan, J. H. Forstater, S. T. Grosser, H. M. Halsey, G. J.
1936   Hughes, J. Jo, L. A. Joyce, J. N. Kolev, J. Liang, K. M. Maloney, B. F. Mann, N. M.
1937   Marshall, M. McLaughlin, J. C. Moore, G. S. Murphy, C. C. Nawrat, J. Nazor, S. Novick,
1938   N. R. Patel, A. Rodriguez-Granillo, S. A. Robaire, E. C. Sherer, M. D. Truppo, A. M.
1939   Whittaker, D. Verma, L. Xiao, Y. Xu and H. Yang, *Science*, 2019, **366**, 1255-1259.
1940 200. C. C. Nawrat, A. M. Whittaker, M. A. Huffman, M. McLaughlin, R. D. Cohen, T.
1941   Andreani, B. Ding, H. Li, M. Weisel and D. M. Tschaen, *Organic Letters*, 2020, **22**,
1942   2167-2172.

1943   201.   J. Ren, P. Yao, S. Yu, W. Dong, Q. Chen, J. Feng, Q. Wu and D. Zhu, *ACS Catalysis*,
1944   2016, **6**, 564-567.
1945   202.   *United States Pat.,* 1996.
1946   203.   *United States Pat.,* 1979.
1947   204.   J. Yin, M. Weisel, Y. Ji, Z. Liu, J. Liu, D. J. Wallace, F. Xu, B. D. Sherry and N. Yasuda,
1948   *Organic Process Research & Development*, 2018, **22**, 273-277.
1949   205.   M. I. Youshko, H. M. Moody, A. L. Bukhanov, W. H. Boosten and V. K. Švedas,
1950   *Biotechnolöy and Bioengineering*, 2004, **85**, 323-329.
1951   206.   M. I. Youshko, L. M. van Langen, E. de Vroom, F. van Rantwijk, R. A. Sheldon and V.
1952   K. Švedas, *Biotechnology and bioengineering*, 2001, **73**, 426-430.
1953   207.   M. A. Wegman, L. M. van Langen, F. van Rantwijk and R. A. Sheldon, *Biotechnology
1954   and bioengineering*, 2002, **79**, 356-361.
1955   208.   M. Furui, T. Furutani, T. Shibatani, Y. Nakamoto and T. Mori, *Journal of Fermentation
1956   and Bioengineering*, 1996, **81**, 21-25.
1957   209.   T. Nagasawa, C. D. Mathew, J. Mauger and H. Yamada, *Applied and Environmental
1958   Microbiology*, 1988, **54**, 1766-1769.
1959   210.   L. G. Encarnacion-Gomez, Ph.D., Georgia Institute of Technology, 2015.
1960   211.   K. Würges, U. Mackfeld, M. Pohl, S. Lütz, S. Wilhelm, W. Wiechert and T. Kubitzki,
1961   *Advanced Synthesis & Catalysis*, 2011, **353**, 2431-2438.
1962   212.   K. Liu, F. Zhu, L. Zhu, G. Chen and B. He, *Biochemical Engineering Journal*, 2015, **98**,
1963   63-67.
1964   213.   B.-K. Cho, J.-H. Seo, T.-W. Kang and B.-G. Kim, *Biotechnology and Bioengineering*,
1965   2003, **83**, 226-234.
1966   214.   B.-K. Cho, J.-H. Seo, J. Kim, C.-S. Lee and B.-G. Kim, *Biotechnology and Bioprocess
1967   Engineering*, 2006, **11**, 299-305.
1968   215.   R. V. Ulijn, A. E. Janssen, B. D. Moore and P. J. Halling, *Chemistry-A European
1969   Journal*, 2001, **7**, 2089-2098.
1970   216.   M. Erbeldinger, X. Ni and P. J. Halling, *Biotechnology and Bioengineering*, 1998, **59**, 68-
1971   72.
1972   217.   U. Eichhorn, A. S. Bommarius, K. Drauz and H.-D. Jakubke, *Journal of Peptide Science*,
1973   1997, **3**, 245-251.
1974   218.   P. Halling, U. Eichhorn, P. Kuhl and H.-D. Jakubke, *Enzyme and Microbial Technology*,
1975   1995, **17**, 601-606.
1976   219.   P. Kuhl, P. J. Halling and H.-D. Jakubke, *Tetrahedron letters*, 1990, **31**, 5213-5216.
1977   220.   K. Oyama, S. Irino, T. Harada and N. Hagi, *Annals of the New York Academy of
1978   Sciences*, 1984, **434**, 095-098.
1979   221.   K. Oyama and K.-I. Kihara, *Chemtech*, 1984, **14**, 100-105.
1980   222.   D. Hülsewede, E. Temmel, P. Kumm and J. v. Langermann, *Crystals*, 2020, **10**, 345.
1981   223.   C. B. Aakeröy, M. E. Fasulo and J. Desper, *Molecular Pharmaceutics*, 2007, **4**, 317-322.
1982   224.   S. Aitipamula, R. Banerjee, A. K. Bansal, K. Biradha, M. L. Cheney, A. R. Choudhury,
1983   G. R. Desiraju, A. G. Dikundwar, R. Dubey, N. Duggirala, P. P. Ghogale, S. Ghosh, P. K.
1984   Goswami, N. R. Goud, R. R. K. R. Jetti, P. Karpinski, P. Kaushik, D. Kumar, V. Kumar,
1985   B. Moulton, A. Mukherjee, G. Mukherjee, A. S. Myerson, V. Puri, A. Ramanan, T.
1986   Rajamannar, C. M. Reddy, N. Rodriguez-Hornedo, R. D. Rogers, T. N. G. Row, P.
1987   Sanphui, N. Shan, G. Shete, A. Singh, C. C. Sun, J. A. Swift, R. Thaimattam, T. S.
1988   Thakur, R. Kumar Thaper, S. P. Thomas, S. Tothadi, V. R. Vangala, N. Variankaval, P.

Vishweshwar, D. R. Weyna and M. J. Zaworotko, *Crystal Growth & Design*, 2012, **12**, 2147-2152.

225. FDA, *Center for Drug Evaluation and Research (CDER), Silver Spring, US*, 2018.

226. L. Yang, D. Wei and Y. Zhang, *Journal of Chemical Technology & Biotechnology*, 2004, **79**, 480-485.

227. C. Schroën, V. A. Nierstrasz, R. Bosma, G. J. Kemperman, M. Strubel, L. P. Ooijkaas, H. H. Beeftink and J. Tramper, *Enzyme and microbial technology*, 2002, **31**, 264-273.

228. G. Kemperman, R. De Gelder, F. Dommerholt, C. Schroën, R. Bosma and B. Zwanenburg, *Green Chemistry*, 2001, **3**, 189-192.

229. T. Grecu, C. A. Hunter, E. J. Gardiner and J. F. McCabe, *Crystal Growth & Design*, 2014, **14**, 165-171.

230. D. Douroumis, S. A. Ross and A. Nokhodchi, *Adv. Drug Deliv. Rev.*, 2017, **117**, 178-195.

231. G. Rama Krishna, M. Ukrainczyk, J. Zeglinski and Å. C. Rasmuson, *Crystal Growth & Design*, 2018, **18**, 133-144.

232. S. J. Bethune, N. Huang, A. Jayasankar and N. Rodríguez-Hornedo, *Crystal Growth & Design*, 2009, **9**, 3976-3988.

233. R. Shaikh, R. Singh, G. M. Walker and D. M. Croker, *Trends in Pharmacological Sciences*, 2018, **39**, 1033-1048.

234. S. Emami, M. Siahi-Shadbad, K. Adibkia and M. Barzegar-Jalali, *Bioimpacts*, 2018, **8**, 305-320.

235. M. Karimi-Jafari, L. Padrela, G. M. Walker and D. M. Croker, *Crystal Growth & Design*, 2018, **18**, 6370-6387.

236. E. Gagniere, D. Mangin, F. Puel, J.-P. Valour, J.-P. Klein and O. Monnier, *Journal of Crystal Growth*, 2011, **316**, 118-125.

237. N. Rodríguez-Hornedo, S. J. Nehm, K. F. Seefeldt, Y. Pagán-Torres and C. J. Falkiewicz, *Molecular Pharmaceutics*, 2006, **3**, 362-367.

238. S. Kudo and H. Takiyama, *Journal of Crystal Growth*, 2014, **392**, 87-91.

239. G. Coquerel, in *Novel Optical Resolution Technologies*, eds. K. Sakai, N. Hirayama and R. Tamura, Springer-Verlag Berlin, Berlin, 2007, vol. 269, pp. 1-51.

240. A. Otero-de-la-Roza, J. E. Hein and E. R. Johnson, *Crystal Growth & Design*, 2016, **16**, 6055-6059.

241. H. Lorenz and A. Seidel-Morgenstern, *Angewandte Chemie International Edition*, 2014, **53**, 1218-1250.

242. A. Palmans, *Molecular Systems Design & Engineering*, 2017, **2**, 34-46.

243. R. Yoshioka, H. Hiramatsu, K. Okamura, I. Tsujioka and S.-i. Yamada, *Journal of the Chemical Society, Perkin Transactions 2*, 2000, 2121-2128.

244. R. M. Kellogg, in *Advances in Organic Crystal Chemistry: Comprehensive Reviews 2015*, eds. R. Tamura and M. Miyata, Springer Japan, Tokyo, 2015, DOI: 10.1007/978-4-431-55555-1_21, pp. 421-443.

245. R. Yoshioka, in *Novel Optical Resolution Technologies*, eds. K. Sakai, N. Hirayama and R. Tamura, Springer Berlin Heidelberg, Berlin, Heidelberg, 2007, DOI: 10.1007/128_2006_094, pp. 83-132.

246. K. Petruševska-Seebach, K. Wuerges, A. Seidel-Morgenstern, S. Luetz and M. P. Elsner, *Chemical Engineering Science*, 2009, **64**, 2473-2482.

2033 247. M. D. Johnson, S. A. May, J. R. Calvin, J. Remacle, J. R. Stout, W. D. Diseroad, N.
2034   Zaborenko, B. D. Haeberle, W.-M. Sun and M. T. Miller, *Organic Process Research &*
2035   *Development*, 2012, **16**, 1017-1038.
2036 248. I. Harriehausen, K. Wrzosek, H. Lorenz and A. Seidel-Morgenstern, *Adsorption*, 2020.
2037 249. C. Viedma, *Physical review letters*, 2005, **94**, 065504.
2038 250. C. Viedma, J. E. Ortiz, T. d. Torres, T. Izumi and D. G. Blackmond, *Journal of the*
2039   *American Chemical Society*, 2008, **130**, 15274-15275.
2040 251. D. G. Blackmond, *Chemistry–A European Journal*, 2007, **13**, 3290-3295.
2041 252. D. G. Blackmond, *Chemistry – A European Journal*, 2007, **13**, 10306-10311.
2042 253. W. L. Noorduin, T. Izumi, A. Millemaggi, M. Leeman, H. Meekes, W. J. P. Van
2043   Enckevort, R. M. Kellogg, B. Kaptein, E. Vlieg and D. G. Blackmond, *Journal of the*
2044   *American Chemical Society*, 2008, **130**, 1158-1159.
2045 254. J. E. Hein, B. Huynh Cao, C. Viedma, R. M. Kellogg and D. G. Blackmond, *Journal of*
2046   *the American Chemical Society*, 2012, **134**, 12629-12636.
2047 255. L. Spix, A. Alfring, H. Meekes, W. J. P. van Enckevort and E. Vlieg, *Crystal Growth &*
2048   *Design*, 2014, **14**, 1744-1748.
2049 256. A. I. Stankiewicz and J. A. Moulijn, *Chemical engineering progress*, 2000, **96**, 22-34.
2050 257. A. Stankiewicz, *Chemical Engineering and Processing: Process Intensification*, 2003,
2051   **42**, 137-144.
2052 258. H. J. Kramer and R. Lakerveld, in *Handbook of Industrial Crystallization*, eds. A. S.
2053   Myerson, D. Erdemir and A. Y. Lee, 2019, pp. 197-215.
2054 259. S. L. Lee, T. F. O'Connor, X. Yang, C. N. Cruz, S. Chatterjee, R. D. Madurawe, C. M. V.
2055   Moore, L. X. Yu and J. Woodcock, *Journal of Pharmaceutical Innovation*, 2015, **10**,
2056   191-199.
2057 260. D. Acevedo, X. Yang, A. Mohammad, N. Pavurala, W.-L. Wu, T. F. O'Connor, Z. K.
2058   Nagy and C. N. Cruz, *Organic Process Research & Development*, 2018, **22**, 156-165.
2059 261. M. B. Diender, A. J. J. Straathof, T. Van der Does, M. Zomerdijk and J. J. Heijnen,
2060   *Enzyme and microbial technology*, 2000, **27**, 576-582.
2061 262. E. Temmel, J. Gänsch, H. Lorenz and A. Seidel-Morgenstern, *Crystal Growth & Design*,
2062   2018, **18**, 7504-7517.
2063 263. C. Wibowo, W. C. Chang and K. M. Ng, *AIChE Journal*, 2001, **47**, 2474-2492.
2064 264. B. L. Åslund and Å. C. Rasmuson, *AIChE Journal*, 1992, **38**, 328-342.
2065 265. R. Zauner and A. G. Jones, *Chemical Engineering Science*, 2002, **57**, 821-831.
2066 266. R. Zauner and A. G. Jones, *Chemical Engineering Research and Design*, 2000, **78**, 894-
2067   902.
2068 267. L. Liu, X. Yang, G. Li, X. Huang and C. Xue, *Advanced Powder Technology*, 2020, **31**,
2069   1088-1099.
2070 268. S. K. Kurt, M. Akhtar, K. D. P. Nigam and N. Kockmann, *Industrial & Engineering*
2071   *Chemistry Research*, 2017, **56**, 11320-11335.
2072 269. D. Acevedo, X. Yang, Y. Liu, T. F. O'Connor, A. Koswara, Z. K. Nagy, R. Madurawe
2073   and C. N. Cruz, *Organic Process Research & Development*, 2019.
2074 270. C. Hu, J. E. Finkelstein, W. Wu, K. Shvedova, C. J. Testa, S. C. Born, B. Takizawa, T. F.
2075   O'Connor, X. Yang, S. Ramanujam and S. Mascia, *Reaction Chemistry & Engineering*,
2076   2018, **3**, 658-667.
2077 271. Y. Yang, L. Song, T. Gao and Z. K. Nagy, *Crystal Growth & Design*, 2015, **15**, 5879-
2078   5885.

2079 272. D. Acevedo, V. K. Kamaraju, B. Glennon and Z. K. Nagy, *Organic Process Research &*
2080 *Development*, 2017, **21**, 1069-1079.
2081 273. T. Köllges and T. Vetter, *Crystal Growth & Design*, 2017, **17**, 233-247.
2082 274. H. Li, J. Wang, Y. Bao, Z. Guo and M. Zhang, *Journal of Crystal Growth*, 2003, **247**,
2083 192-198.
2084 275. T. Vetter, C. L. Burcham and M. F. Doherty, *Chemical Engineering Science*, 2014, **106**,
2085 167-180.
2086 276. G. Ruecroft, D. Hipkiss, T. Ly, N. Maxted and P. W. Cains, *Organic Process Research &*
2087 *Development*, 2005, **9**, 923-932.
2088 277. Y. Mo and K. F. Jensen, *Reaction Chemistry & Engineering*, 2016, **1**, 501-507.
2089 278. T. Jung, W.-S. Kim and C. K. Choi, *Crystal Growth & Design*, 2004, **4**, 491-495.
2090 279. M. Su and Y. Gao, *Industrial & Engineering Chemistry Research*, 2018, **57**, 3781-3791.
2091 280. A. R. Oroskar and R. M. Turian, *AIChE Journal*, 1980, **26**, 550-558.
2092 281. T. Mikami, T. Sakuma and I. Hirasawa, *Chemical Engineering Research and Design*,
2093 2010, **88**, 1200-1205.
2094 282. D. A. Berry and K. M. Ng, *AIChE journal*, 1997, **43**, 1737-1750.
2095 283. V. V. Kelkar and K. M. Ng, *AIChE journal*, 1999, **45**, 69-81.
2096 284. K. L. Choong and R. Smith, *Chemical engineering science*, 2004, **59**, 1529-1540.
2097 285. J. W. Schroer and K. M. Ng, *Industrial & Engineering Chemistry Research*, 2003, **42**,
2098 2230-2244.
2099 286. D. Sarkar, S. Rohani and A. Jutan, *AIChE journal*, 2007, **53**, 1164-1177.
2100 287. H.-Y. Wang and J. D. Ward, *Industrial & Engineering Chemistry Research*, 2015, **54**,
2101 9360-9368.
2102 288. A. Dafnomilis, S. Diab, A. D. Rodman, A. G. Boudouvis and D. I. Gerogiorgis,
2103 *Industrial & Engineering Chemistry Research*, 2019, **58**, 18756-18771.
2104 289. L. L. Simon, H. Pataki, G. Marosi, F. Meemken, K. Hungerbühler, A. Baiker, S.
2105 Tummala, B. Glennon, M. Kuentz, G. Steele, H. J. M. Kramer, J. W. Rydzak, Z. Chen, J.
2106 Morris, F. Kjell, R. Singh, R. Gani, K. V. Gernaey, M. Louhi-Kultanen, J. O'Reilly, N.
2107 Sandler, O. Antikainen, J. Yliruusi, P. Frohberg, J. Ulrich, R. D. Braatz, T. Leyssens, M.
2108 Von Stosch, R. Oliveira, R. B. H. Tan, H. Wu, M. Khan, D. O'Grady, A. Pandey, R.
2109 Westra, E. Delle-Case, D. Pape, D. Angelosante, Y. Maret, O. Steiger, M. Lenner, K.
2110 Abbou-Oucherif, Z. K. Nagy, J. D. Litster, V. K. Kamaraju and M.-S. Chiu, *Organic*
2111 *Process Research & Development*, 2015, **19**, 3-62.
2112 290. H. Alatalo, J. Kohonen, H. Qu, H. Hatakka, S.-P. Reinikainen, M. Louhi-Kultanen and J.
2113 Kallas, *Journal of Chemometrics*, 2008, **22**, 644-652.
2114 291. H. Qu, H. Alatalo, H. Hatakka, J. Kohonen, M. Louhi-Kultanen, S.-P. Reinikainen and J.
2115 Kallas, *Journal of Crystal Growth*, 2009, **311**, 3466-3475.
2116 292. M. Su, L. Wang, H. Sun and J. Wang, *Frontiers of Chemical Engineering in China*, 2009,
2117 **3**, 282-288.
2118 293. J. Worlitschek, T. Hocker and M. Mazzotti, *Particle & Particle Systems*
2119 *Characterization*, 2005, **22**, 81-98.
2120 294. H. Li, M. A. Grover, Y. Kawajiri and R. W. Rousseau, *Chemical Engineering Science*,
2121 2013, **89**, 142-151.
2122 295. Q.-L. Su and M.-S. Chiu, *JOURNAL OF CHEMICAL ENGINEERING OF JAPAN*, 2016,
2123 **49**, 680-688.
2124 296. Y. Wang, S. Ma and X. Lv, *Cryst. Res. Technol.*, 2012, **47**, 848-862.

2125 297. W. J. Liu, C. Y. Ma, J. J. Liu, Y. Zhang and X. Z. Wang, *AIChE Journal*, 2015, **61**, 503-
2126   517.
2127 298. H. Alatalo, H. Hatakka, J. Kohonen, S.-p. Reinikainen and M. Louhi-kultanen, *AIChE*
2128   *Journal*, 2010, **56**, 2063-2076.
2129 299. Z. K. Nagy, M. Fujiwara and R. D. Braatz, *Journal of Process Control*, 2008, **18**, 856-
2130   864.
2131 300. V. Liotta and V. Sabesan, *Organic Process Research & Development*, 2004, **8**, 488-494.
2132 301. C. Cheng and M.-S. Chiu, *Chemometrics and Intelligent Laboratory Systems*, 2005, **76**,
2133   1-13.
2134 302. Q. Su, M.-S. Chiu and R. D. Braatz, *AIChE Journal*, 2017, **63**, 5007-5018.
2135 303. H. M. Alatalo, H. Hatakka, M. Louhi-Kultanen, J. Kohonen and S.-P. Reinikainen, *Chem.*
2136   *Eng. Technol.*, 2010, **33**, 743-750.
2137 304. W. Meng, E. Sirota, H. Feng, J. P. McMullen, L. Codan and A. S. Cote, *Organic Process*
2138   *Research & Development*, 2020, DOI: 10.1021/acs.oprd.0c00307.
2139 305. P. Cui, D. P. McMahon, P. R. Spackman, B. M. Alston, M. A. Little, G. M. Day and A. I.
2140   Cooper, *Chemical science*, 2019, **10**, 9988-9997.
2141 306. S. L. Morissette, Ö. Almarsson, M. L. Peterson, J. F. Remenar, M. J. Read, A. V.
2142   Lemmo, S. Ellis, M. J. Cima and C. R. Gardner, *Adv. Drug Deliv. Rev.*, 2004, **56**, 275-
2143   300.
2144 307. T. Togkalidou, H. H. Tung, Y. K. Sun, A. Andrews and R. D. Braatz, *Organic Process*
2145   *Research & Development*, 2002, **6**.
2146 308. Z. Q. Yu, P. S. Chow and R. B. H. Tan, *Crystal Growth & Design*, 2010, **10**, 2382-2387.
2147 309. Q. Wang, X. Li, L. Wang, Y. Cheng and G. Xie, *Industrial & Engineering Chemistry*
2148   *Research*, 2005, **44**, 261-266.
2149 310. M. A. McDonald, A. S. Bommarius, R. W. Rousseau and M. A. Grover, 2018.
2150 311. S. C. Barthe, M. A. Grover and R. W. Rousseau, *Crystal Growth & Design*, 2008, **8**,
2151   3316-3322.
2152 312. M. R. Abu Bakar, Z. K. Nagy and C. D. Rielly, *Crystal Growth & Design*, 2010, **10**,
2153   3892-3900.
2154 313. J. Heinrich and J. Ulrich, *Chem. Eng. Technol.*, 2012, **35**, 967-979.
2155 314. T. Tosa, M. Furui, N. Sakata, O. Otsuki and I. Chibata, *Annals of the New York Academy*
2156   *of Sciences*, 1988, **542**, 440-443.
2157 315. L. Wang, A. Sklyarenko, D. Li, A. I. Sidorenko, C. Zhao, J. Li and S. V. Yarotsky,
2158   *Bioprocess and Biosystems Engineering*, 2018, **41**, 1851-1867.
2159 316. E. Simone, A. Saleemi and Z. Nagy, *Organic Process Research & Development*, 2014,
2160   **19**, 167-177.
2161 317. L. Simon, S. Reinlein and K. Hungerbuehler, 2011.
2162 318. K. B. Konstantinov and C. L. Cooney, *Journal of Pharmaceutical Sciences*, 2015, **104**,
2163   813-820.
2164 319. C. Hu, C. J. Testa, W. Wu, K. Shvedova, D. E. Shen, R. Sayin, B. S. Halkude, F. Casati,
2165   P. Hermant and A. Ramnath, *Chemical Communications*, 2020.
2166 320. W. Wu, M. G. Lesher, C. Hu, K. Shvedova, B. Takizawa, T. F. O'Connor, X. Yang, S.
2167   Ramanujam and S. Mascia, *Organic Process Research & Development*, 2018, **22**, 1214-
2168   1221.
2169 321. T. Lee, H. Y. Lin and H. L. Lee, *Organic Process Research & Development*, 2013, **17**,
2170   1168-1178.

2171   322.   M. E. Vilt and W. W. Ho, *Journal of Membrane Science*, 2011, **367**, 71-77.
2172   323.   C. A. Quist-Jensen, J. M. Sørensen, A. Svenstrup, L. Scarpa, T. S. Carlsen, H. C. Jensen,
2173   L. Wybrandt and M. L. Christensen, *Desalination*, 2018, **440**, 156-160.
2174   324.   K. Y. Fung, K. M. Ng and C. Wibowo, *Industrial & Engineering Chemistry Research*,
2175   2005, **44**, 910-921.
2176   325.   J. Wöltinger, K. Drauz and A. S. Bommarius, *Applied Catalysis A: General*, 2001, **221**,
2177   171-185.
2178   326.   S. Ferguson, F. Ortner, J. Quon, L. Peeva, A. Livingston, B. L. Trout and A. S. Myerson,
2179   *Crystal Growth & Design*, 2013, **14**, 617-627.
2180   327.   C. Wibowo and K. M. Ng, *AIChE Journal*, 2001, **47**, 107-125.
2181